OUTDOOR WIRELESS VISIBLE LIGHT COMMUNICATIONS FOR INFRASTRUCTURE TO VEHICLE APPLICATIONS USING MIMO TECHNIQUE

ADISORN KAEWPUKDEE

A Thesis Submitted in Partial Fulfillment of the Requirements for the Degree of Doctor of Philosophy in Telecommunication and Computer Engineering

Suranaree University of Technology

Academic Year 2023

การสื่อสารไร้สายด้วยแสงที่มองเห็นภายนอกอาคารเพื่อประยุกต์ใช้งานระหว่างโครงสร้างพื้นฐานกับยานพาหนะโดยใช้เทคนิคไมโม

นายอดิศร แก้วภักดี

วิทยานิพนธ์นี้เป็นส่วนหนึ่งของการศึกษาตามหลักสูตรปริญญาวิศวกรรมศาสตรดุษฎีบัณฑิต
สาขาวิชาวิศวกรรมโทรคมนาคมและคอมพิวเตอร์
มหาวิทยาลัยเทคโนโลยีสุรนารี
ปีการศึกษา 2566

OUTDOOR WIRELESS VISIBLE LIGHT COMMUNICATIONS FOR INFRASTRUCTURE TO VEHICLE APPLICATIONS USING MIMO TECHNIQUE

Suranaree University of Technology has approved this thesis submitted in partial fulfillment of the requirements for The Degree of Doctor of Philosophy.

Thesis Examining Committee

C. Thaijiam

(Assoc. Prof. Dr. Chanchai Thaijiam)
Chairperson

(Assoc. Prof. Dr. Peerapong Uthansakul)
Member (Thesis Advisor)

(Assoc. Prof. Dr. Piyaporn Mesawad)
Member

(Assoc. Prof. Dr. Monthippa Uthansakul)
Member

(Dr. Dheerasak Anantakul)
Member

(Assoc. Prof. Dr. Yupaporn Ruksakulpiwat)
Vice Rector for Academic Affairs
and Quality Assurance

(Assoc. Prof. Dr. Pornsiri Jongkol)
Dean of Institute of Engineering

อดิศร แก้วภักดี : การสื่อสารไร้สายด้วยแสงที่มองเห็นภายนอกอาคารเพื่อประยุกต์ใช้งานระหว่างโครงสร้างพื้นฐานกับยานพาหนะโดยใช้เทคนิคไมโม (OUTDOOR WIRELESS VISIBLE LIGHT COMMUNICATIONS FOR INFRASTRUCTURE TO VEHICLE APPLICATIONS USING MIMO TECHNIQUE)
อาจารย์ที่ปรึกษา : รองศาสตราจารย์ ดร.พีระพงษ์ อุฑารสกุล 145 หน้า

คำสำคัญ: การสื่อสารด้วยแสงที่สามารถมองเห็นได้/โครงสร้างพื้นฐานกับยานพาหนะ/ผลตอบสนองช่องสัญญาณ/ไฟถนนอัจฉริยะ

ปัจจุบันข้อมูลการเสียชีวิตและบาดเจ็บของมนุษย์มีสาเหตุมาจากอุบัติเหตุเป็นสำคัญ ซึ่งเป็นอุบัติเหตุเกิดขึ้นจากการจราจรบนถนนเป็นหลัก เพื่อป้องกันและลดปัญหาการเกิดอุบัติเหตุ และช่วยลดจำนวนการเสียชีวิตและบาดเจ็บของมนุษย์ จึงได้นำระบบการขนส่งอัจฉริยะ (Intelligent Transportation System, ITS) ใช้สำหรับการบริหารจัดการเกี่ยวกับการจราจรบนท้องถนน อีกทั้งยังช่วยลดปัญหาการจราจรติดขัด ลดการใช้พลังงานอย่างสิ้นเปลือง และลดการปล่อยก๊าซคาร์บอนไดออกไซด์ซึ่งเป็นปัญหาการเกิดสภาวะโลกร้อน ดังนั้น เมื่อยานพาหนะมีความฉลาดสามารถนำทางด้วยตัวเองได้ สามารถป้องกันการชน สามารถความคุมความเร็วแบบปรับค่าได้ สิ่งเหล่านี้ต้องอาศัยระบบการตรวจจับ การสื่อสารข้อมูล การส่งสัญญาณข้อมูลต่าง ๆ ระหว่างยานพาหนะและเครือข่ายการสื่อสารในระบบการขนส่งแบบอัจฉริยะ อาทิเช่น การสื่อสารด้วยคลื่นวิทยุคลื่นสั้น (Dedicate Short-Range Communication, DSRC) ซึ่งมีทั้งรูปแบบการสื่อสารระหว่างยานพาหนะกับยานพาหนะ (Vehicle-to-Vehicle, V2V) การสื่อสารระหว่างยานพาหนะกับโครงสร้างพื้นฐาน (Vehicle-to-Infrastructure, V2I) หรือการสื่อสารระหว่างโครงสร้างพื้นฐานกับยานพาหนะ (Infrastructure-to-Vehicle, I2V) เป็นต้น และในเครือข่ายการสื่อสารแบบเซลลูลาร์-ยานพาหนะกับทุกสรรพสิ่ง (Cellular Vehicle-to-Everything, C-V2X) ได้ทำการทดสอบระบบการใช้งานในประเทศแถบยุโรป ด้วยคลื่นความถี่ 5.9 กิกะเฮิร์ต คาดการณ์ว่าจะนำมาแทนที่หรือใช้งานร่วมกันกับระบบการสื่อสารแบบ DSRC ซึ่งเครือข่ายการสื่อสารที่กล่าวมานั้นเป็นการสื่อสารด้วยคลื่นความถี่วิทยุ (Radio Frequency, RF) ณ ปัจจุบันการใช้งานแถบคลื่นวิทยุมีความแออัดอย่างมาก การใช้งานต้องขออนุญาต และมีต้นทุนที่สูง

ระบบการขนส่งอัจฉริยะได้นำเทคโนโลยีการสื่อสารด้วยแสงที่มองเห็น (Visible Light Communication, VLC) มาประยุกต์ใช้งานเพื่อเป็นทางเลือกให้กับระบบการขนส่งอัจฉริยะ ข้อดีสำหรับการใช้งานแถบคลื่นแสงที่มองเห็น มีต้นทุนต่ำ ไม่ต้องขออนุญาต ร่วมกับเทคโนโลยีการผลิต

หลอดแอลอีดีที่ให้ความสว่างที่เพิ่มขึ้นในขณะที่ต้นทุนการผลิตลดลง หลอดแอลอีดีในอนาคตที่จะนำไปแทนที่หลอดไฟแบบเดิมเพราะมีข้อดี อาทิเช่น ให้แสงสว่างที่มากกว่า อายุการใช้งานที่ยาวนาน ประหยัดไฟมากกว่า สามารถนำไปใช้ในระบบการสื่อสารข้อมูล เป็นต้น ดังนั้นงานวิจัยฉบับนี้ได้ศึกษาการสื่อสารไร้สายด้วยแสงที่มองเห็นภายนอกอาคาร (Outdoor Wireless Visible Light Communication, OWVLC) เพื่อประยุกต์ใช้งานระหว่างโครงสร้างพื้นฐานกับยานพาหนะ (I2V) โดยใช้เทคนิคแบบไมโม (Multiple-Input Multiple-Output, MIMO)

ออกแบบวงจรภาครับสำหรับช่องสัญญาณที่มีการเปลี่ยนตามการเคลื่อนที่ของยานพาหนะ เพื่อให้สามารถถอดรหัสสัญญาณกลับคืนได้อย่างถูกต้อง แสดงสมรรถนะของระบบด้วยการจำลองผลด้วยโปรแกรมการประมวลผลสัญญาณทางไฟฟ้าแสดงให้เห็นว่าระบบที่ได้ออกแบบสามารถส่งข้อมูลได้มากกว่าระบบเดิม ระบบการสื่อสารในงานวิจัยนี้มีข้อจำกัดคือ ระบบทำงานเฉพาะช่วงเวลากลางคืน หรือตามปกติที่ไฟส่องสว่างบนถนนทำงานแบบอัตโนมัติ แสงประดิษฐ์และแสงแวดล้อมเป็นอุปสรรคสำคัญของการสื่อสารด้วยแสงที่มองเห็นภายนอกอาคารนี้

สาขาวิชา วิศวกรรมโทรคมนาคม ลายมือชื่อนักศึกษา ....

ปีการศึกษา 2566 ลายมือชื่ออาจารย์ที่ปรึกษา ....

ADISORN KAEWPUKDEE : OUTDOOR WIRELESS VISIBLE LIGHT COMMUNICATIONS FOR INFRASTRUCTURE TO VEHICLE APPLICATIONS USING MIMO TECHNIQUE. THESIS ADVISOR : ASSOC. PROF. PEERAPONG UTHANSAKUL, Ph.D., 145 PP.

Keyword: VISIBLE LIGHT COMMUNICATION/MIMO/INFRASTRUCTURE TO VEHICLE/ CHANNEL IMPULSE RESPONSE/SMART STREET LIGHT

Nowadays, the statistics of deaths and person's injuries are mainly caused by accidents in which the main accident occurs from road traffic. Therefore, the Intelligent Transportation System (ITS) has introduced to manage road traffic, prevent accidents, reduce the number of fatalities and injuries. It also helps to reduce the traffic congestion, energy consumption and carbon dioxide emissions, which has been the main global warming issues. Furthermore, the modern vehicle has an intelligence such as autonomous driving, ability to prevent the collisions and adaptive control speed, etc. The ITS requires a detection system and a data communication network. A radio frequency (RF) system for ITS communication network such as Dedicated Short-Range Communication (DSRC) has the following three communication schemes, i.e. Vehicle-to-Vehicle (V2V) and Vehicle-to-Infrastructure (V2I) and infrastructure-to-vehicle (I2V). In addition, Cellular-Vehicle to Everything (C-V2X) has been tested the platform to ITS, C-V2X will cooperate with DSRC where the cellular network uses 5G and 6G technologies. However, RF spectrum has the congestion and high licensed cost, then researcher is looking for alternative spectrum as the optical spectrum to be used for ITS.

ITS has applied Visible Light Communication (VLC) technology as an alternative for V2V, I2V and V2I communication systems. VLC based-on White LED has free license and low cost. There are two main devices; Photo Diode (PD) and Light Emitting Diode (LED). LED is provided more luminance while the cost is reduced. In future, LEDs will replace all kinds of the traditional bulbs because they have more advantages such as providing more luminance, long lifetime, low consumption, cooler operation and usage in the data communication system etc.

In this thesis, researcher studies the possibility of I2V communication system to support ITS by designing a new configuration of I2V system, based on VLC system. Both Single-Input Single-Output (SISO) and Multiple-Input Multiple-Output (MIMO) techniques are used for Outdoor Wireless Visible Light Communication, Infrastructure to Vehicle (OWVLC-I2V) system. The street lamp, which has an array of LEDs, transmits the traffic information from Road Side Unit (RSU) to the vehicles on the road at nighttime. Depending on the setting, the photodetector can be placed either on the car's dashboard or on the rooftop, serving as a receiver. This thesis illustrates the channel impulse response that changes with respect to the movement of vehicle and shows the relationship between throughput and vehicle speed for SISO and MIMO systems.

School of Telecommunication Engineering Student's Signature ....

Academic Year 2023 Advisor's Signature ....

ACKNOWLEDGEMENT

I would like to sincerely thank Assoc. Prof. Dr. Peerapong Uthansakul, my thesis advisor, for his unwavering support and encouragement during this project. I am immensely thankful to him for his valuable guidance and instruction regarding research methodology as well as many other difficult life experiences. Without all of the encouragement I have always gotten from him, I could not have accomplished this much, nor could I have finished my thesis.

Furthermore, I express my gratitude to the entire staff of the Department of Telecommunication Engineering as well as other individuals for their recommendations and assistance. I express my gratitude to the Ministry of Higher Education, Science, and Research Innovation of Thailand for funding my Ph.D. studies at Suranaree University of Technology (SUT) and to Nakhon Pathom Rajabhat University (NPRU), my affiliated institution, for enabling me to pursue this academic endeavor.

Finally, I want to convey my heartfelt thanks to my spouse, my child, my parents, and my friends for their unwavering support throughout this research endeavor.

Adisorn Kaewpukdee

TABLE OF CONTENTS

TABLE OF CONTENTS (Continued)

TABLE OF CONTENTS (Continued)

TABLE OF CONTENTS (Continued)

LIST OF TABLES

Table Page

LIST OF FIGURES

Figure | Page

LIST OF FIGURES (Continued)

LIST OF FIGURES (Continued)

Figure Page

LIST OF FIGURES (Continued)

LIST OF FIGURES (Continued)

Figure **Page**

LIST OF ABBREVIATIONS

VLC	=	Visible Light Communication
C-V2X	=	Cellular-Vehicle to Everything
C-ITS	=	Cooperative Intelligent Transportation System
RF	=	Radio Frequency
DSRC	=	Dedicated Short-Range Communication
V2I	=	Vehicle-to-Infrastructure
LOS	=	Line of Sight
I2V	=	Infrastructure-to-Vehicle
V2V	=	Vehicle –to-Vehicle
NLOS	=	Non-Line of Sight
LED	=	Light Emitting Diode
SNR	=	Signal to Noise Ratio
WAVE	=	Wireless Access in Vehicular Environments
FOV	=	Field of View
ITS	=	Intelligent Transportation System
PD	=	Photodetector
BER	=	Bit Error Rate
SINR	=	Signal Interference to Noise Ratio
VANETs	=	Vehicle Ad-hoc Networks
RSU	=	Road-side Units
ISNR	=	Interference Signal to Noise Ratio
OBU	=	On-Board Units
IWVLC	=	Indoor Wireless Visible Light Communication
5G	=	Fifth Generation
LTE	=	Long-Term Evolution
OWVLC	=	Outdoor Wireless Visible Light Communication

LIST OF ABBREVIATIONS (Continued)

OWC	=	Optical Wireless Communication
WHO	=	World Health Organization
OOK	=	On-Off-Keying
OW	=	Optical Wireless
FSO	=	Free-Space Optical
CO2	=	Carbon Dioxide
IT	=	Information Technology
C-ITS	=	Cooperative-Intelligent Transportation Systems
SSL	=	Solid-State Lighting
InGaN	=	Indium Gallium Nitride
LPF	=	Low-pass filter
V2X	=	Vehicle to Everything
IM/DD	=	Intensity Modulation/Direct Detection

CHAPTER I

INTRODUCTION

1.1 Background and problem statement

The requirements of answers to traffic issues like collisions, traffic jams, greenhouse gases emission (CO_2), and pollution (P.M. 2.5) are increasing daily. Because there hasn't been enough investment in road construction to meet the rising demand from registered drivers, traffic on highways, urban streets, and conventional roads is getting worse every year and used vehicles in general. Traffic congestion not only inconveniences users but also leads to significant economic losses. World Health Organization (WHO) in December 2018 has announced the quantity road traffic deaths of 1.35 million. This was the 8th leading cause of death in the world (as shown in Figure 1.1). Road traffic injuries is now the leading killer of people aged 5 to 29 years (*Global Status Report on Road Safety 2018*, 2018). The responsibility is disproportionately borne by pedestrians, cyclists, and motorcyclists, in particular those living in developing countries. WHO predicts that road traffic injuries will rise to become the fifth leading cause of death by 2030. Intelligent Transportation Systems (ITS) ("Intelligent Transportation System," 2021) has garnered considerable attention for addressing traffic issues. ITS integrates persons, roads, and cars with advanced Information Technology. (IT), novel information systems have been developed to address road transportation issues. The objective is to optimize traffic flow and minimize the environmental impact. Numerous projects worldwide are now being researched and implemented in the field of Intelligent Transportation Systems (ITS), including the PREvent project. ("Communications Access for Land Mobiles," 2020), and CALM (*CAR 2 CAR Communication Consortium*, 2020) to reduce road fatalities. VIDAS (Kumar et al., 2008, 2009) Visible Light Communication for Advanced Driver Assistance Systems (VLC-ADAS) is a project that was established under a certain framework.

As seen in Figure 1.2, the idea of vehicular collaboration—that is, sharing information with other vehicles or roadside units—is crucial for a variety of ITS applications. The information-sharing concept known as Cooperative Intelligent Transportation Systems (C-ITS) uses technologies to minimize the impact of transportation on the environment, ease traffic congestion, and most importantly, drastically lower the number of traffic accidents. For any C-ITS application, ensuring dependable vehicle communications that meet safety standards has always been of utmost importance. Numerous academics study the radio frequency (RF) and visible light communication (VLC) systems used in intelligent transportation systems (ITS).

Figure 1.1 Report of road traffic injuries in 2018 by WHO (*Global Status Report on Road Safety 2018*, 2018).

Vehicle to Everything (V2x) communication allows cars to communicate with the infrastructure and with one another to share data, which enhances traffic safety and increases transportation system efficiency. Based on IEEE 802.11p, Direct Short-Range Communication (DSRC) has been the focus of much standardization, product development, and field testing by all parties involved, demonstrating its utility for V2x. In contrast to cellular technology, DSRC tackles the most difficult V2x use-cases and is currently prepared for V2x deployment. It's incredibly alluring to think about cars cooperating and exchanging data to make transportation safer, more environmentally friendly, and more fun. Together, these technologies—collectively referred to as C-ITS—promise to diminish the negative effects of transportation on the environment, relieve traffic congestion, and drastically lower the frequency of fatal traffic accidents. Wireless communication, which includes infrastructure-to-vehicle (I2V), infrastructure-to-vehicle (V2V), and vehicle-to-vehicle (V2I) communication, is a crucial enabling technology of C-ITS (as indicated in Figure 1.2). These wireless transactions are collectively referred to as V2x communication. The RF communication system is the foundation for them.

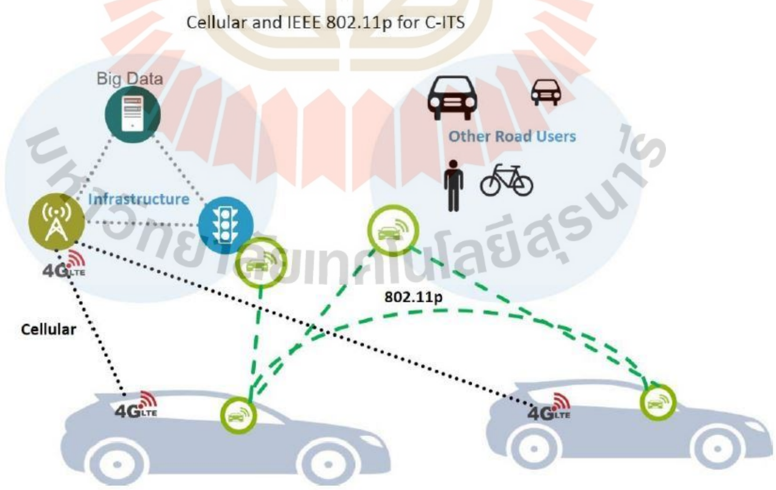

Figure 1.2 Comparison between IEEE 802.11p (DSRC) and cellular (C-V2x) connectivity to the vehicle (*Why 802.11p Beats LTE and 5G for V2x*, 2016).

VLC technology is promising to be a part of wireless communication technology in the next future for 6G networks (Căilean & Dimian, 2017), It serves as a substitute for the current wireless radio frequency (RF) communications system. When it comes to data transport, VLC uses a wavelength range of 380–780 nm, which provides 1000 times more bandwidth than RF communications. Furthermore, Because VLC is not regulated, the cost of the technology is greatly decreased. The vast amount of available spectrum enables VLC to achieve extremely high data speeds, which may now reach tens of gigabits per second (Chun et al., 2016; Hussein et al., 2015). Indoor VLC shows the achievement data rate within a span of fewer than ten years from its establishment, it is obvious that VLC's potential in terms of data transmission speed and network stability is substantially greater. Transmission higher data rates could be achieved by using Multiple Input Multiple Output (MIMO) communication techniques. These characteristics offer VLC to be a part of future 6G technologies (Ayyash et al., 2016; Strinati et al., 2019). VLC and RF technologies are also compatible for wireless communication system, the both can complement each other, creating hybrid or various networks and improve communication performances (Li et al., 2015).

Figure 1.3 Modeling of ITS infrastructure.

The ITS is used to decrease the quantity of collisions and related casualties. Moreover, the ITS goals to enhance the effectiveness of the transport scheme and therefore, to make the traffic safety more, to reduce the CO_2 emission and to reduce the P.M. 2.5 that make the environment better. Intelligent Transportation Systems (ITS) utilize I2V/V2I and V2V communications to gather traffic data, which is subsequently analyzed and disseminated to enhance vehicle awareness. Moreover, this data facilitates the effective administration of the transport scheme, enhancing productivity and alleviating traffic congestion. The aggregate information is utilized to autonomously adapt the transport scheme to varying travel routes. Hence, a significant component of ITS is the extensive dissemination. However, for ITS to be effective, the system necessitates a widespread communication network that encompasses intelligent vehicles and intelligent infrastructures. This network facilitates the collection of extensive traffic data and its efficient distribution. One significant obstacle for the ITS is to minimize the installation cost while ensuring the reliability of the I2V system remains unaffected. The advantages of enabling ITS are the management and efficiency monitoring of the traffic system and can help reduce the traffic jams and provide optimized alternative routes. The advantages of incorporating intelligence into the transportation system lie in the effective surveillance and control of traffic, which are contingent upon the prevailing traffic conditions. Furthermore, enhancing the efficacy of the ITS will contribute to time and cost savings, as well as a reduction in CO2 emissions.

This thesis has investigated and designed an OWVLC system for infrastructure to vehicle application using MIMO technique. This study will support the ITS for the road safety applications. The transmitter is LED array as streetlight installed on the road. We designed the LED array to illuminate the lighting for the road at night. The I2V communication is based on VLC technology, we used MIMO technique for increasing the data rate and more efficacy of the I2V system. Our receiver is installed on/in the car's dashboard. The vehicle moves through the lighting areas and then the channel response is studied for simulating the received signal. The results are shown the performance VLC-I2V system such as the power distribution, the channel response, the signal to noise ratio, the data rate based 10^{-4} BER.

1.2 Thesis objectives

1.2.1 To investigate the signal impulse response of the pathway OWVLC scheme for I2V applications, both SISO and MIMO techniques, especially at nighttime.

1.2.2 To design the transceiver schemes of OWVLC scheme for I2V applications based on the simulation.

1.2.3 To investigate the performance of an OWVLC system for I2V applications by designing and comparing differences in scenarios.

1.3 Scope and limitation of the thesis

1.3.1 The limitation of the OWVLC-I2V scheme is in the daytime caused by the ambient sunlight, and the streetlight is probably turned on at night or when it has to rain, gloomy and cloudy.

1.3.2 The OWVLC-I2V system is a single communication from a streetlight to the vehicle. It is used for broadcasting traffic information to vehicles and cooperates with RSU.

1.4 Contributions

1.4.1 This thesis has shown a new concept of the OWVLC system for I2V applications. Moreover, we have illustrated the modeling of the OWVLC scheme for I2V and then investigated the pathway of the OWVLC scheme for I2V's signal impulse response when the vehicle is driving.

1.4.2 We introduced communication solutions for the I2V system using the OWVLC scheme. Within the SISO and MIMO methodologies, the framework has the capability to establish the correlation between the speed of the vehicle and the throughput.

1.4.3 We have demonstrated the receiver create of the OWVLC scheme for the I2V system that performs the bit error rate (BER) of the process for both SISO and MIMO techniques.

1.5 Organization of the thesis

The thesis comprises five distinct segments. The following sections provide a concise outline of the subsequent chapters. Chapter 2 presents the VLC framework theory and provides a comprehensive review of the pertinent literature on I2V communications employing VLC. This includes an examination of VLC technology spanning from its origins to the current state, as well as an exploration of relevant theories crucial for understanding. Additionally, the chapter delves into the application of digital modulation theory in the context of wireless optical communications. In Chapter 3, the OWVLC (Optical Wireless Visible Light Communication) system for I2V communication is outlined, employing Single-Input Single-Output (SISO) techniques. The chapter provides insights into the system configuration and channel response when the vehicle is in motion. Furthermore, it involves the simulation of visible light wireless communication in the context of I2V communication within an ITS. The chapter also details the simulations conducted to experiment with data transmission. In Chapter 4, optical wireless communication employing Multiple-Input Multiple-Output (MIMO) techniques is introduced with the aim of enhancing throughput. The chapter includes experiments conducted through numerical simulations to validate these enhancements. In addition, the chapter thoroughly describes the receiver circuit used in optical wireless communication employing MIMO techniques. Chapter 5 showcases the experimental findings and thoroughly examines the proposed approach. The outcomes stem from numerical simulations of data transmission, encompassing both SISO and MIMO communication within ITS. Chapter 6 outlines the forthcoming research directions. The discussion covers various aspects that require further exploration, including scenarios like external light disturbances and challenges associated with daytime communication, such as light path obstructions.

CHAPTER II

BACKGROUND THEORY

2.1 Background

In 1880, Alexander Graham Bell demonstrated sound transmission through light using a vibrating mirror. Bell's photophone shields the sound passing through the instrument to the glass. Sound vibrations produce mirror-like vibrations. The glass receives sunlight from the bell, which records the mirror's vibrations and reflects them onto the receiving mirror. After the projection, the signal will switch back to audio. Similar to a phone, a photophone functions. Except that the photophone projects information using light. Even if the phone uses electricity, although the distance of communication by photophone over hundreds of meters was illustrated, in practice, the limitation of technology was the interferences from outside. Meanwhile, the original signaling system with flashing lights, based on Morse code used for messaging between ships.

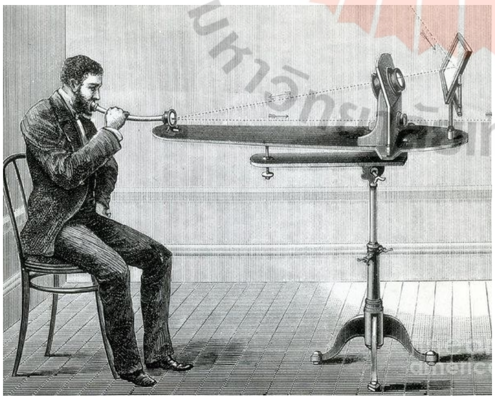

(a) Transmitter.

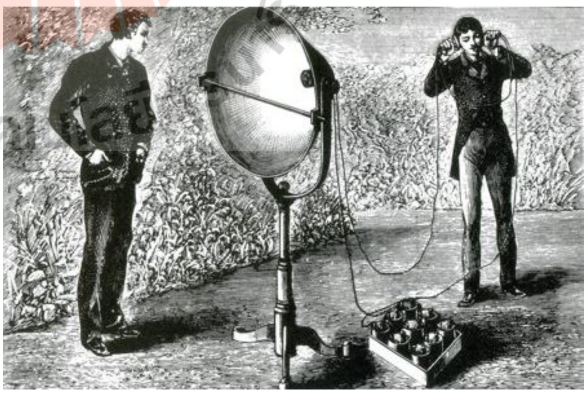

(b) Receiver.

Figure 2.1 Photophone, first of light communication (Bell, 1881).

In the 1990's (Komine, 2005), LED (Light Emitting Diodes) technology was developed and studied for various purposes. Indium gallium nitride (InGaN) is based on blue and green LED with YAG phosphor that can produce the white LED to create white light. It will be significant for lighting technologies in the future (Komine, 2005). White LEDs have a ton of benefits over conventional bulbs like incandescent and fluorescent lighting, for instance: reduced electricity usage, cooler operation, longer lifespan, a smaller dimensions, and lower voltage etc. The development of LEDs has impacted three key focal areas. The first category includes uses in motor vehicles and devices for traffic regulation, such as headlights, taillights, traffic lights, and other types of lighting. The second is community message boards like billboards, LED signs, etc. that can disseminate news and additional information. The third is seen in common lighting fixtures like architectural lights. There is a hospital fire Interior illumination for automobiles and aircraft flashlights, emergency and exit lighting, etc.

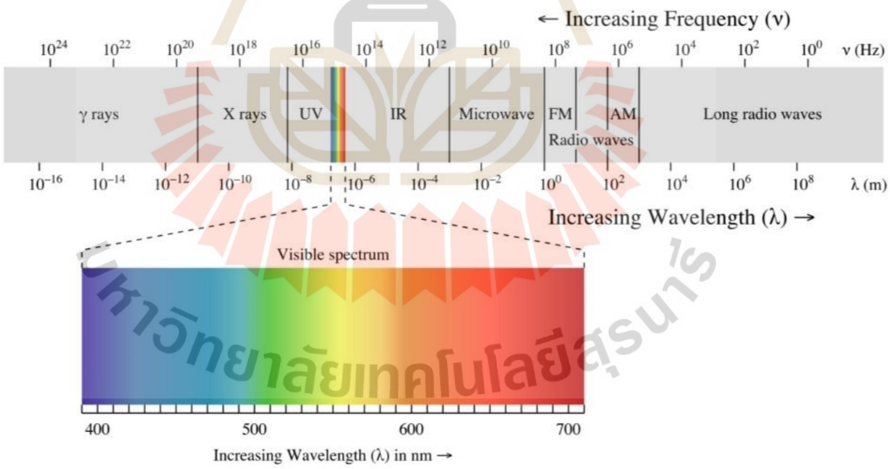

Figure 2.2 A visible light spectrum.

Visible Light Communication (VLC) began in 2004 at Keio University's Nakagawa Laboratory in Japan (Komine, 2005; Komine & Nakagawa, 2004), followed by top-notch research and development. Their research involved indoor wireless visible light communication (IWVLC), and to establish the lighting source, a typical modelling room was built with four LED array lamps put on the ceiling. Based on numerical analyses, they looked at how interference and reflection affected the next-generation of VLC indoor system. The electromagnetic spectrum is depicted in Figure 2.2, with the visible light spectrum's wavelengths falling between 780 and 380 nm. Visible light is just a tiny component of the electromagnetic radiation spectrum. Electromagnetic waves having shorter wavelengths and higher frequencies include UV, X, and gamma rays. Infrared light, microwaves, radio waves, and television waves are examples of electromagnetic waves with longer wavelengths and lower frequency.

2.2 Optical wireless communication system

The OWC system operates in the visible light wavelength range of 390 -750 nm. This wavelength range is called Visible light communication (VLC). LED bulbs can produce light through the VLC system, additionally referred to as light-emitting diodes (LEDs). Extremely fast impulses can activate LED devices without degrading the light intensity or harming the human eye. The VLC system is applied in a variety of areas, including wireless local area networks (WLAN), wireless personal area networks and vehicle networks, etc.. (“Optical Wireless Communications,” 2021). The ground-based point-to-point OWC system, often referred to as free space optics (FSO) systems (Khalighi & Uysal, 2014), operates at frequencies close to the infrared (750–1600 nm). These systems, which use laser transmitters, provide a workable remedy for backhaul constraints and transparent protocol connectivity at significant data rates, such as 10 Gbit/s per wavelength. Due to recent developments in solid state optical sources and detectors that operate in the solar-blind UV spectrum (200-280 nm), there has also been an increase in interest in ultraviolet communication (UVC). At ground level, the sun's light is insignificant in this so-called deep UV band. This enables the development of a photon counting detector with a wide field of vision receiver that boosts received energy while introducing little additional background noise.

Table 2.1 History of optical wireless communication system (Ghassemlooy et al., 2019).

Date	Systems/Devices/Standards
800 BC	Fire beacons —by the ancient Greeks and Romans
150 BC	Smoke signals —by the American Indians
1790	Optical telegraph —by Claude Chappe, France
1880	Photophone—by Alexander Graham Bell, USA
1960	Laser
1970	FSO mainly used in secure military applications
1979	Indoor OWM systems—F. R. Gfeller and G. Bapst
1993	Open standard for IR data communications—The Infrared Data Association (IrDA)
2003	The Visible Light Communications Consortium (VLCC)–Japan
2008	Global standards for home networking (infrared and VLC technologies)—Home Gigabit Access (OMEGA) Project—EU
2009	IEEE802.15.7—Standard on VLC
2017	The IEEE 802.15.13 – standard on was introduced to offer data rates reaching 10 Gbps, covering distances of approximately 200 meters. (Khalighi & Uysal, 2014).
2018	The IEEE has introduced a fresh task group dedicated to establishing a global standard in wireless local area networks through visible light communication. This standard, designated as IEEE 802.11bb, aims to collaborate with manufacturers, operators, and end users in the development of the system. (Khalighi & Uysal, 2014).
2019	Designed a packet-based VLC protocol based on the IEEE 802.11ac frame structure, which can be utilized for the simulation, analysis, and testing of a wireless VLC communication system (Zeshan & Baykas, 2019).

This design is very suitable for a "concrete" outdoor setup. Non-line-of-sight to accommodate short-range low-power UVCs such as wireless sensors and ad hoc networks. Table 2.1 depicts the development of optical wireless communications from 800 BC to the present (Ghassemlooy et al., 2019).

In the deployment of OWC in the communications landscape, Table 2.2 compares radio frequency (RF) and optical wireless (OW) communication systems. Figure 2.2 provides a summary of the system coverage and data rates offered in traditional RF and OWC systems. OWC systems can deliver data rates in excess of 10 Gbps. (Khalighi & Uysal, 2014). However, the OW system's implementation is fraught with difficulties. Fog, rain, and dust, for example, limit the data rate and outside coverage of free space optics (FSO).

Table 2.2 Comparison of RF and OW system (Khalighi & Uysal, 2014).

Property	**OW System**	**RF System**
Transmitted Power	Restricted (Eye safety and interference)	Restricted (Interference)
Noise Sources	Sun light and Ambient Light	Other Users and Systems
Power consumption	Relatively low	Medium
Multipath Fading	No	Yes
RF Electromagnetic interference	No	Yes
Passes through walls	No	Yes
Technology Cost	Low	High
Beam Directionality	Medium	Low
Available bandwidth	Very high	Low
Bandwidth Regulated	No	Yes
Security	High	Low

2.3 Channel modeling

Understanding the channel characteristics is critical for designing, installing, and operating an efficient optical communication system. The channel impulse response determines the communication channel's properties, which are subsequently utilized to study and battle the impacts of channel distortion. Much work on channel characterization has been published. It includes experimental measurements and computer simulations of indoor and outdoor systems. Two types of power are directly tied to the channel: Investigating optical path loss and multipath dispersion involves analyzing two distinct types of optical wireless channels. The reflection is ignored in direct LOS and tracked settings. To determine path loss, one needs to consider the variance in the transmitter beam, the dimensions of the receiver, and the distance of separation. On the other hand, a non-LOS arrangement, also known as a light distribution system (often utilized in indoor contexts), takes advantage of reflections off room surfaces and furnishings. Path loss predictions could be made more difficult by these reflections, are considered undesired signals or distortions caused by multipath interference. Additionally, the article discusses how artificial light interference can influence the link's operational efficiency. The diverse and dynamic surroundings of the atmosphere's outside channels can change the properties of a beam. This causes turbulence-induced amplitude and phase variations as well as light loss. There have been a few models presented to explain the statistical makeup of the atmospheric cavity. Additionally, a practical test stand is available for keeping track of the measured data as well as how the atmosphere affects the free space optical interface.

2.4 Indoor optical wireless communication channel

The topologies used by VLC for indoor applications vary widely, and they are distinguished by (1) how the receiver and transmitter are oriented. and (2) Whether a LOS path exists between the emitter and receiver. Intensity modulation with direct detection (IM/DD) is a workable technique for optical wireless applications due to its low cost and minimal complexity. The modulated signal directly modifies the drive current that is being driven by the optical source $m(t)$, the modulated signal directly modifies the drive current of the optical source $x(t)$ (see Figure 2.3). An electric current $y(t)$ is produced by the instrument's photodetector, which combines tens of thousands of incident light signals with very short wavelengths. This luminous current is directly inversely proportional to the square of the received electric field or the instantaneous power of light. In IM/DD-based optical wireless systems, the high-frequency properties of the optical carrier are concealed by an equivalent baseband model. Figure 2.4 depicts the model in the discussion, where $x(t)$ is the lighting signal in free-space, $h(t)$ is the baseband channel impulse response, R is the photodetector responsivity, $y(t)$ is received signal output from the photodetector, and $n(t)$ is the signal-independent shot noise , as the additive white Gaussian noise (AWGN) with a double-sided power spectral density (PSD) of $N_0/2$.

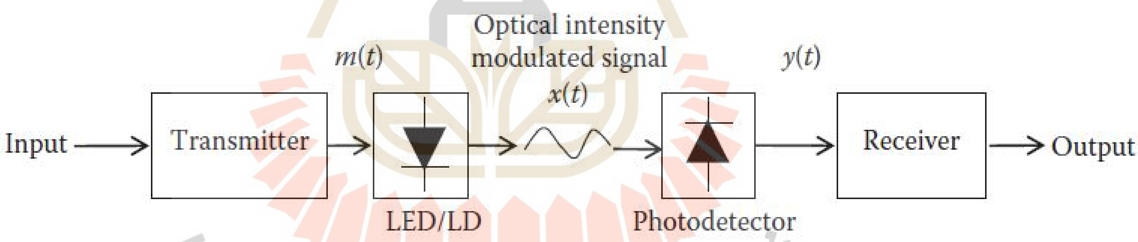

Figure 2.3 Block diagram of an optical intensity, direct detection communications channel.

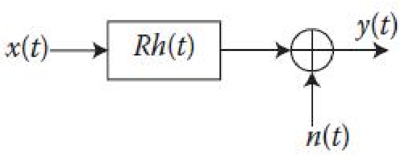

Figure 2.4 An optical wireless system using IM/DD.

Non-LOS communications experience multi-path propagation effects in a similar fashion to RF systems, although these impacts are stronger, particularly in indoor applications. The performance of these links can be significantly impacted by multi-path, as will be covered in later chapters. The electric field that is impacted by strong amplitude at wavelengths fades due to multipath propagation. If detector size is proportional to one wavelength or less, detectors experience fading from numerous directions. Thankfully, OWC receivers employ sensor with an exposed area of several million square meters or more. Additionally, the determination is based on the integration of optical energy across the complete surface of the photodetector and how much photocurrent is generated overall, as demonstrated in Figure 2.5, this offers an intrinsic spatial diversity (Ghassemlooy et al., 2019).

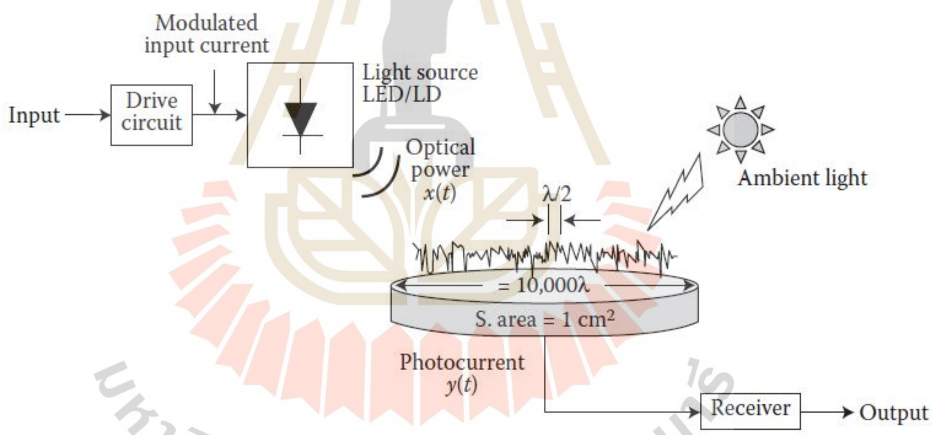

Figure 2.5 Baseband representation of an optical wireless system employing IM/DD.

Although multi-path fading does not impair indoor OWC networks, the dispersion effect is evident in symbolic inter-interference (ISI). A signal representing the distribution's linear baseband channel response was modeled as $h(t)$. The OWC link's channel parameters are fixed for a certain transmitter, receiver, and intervening reflective object position. When there is a shift in these communication components of a few millimeters or less, the channel characteristics change. The room's relatively modest movement of objects and people, combined with the high bit rate. The channels are considered static because their only variation is in the length of numerous bit intervals.

The following equations below serve as a summary of the baseband representation of an optical wireless system employing IM/DD

$$\begin{aligned} y(t) &= Rx(t)\otimes h(t)+n(t) \\ &= \int_{-\infty}^{\infty} Rx(\tau)h(t-\tau)\,dt+n(t) \end{aligned} \tag{2.1}$$

where the symbol $\otimes$ denotes the convolution.

The response of the system to an impulse signal $h(t)$, it is possible to examine or simulate the impacts of multi-path dispersion in internal optical wireless communication channels utilizing impulse signals. Modeling of the channel impulse response (F. R. Gfeller & Bapst, 1979)

$$h(t)=f(x)=\begin{cases} \dfrac{2t_0}{t^3\sin^2(FOV)}, & t_0\le t\le \dfrac{t_0}{\cos(FOV)} \\ 0, & elsewhere \end{cases} \tag{2.2}$$

where t_0 is the minimum delay.

Unlike traditional electric or radio systems, optical wireless communications systems are a linear filter channel with AWGN (Equation 2.1). This is due to the immediate optical power's relationship to the electric current that is generated. Power over amplitude is represented by $x(t)$. Transmission is subject to two restrictions as a result. To begin with, $x(t)$ must be non-negative, that is

$$x(t)\ge 0 \tag{2.3}$$

Furthermore, the maximum amount of light that can be used is constrained by eye safety regulations. The main restriction is often the average electricity demand of $x(t)$ must not go over a certain maximum power $P_{\max}$, that is

$$P_{\max}=\lim_{T\to\infty}\frac{1}{2T}\int_{-T}^{T}x(t)dt \tag{2.4}$$

This is opposite to the signal's time-averaged value $|x(t)|^2$, such is the case when the amplitude is represented by $x(t)$ for the standard RF channels.

These variations significantly impact the system design. A typical RF channel's signal-to-noise ratio (SNR) is inversely proportional to the average received power. The square of the average optical signal power received determines the optical wireless communication link.

$$SNR = \frac{R^2 H^2(0) P_r^2}{R_b N_0} \tag{2.5}$$

Where N_0 is the noise spectral density and $H(0)$ is the channel DC gain given by

$$H(0) = \int_{-\infty}^{\infty} h(t) dt \tag{2.6}$$

Systems for optical communication need a lot of optical transmission power, and they can only withstand a certain amount of route losses. However, the modulation strategy with a high peak-to-average power ratio is the most beneficial because the average output power is constrained. Essentially, power efficacy and bandwidth efficacy are being traded. The SNR and photodetection area are both inversely correlated in the presence of short noise, due to the short-term noise variability and the electric power received are proportional to A_d^2 and A_d , respectively, where A_d is the receiver detector area. The one-piece receiver is a vast area detector as a result. However, when the detecting area grows, the receiver's bandwidth-limiting capacity also grows. Contrasting sharply with this are the higher bandwidth needs connected with energy-efficient modulation methods. As a result, these two criteria are trade-offs.

The equation (2.7) below defines the optical wireless channel transfer function.

$$H_{OW}(f) = H_{los}(f) + H_{diff}(f) \tag{2.7}$$

Where H_{los} the LOS channel response effect known as HLOS is primarily independent of the modulation frequency. The distance between the transmitter and receiver will determine this and the receiver-transmitter's angle concerning the LOS, whereas H_{diff} the channel response brought on by light signal diffusion reflecting off the room wall.

In a direct link, it is possible to increase the power ratio between the diffusion link and the LOS in a direct link. This is measurable using equation (2.8), can be quantified by the Rician factor.

$$k_{rf} = \left(\frac{H_{los}}{H_{diff}}\right)^2 \tag{2.8}$$

Its definition is based on the electrical signal powers, same like in radio communications.

2.4.1 Line-of-sight propagation model

LEDs are typically used as light sources and photodetectors as large area photodetectors in indoor OWC systems. The following distribution of typical Lambertian radiation intensities was used to represent the angular distribution of the radiation intensity pattern (Lambert, 1760).

$$R_0(\phi) = \begin{cases} \frac{(m_1+1)}{2\pi}\cos^{m_1}(\phi), & for \phi \in (-\pi/2, \pi/2) \\ 0, & for \phi \geq \pi/2 \end{cases} \tag{2.9}$$

Where m_1 is the Lambert's mode number expressing directivity of the source beam, $\phi = 0$ is the angle of maximum radiated power. The order of Lambertian emission m_1 is related to the LED semi-angle at half power $\Phi_{1/2}$ by (Kahn & Barry, 1997)

$$m_1 = \frac{-\ln 2}{\ln(\cos \Phi_{1/2})} \tag{2.10}$$

The equation (2.11) determines the radiation intensity.

$$S(\phi) = P_t \frac{(m_1+1)}{2\pi}\cos^{m_1}(\phi) \tag{2.11}$$

When light is incident on the detector at ψ angles, it is collected as though it were an active area of A_r that is smaller than the detector FOV. Equation (2.12) was used to calculate the detector's effective collection area.

$$A_{eff}(\psi) = \begin{cases} A_r \cos(\psi), & 0 \le \psi \le \pi/2 \\ 0, & \psi > \pi/2 \end{cases} \tag{2.12}$$

For indoor OWCs, large area detectors work best to capture as much energy as feasible. However, in fact, it leads to a number of issues, such as rising production costs, expanding channel capacity, reducing receiver bandwidth, and increasing receiver signal noise. As a result, using non-imaging probes provides an affordable way to expand the total effective collection area. Equation (2.13) determines the optical gain of a perfect non-imaging probe with an intrinsic refractive index of n (Kahn & Barry, 1997).

$$g(\psi) = \begin{cases} \dfrac{n^2}{\sin^2(\Psi_c)} & , 0 \le \psi \le \Psi_c \\ 0 & , \psi > \Psi_c \end{cases} \tag{2.13}$$

where $\Psi_c \le \pi/2$ is the FOV.

The FOV of the receiver system is found to be related to the optical detection area and the collecting area of the A_{coll} lens by the radiation constant theorem (O'Brien et al., 2005).

$$A_{coll} \sin\left(\Psi_c/2\right) \le A_r \tag{2.14}$$

Naturally from equation (2.14), as the FOV declines, the photoreceptor gain increases.

For indoor OWC, the link length is fairly modest and as a result, relatively little attenuation is caused by absorption and scattering. Taking into account the OWC association, a receiver equipped with an optical transmission bandpass filter $T_s(\psi)$ and a non-imaging concentrator of gain $g(\psi)$, the DC gain for a receiver positioned at a distance of d and angle ϕ regarding to transmitter (see Figure 2.6) may be estimated as (Ghassemlooy et al., 2019)

$$H_{los}(0)=\begin{cases}\dfrac{A_r(m_1+1)}{2\pi d^2}\cos^{m_1}(\phi)T_s(\psi)g(\psi)\cos(\psi) & ,0\le\psi\le\Psi_c\\ 0 & ,\text{elsewhere}\end{cases} \tag{2.15}$$

The received power therefore becomes (as shown in Figure 2.7)

$$P_{r-los}=H_{los}(0)P_t \tag{2.16}$$

Equation (2.17) can be utilized for determine the magnitude of the LOS signal in a LOS link when the transmitter and receiver are lined up.

$$H_{los}(m_1)=\frac{(m_1+1)}{2}H_{los} \tag{2.17}$$

where H_{los} refers to a Lambertian transmitter with $m_1=1$.

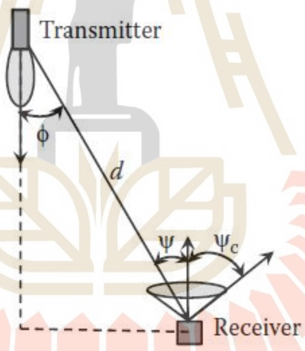

Figure 2.6 Geometry LOS propagation model (Ghassemlooy et al., 2019).

Multipath propagation is rarely an issue in short-range LOS communications, and LOS link channels are frequently described as linear attenuation and delay. Path loss for optical LOS lines is dependent on the square of the distance between transmitter and receiver and is regarded as non-frequency selective. Equation (2.18) describes how the impulse response signal can be expressed.

$$h_{los}(t)=\frac{A_r(m_1+1)}{2\pi d^2}\cos^{m_1}(\phi)T_s(\psi)g(\psi)\cos(\psi)\delta\left(t-\frac{d}{c}\right) \tag{2.18}$$

where c is the speed of the light in free space, $\delta(.)$ is the Dirac function and $\delta(t-d/c)$ represents the signal propagation delay. The expression assumes that $\phi < 90^o$ and $\psi < FOV$ and $d \gg \sqrt{A_r}$.

2.4.2 Non-LOS propagation model

Non-linear propagation from transmitter to receiver characterizes LOS. It is harder to forecast diffuse links with optical path loss. Due to the fact that there are numerous variables, like the room's size, the ceiling's reflection, the room's walls, and other furnishings, the transmitter and receiver's position and orientation, the size and placement of the windows, and other physical aspects of the space. Equation (2.19) is a general expression for the energy obtained.

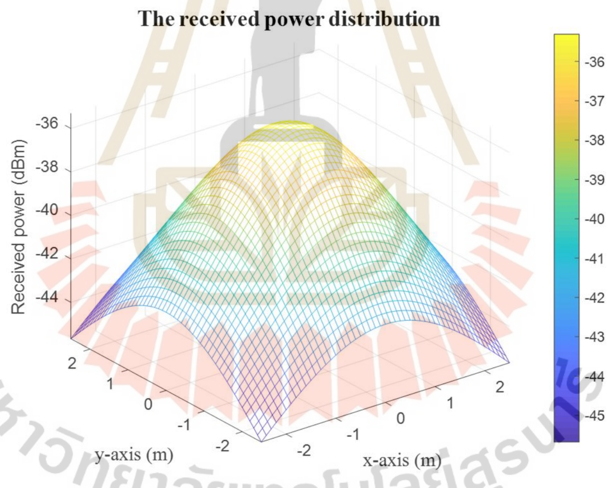

Figure 2.7 The received power distribution of the LOS link.

$$P_{r-nlos} = \left[H_{los}(0) + H_{nlos}(0)\right]P_t$$

$$= \left(H_{los}(0) + \sum_{reflections} H_{reflections}(0)\right)P_t \tag{2.19}$$

where $H_{reflections}$ represents the reflected path.

The wavelength of light passed through an object surface affects its ability to reflect light in a room such as wavelength of transmission, the surface material, and the angle of incidence θ_i and roughness of the surface relative to the wavelength. The Rayleigh criteria is largely used to determine the shape of the reflectance pattern and the texture of the surface (F. R. Gfeller & Bapst, 1979).

According to this standard, a surface is deemed to be flat if the greatest height of the surface's unevenness satisfies the requirements listed below.

$$h_{si} < \frac{\lambda}{8\sinh(\theta_i)} \tag{2.20}$$

To estimate path loss for diffuse and undirected non-LOS links, analyzing the optical power distribution in a certain environment is necessary. To precisely characterize indoor optical features, many efforts have been performed.

To calculate the impulse response effect of the optical wireless medium, all the component energies received after multipath propagation were added together. In the case of non-LOS links, the received signal comprises components traveling down several pathways. Depending on the proportions of the room's design, the length of the corridor for these elements varies. Therefore, the pulse signal must be amplified to be strong. The LOS component's channel gain, measured in decibels (dB), is distributed according to the gamma dispersion. Adding the channel in decibel (dB) for the LOS pathway, including total reflection, is a Rayliegh scatter pattern that considers the transmitter-to-receiver path. (Carruthers & Carroll, 2005). One parameter that is frequently used to measure the time-dispersion characteristics of multipath channels is the root mean square mean of spread delay D_{rms}. Defined as the square root of the center moment squared of the channel impulse response. which can be calculated using equation (2.21).

$$D_{rms} = \left[\frac{\int (t-\mu) h^2(t)\,dt}{\int h^2(t)\,dt} \right]^{1/2} \tag{2.21}$$

where μ is the mean delay spread, it can be calculated from equation (2.22).

$$\mu = \frac{\int th^2(t)\,dt}{\int h^2(t)\,dt} \tag{2.22}$$

The room's optical power distribution is adequate to determine the basic power consumption. Because multipoint reflection is not taken into consideration, the power modulation cannot be accurately predicted due to multipath propagation. Two or more reflections only entail a minimal amount of optical power. But compared to a single reflection, the signal travels to the receiver far more slowly. Therefore, it cannot be disregarded while thinking about distributed linkage and non-directional high-speed LOS. To create an impulse response that includes reflections of higher order. Barry et al. (Barry et al., 1993) designed a raytracing technique that calculates the attenuation and propagation delay experienced by a signal along a route that includes a certain number of reflections. After that, the algorithm totals up each contribution to produce the overall impulse response. The author imagines a rectangle room that is vacant. The photoreceptors are considered to face vertically upward, toward the ceiling. Taking into account the room's receiver (Rx), which is a single source. An infinite sum can be used to represent the impulse response. After that, the algorithm totals up each contribution to produce the overall impulse response. designed as a blank rectangular space with the assumption that the photoreceptors face vertically above of the room. The reaction of a system to an impulse signal can be expressed as an infinite sum when a single source receiver (Rx) and a chamber receiver are taken into account.

$$h_{nlos}(t,S,R_x) = \sum_{k=0}^{\infty} h_{nlos}^{(k)}(t,S,R_x) \tag{2.23}$$

where $h_{nlos}^{(k)}(t,S,R_x)$ is the Impulse response due to reflected light exactly k reflections.

For K multiple sources the previously mentioned equation can be changed to

$$h_{nlos}(t,S,R_x) = \sum_{i=0}^{K} \sum_{k=0}^{\infty} h_{nlosK}^{(k)}(t,S,R_x) \tag{2.24}$$

After k reflection the impulse response $h^{(k)}(t,S,R_x)$ can be assessed with the recursive technique described in (Barry et al., 1993).

$$h_{nlos}(t,S,R_x) = \frac{(m_1+1)}{2\pi}\sum_{j=1}^{K}\rho_j\cos(\phi_j)\frac{\cos(\psi)}{d_{Sj}^2}rect\left(\frac{2\psi}{\pi}\right) \times h_{nlos}^{(k-1)}\left(t-\frac{d_{Sj}}{c},S,R_x\right)\Delta A \tag{2.25}$$

where ΔA is area of the reflective element, K is The quantity of reflected surfaces in the space as a whole, ρ_j is the a reflection factor of j, d_{sj} is the distance from S to j, $h^{(k-1)}(t,S,R_x)$ is the impulse response of order $k-1$ between reflector j and R_x. Since $\left\|h^{(k)}(t,S,R_x)\right\| \to 0$, $k \to \infty$, it is possible to evaluate the channel impulse response by taking the first $\Re$. We can get a good approximation of the channel by using recursive algorithms or iterative approaches, and just taking 10 reflections into account.

The surface of the room is divided by $\Re$ the reflective component in order to first evaluate the diffuse reflectivity with an area of ΔA. Two elements can be used to describe the channel: (a) the first element is each element of the surface with an area of ΔA considered as a receiver and (b) The light-collected signal is then scaled by reflectivity and each component is thought of as a point source that reemits it ρ_j. Following are some approximations for the impulse response of a channel after a single reflection off the ceiling (see Figure 2.8).

$$h_{nlos}^1(t,S,R_x) = \sum_{j=1}^{\Re}\frac{(m_1+1)\rho_j A_r \Delta A}{2\pi d_{Sj}^2 d_{R_xj}^2}\cos(\phi_{sj})\times\cos(\psi_{sj})\cos(\psi_{Rj})\delta\left(t-\frac{d_{Sj}+d_{Rj}}{c}\right) \tag{2.26}$$

The orientation angles of the transmitter and receiver are expressed as azimuth and elevation angles using the values given in Table 2.3, where the transmitter is at the ceiling. Figure 2.9 depicts the impulse response of the first LOS connection and diffuse reflection. Distribution of propagation, average delay, RMS delay, D_{rms} Figure 2.10 depicts the maximum possible data rate diagram and the mean square value of the channel delay. In indoor optical wireless communications systems, the channel impulse response is position dependent and fluctuates with receiver movement. One of the most critical factors limiting data rate is the first reflection. The typical delay propagation for the system under study ranges between 10 and 16 ns. D_{rms} 0.3–0.6 ns corresponding. As a result, the highest possible data rate ranges from 180 to 360 Mbps. The achieved data rate is substantially reduced (as indicated in Figure 2.8).

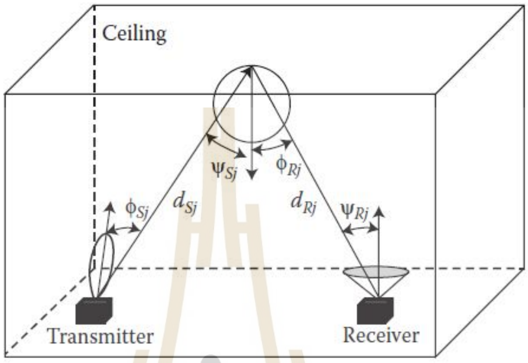

Figure 2.8 Geometry used to describe the single-refection propagation model (Ghassemlooy et al., 2019).

Table 2.3 Simulation Parameters (Ghassemlooy et al., 2019).

	Parameters	Values
Transmitter	Room size	5 x 5 x 3 m^3
	Location (x, y, z)	(2.5, 2.5, 3)
	Lambert's order	1
	Wall reflective index	0.8
	Elevation	-90°
	Power	1 W
	Azimuth	0°
Receiver	Location (x, y, z)	(1.5, 1.5, 0)
	Elevation	90°
	Half angle (FOV)	85°
	Active area (A_R)	1 cm^2
	Azimuth	0°
	Δ_t	0.5 ns

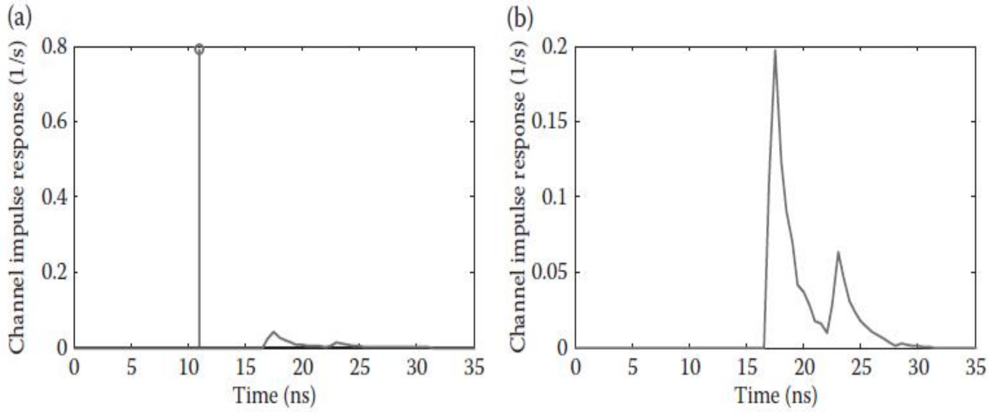

Figure 2.9 Impulse responses of the diffused links: (a) with a LOS path and (b) without LOS path (Ghassemlooy et al., 2019).

2.5 Visible light communication system

Visible light communication is a part of the optical communications system that the spectrum of visible light is between 430 and 790 THz (780 – 380 nm) (as shown in Figure 2.2). Normally, the ordinary lamps are the fluorescent and incandescent lamps. So, as we know LED stand for light emitting diode which creates from the semiconductor materials, LED lamps have been replace the traditional lamps because There are numerous advantages, such as long lifetime, low power consumption, smaller size, and so on. In comparison to standard incandescent (with a brightness efficacy of 52 lm/W) and fluorescent (with a brightness efficacy of 90 lm/W) lighting bulbs, (Al Naboulsi et al., 2004), White LEDs have a peak efficiency of more than 260 lm/W (far lower than the theoretically expected luminous effectiveness of up to 425 lm/W). (Bouchet et al., 2008). Furthermore, LED that uses for lighting and it can carrier the data at the same time. Because of these benefits, white LEDs are appropriate sources for the next generation lighting (both indoor and outdoor) that require both illumination and data transfers.

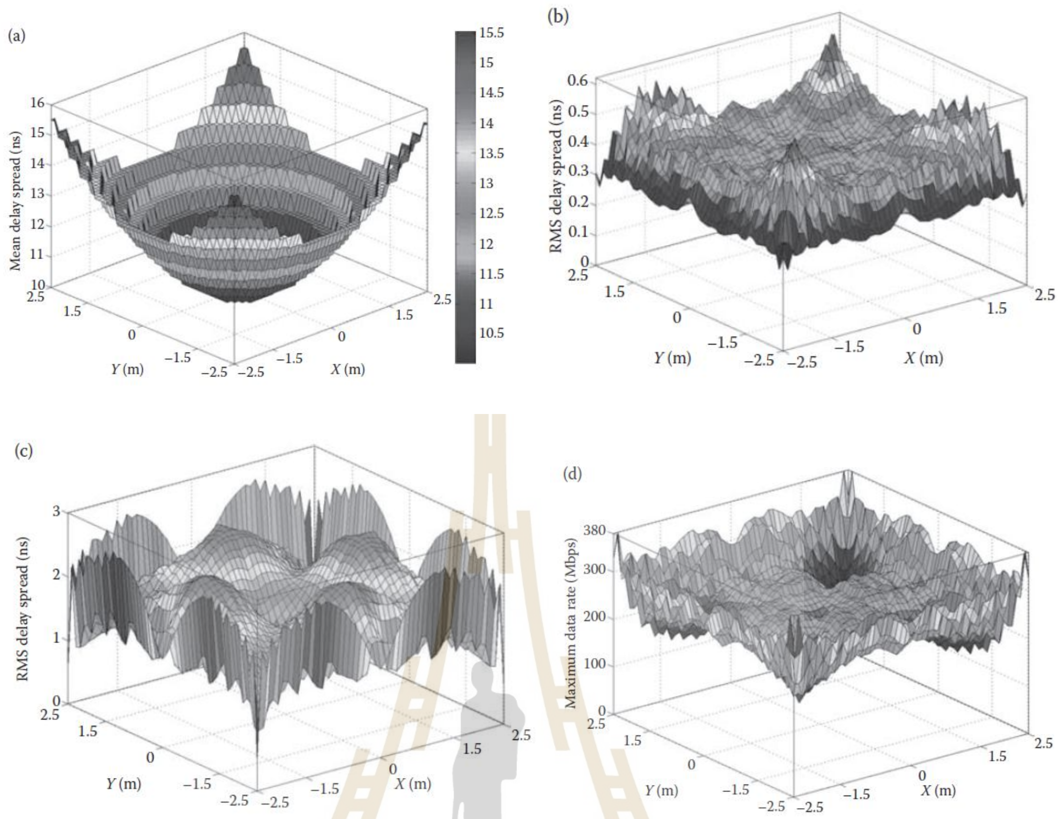

Figure 2.10 Channel delay spread: (a) mean delay spread, (b) RMS delay spread with LOS component, (c) RMS delay spread without LOS component and (d) maximum data rate distributions (Ghassemlooy et al., 2019).

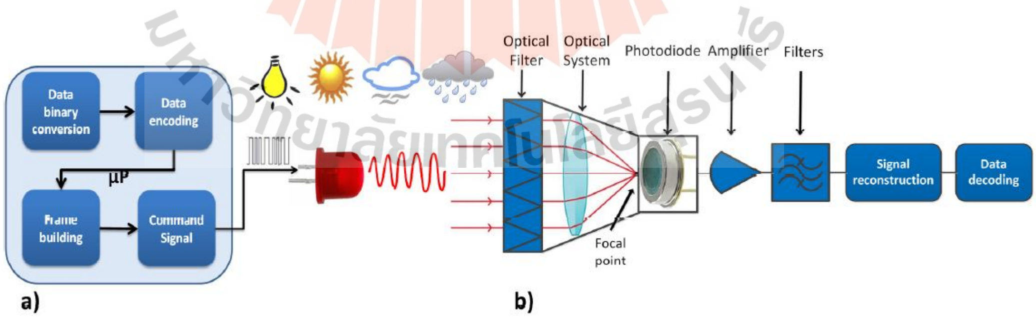

Figure 2.11 Basic architecture of a visible light communication system : a) transmitter, b) receiver. (Căilean & Dimian, 2017).

A VLC system comprises primarily of a transmitter that modulates the light emitted by the LED and a receiver based on a photosensitive element (often a positive-intrinsic-negative (PIN) photodiode or an image sensor) that extracts the information transmitted via the modulated light beam. Despite being physically separated, the transmitter and receiver exchange information through the VLC channel. Line-of-sight (LOS) is a requirement for VLC systems. Figure 2.11 is a diagram illustrating a VLC scheme. Because the structure of the VLC system is explained in (Căilean & Dimian, 2017), this part will just provide the necessary information to comprehensively grasp the remaining content of the paper, instead of covering all elements associated with the hardware advancement and execution of VLC schemes.

2.5.1 Transmitter

In VLC, the transmitter is light emitting diode (LED) as the diode to transfer data. The visible light spectrum can be used to transmit LED light through the free-space optical (FSO) medium. The VLC system's objective is to offer illumination while also transmitting data. However, data transfer must not interfere with illumination or signaling functions. As a result, the transmitter must employ the same optical power or, or, if needed, accommodate for light attenuation. Furthermore, there must be no visible flashing from the VLC transmitter. The encoder, which turns data into a modulated message, is the essential component of the VLC transmitter. Determining the appropriate data rate and using the binary data, the encoder controls the LED switching. The outcome is a modulated light beam that represents binary data. The most basic case is modulating the data employing OOK, but moreover advanced converting data methods may also be utilized. Other modulation techniques utilized in VLC applications are discussed in detail in (Khalighi & Uysal, 2014).

(a) Application of LED in transportation system. (b) LED lighting system in vehicles.

Figure 2.12 LED use to be the transmitter for VLC system application for ITS.

Transmitters for VLC systems are essentially constrained by the LEDs' properties. The data rate is determined by the LEDs' switch ability (i.e. transmission frequency). The luminous area of an LED lamp is determined by the power distribution and the luminous pattern (i.e. radiative angle). The solid-state lighting (SSL) manufacturing sector was able to produce LEDs with versatile functionality, featuring switching frequencies in the tens of megahertz, eventually maturing into a high switching rate of several Gb/s.

2.5.2 Receiver

The VLC receiver utilizes the photodetector to extract data from the modulated light beam. The photodetector transforms light into an electrical signal, while the receiver module demodulates and decodes it. Typically, VLC receivers use photosensitive components that have wide bandwidths and can transmit data at high rates. However, because of the presence of extraneous light from many sources (both artificial and natural), the receiver is vulnerable to significant interference. To enhance the performance of the VLC receiver, one may use an optical filter that effectively removes undesirable spectrum elements, including the infrared element. Furthermore, in applications requiring rapid utilizing white light, the optical filter selectively permits just a small range of blue radiation to transmit. This method is used because of the production of white light through the merging of blue LEDs and yellow phosphors. However, signal processing exclusively utilized the blue segment of the white light. (Căilean & Dimian, 2017).

(a) VLC Receiver photodetector based.

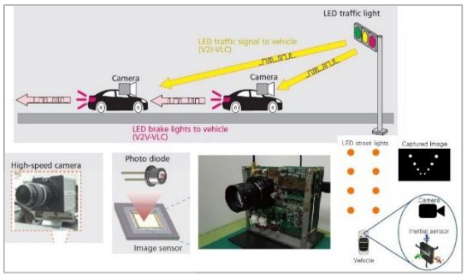

(b) VLC Receiver camera based.

Figure 2.13 Receiver devices for application in VLC system.

Given the large number of devices that already have cameras (e.g., laptops, tablets, smartphones, or autos), image sensors are employed in VLC technologies to receive light. As a comprehensive exploration of optical communications using image sensors, this article will just highlight certain significant image sensor reception properties. The image sensor is made up of numerous light sensors arranged in a grid pattern or integrated onto a circuit. Despite their widespread availability, such devices have significant downsides when it comes to VLC usage. The first issue is that their noise performance is poorer than those of separate photoelements. Nevertheless, the biggest restrictions stem from the camera's low frame rate (fps), which limits communication performance. Because the vast majority of inexpensive cameras are only capable of capturing up to fifty frames per second, it may be inferred that these kinds of devices can only achieve relatively limited bandwidth. Additionally, the data rate may be boosted to numerous kilobytes per second by employing the rolling shutter function of the photographic device (Roberts, 2013a, 2013b). Reading the pixels in the matrix row by row is accomplished by the use of the rolling shutter, as opposed to scanning the full matrix in a single pass. Therefore, the outcomes are only applicable to static applications and have a modest data flow. (Ji et al., 2014) presents an effort to build vehicle-level control (VLC) systems for automobiles by making use of inexpensive image sensors. However, since the communication distance is smaller than one meter, its applicability in automobiles is restricted.

2.6 Visible light communication for intelligent transportation system literature reviews

Both the number of cars using the transportation system and the number of persons killed each year are on the rise. (*Global Status Report on Road Safety 2018*, 2018). found that road accidents are among the leading causes of mortality. Also, the leading cause of mortality for people in this age group (between 15 and 29) is vehicular accidents. To make roads and vehicles safer, researchers, businesses, and government agencies are working together in this area. Finding ways to help individuals prevent accidents is the main focus of the study. Many think that transportation systems may be made more safer and more efficient with the use of wireless connections that allow for the real-time transfer of data between cars and traffic infrastructures. By combining communications between vehicles and infrastructures, this technology allows for seamless mobility. (A.-M. Cailean et al., 2014) found that VLC technology might greatly elevate the performance of automobile connections, particularly in densely populated areas, as it remains unaffected by the occurrence of broadcasting storm phenomena (Tonguz et al., 2006a, 2006b).

According to (Papadimitratos et al., 2009)), one way to lower accident and fatality rates is via the Intelligent Transportation System (ITS), which plans to include state-of-the-art collaborative technologies. There is an additional goal of ITS to reduce carbon dioxide emissions by making the transportation system more efficient. Intelligent transportation systems (ITS) benefit transportation networks by providing crucial traffic data in real-time. Through I2V/V2I and V2V communications, ITS constantly gathers, analyzes, and transmits traffic data to increase vehicle awareness.

In addition, the data helps with transportation system management, which improves efficiency and gets rid of traffic jams. By analyzing the gathered data, the transportation system may automatically adjust to new traffic circumstances. Consequently, the ITS relies heavily on its extensive dissemination. The system's efficacy, however, hinges on the widespread deployment of intelligent cars and intelligent infrastructures across a variety of geographies. This will enable the system to gather and transmit data more effectively. Keeping deployment costs as low as possible while ensuring dependability is a major concern for the ITS. One benefit of integrating intelligence into the transportation system is the ability to effectively monitor and control traffic. This helps to decrease congestion and offers alternative routes that are optimized according to the current traffic conditions. Time and money may be saved and emissions can be decreased by making the transportation system more efficient.

Current VLC prototypes provide low-error communication lengths of 40-60 meters for photodiode-based systems(Căilean et al., 2015; Lourenço et al., 2012; Okada et al., 2009) and up to 100 meters for camera-based systems (Goto et al., 2016; Takai et al., 2013, 2014a; Yamazato et al., 2014). Therefore, increasing the connection distance is necessary for complete compatibility with the automotive sector. In Table 2.4, we can see a comparison between this thesis and a number of important I2V/V2V prototypes in terms of their technical specifications.

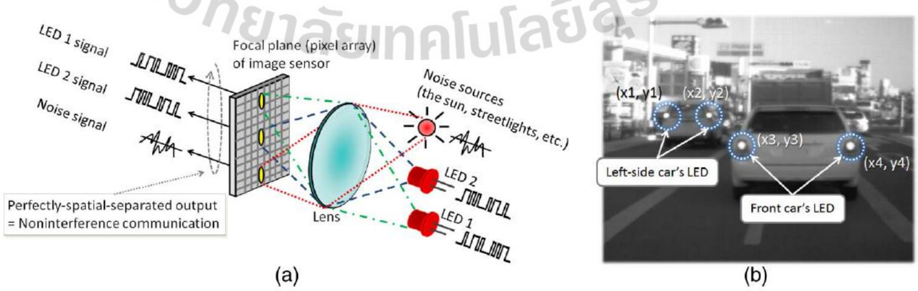

Figure 2.14 Characteristics of the IS-OWC system. (a) Noninterference communication. (b) Identifications of sources (Takai et al., 2013).

Table 2.4 Overview of the current research on experimental demonstrations of I2V and V2V (Căilean & Dimian, 2017).

References	Receiver type	Scenario	Receiver FOV	Data rate	Max. Distance	Modulation and/or coding technique	Merits, observation or particularities
(Takai et al., 2013, 2014b; Yamazato et al., 2014)	Camera-based	I2V static	22°	10-20 Mb/s	2 m	OFDM/QAM/ Manchester code	Present in different configurations, the prototype is probably one of the best existing VLC systems for automotive applications. However, it is also one of the most complex ones, and therefore the price makes it rather inaccessible for general usage.
				10 Mb/s	20 m		
(Yamazato et al., 2014)		I2V mobile		32 kb/s	70 m		
				2 kb/s	110 m		
(Goto et al., 2016)		I2V static		55 Mb/s	1.5 m	OFDM	
(Căilean et al., 2015)	Photodiode based	I2V static	10°	15 kb/s	50 m	OOK with Manchester or Miller coding	One of the best photodiode-based VLC system for automotive applications in terms of raw BER ($<10^{-7}$) and communication distance. Developed under budget constraints.
(Saito et al., 2008)	Photodiode based receiver + emitter tracking system based of low-cost camera	I2V	1.3°	4.8 kb/s	90 m	2PPM	Combines mobility camera-based receivers with the benefits of photodiode-based receivers. Uses a rather complex emitter tracking system.
(Okada et al., 2009)		I2V mobile	0.4°	1 Mb/s	60 m	QPSK	
				2 Mb/s		16 QAM	

Table 2.4 Overview of the current research on experimental demonstrations of I2V and V2V (Căilean & Dimian, 2017) (Continued).

References	Receiver type	Scenario	Receiver FOV	Data rate	Max. Distance	Modulation and/or coding technique	Merits, observation or particularities
(A. Cailean et al., 2012)	Photodiode based	V2V static	20° +	15 kb/s	15 m	OOK with Manchester or Miller coding	Communication distance is sacrificed to increasing the noise robustness. Wide FOV.
(Kumar et al., 2012; Lourenço et al., 2012a; Terra et al., 2011)	Photodiode based	I2V static	NA (not available)	20 kb/s	50 m	DSSS	Highly robust to noise due to the DSSS modulation.
(A.-M. Cailean et al., 2013)	Photodiode based	I2V2V	10°	15 kb/s	23 m	OOK with Manchester or Miller coding	First experimental demonstration of a I2V and V2V cooperative VLC system.

Table 2.4 Overview of the current research on experimental demonstrations of I2V and V2V (Căilean & Dimian, 2017) (Continued).

References	Receiver type	Scenario	Receiver FOV	Data rate	Max. Distance	Modulation and/or coding technique	Merits, observation or particularities
(Corsini et al., 2012)	Photodiode based	Emission angle 18° and 25 mm focal length lens at the receiver	25 mm focal length and 25 mm diameter	115 kb/s	31 m	OOK	Clearly points out the significant influence of the light emission angle and of the focal lens (narrow FOV).
(Corsini et al., 2012)	Photodiode based	Emission angle 120°	No focal lens	115 kb/s	1 m	OOK	Clearly points out the significant influence of the light emission angle and of the focal lens (narrow FOV).
My Research	Photodiode based	I2V (Street light to vehicle at nighttime), LED array for optical power distribution.	90°-120°	20 Mb/s	4.9 m	OOK with Manchester coding	Present a different configuration of I2V system, simulation the channel response while the receiver on the move both SISO and MIMO techniques for I2V system.

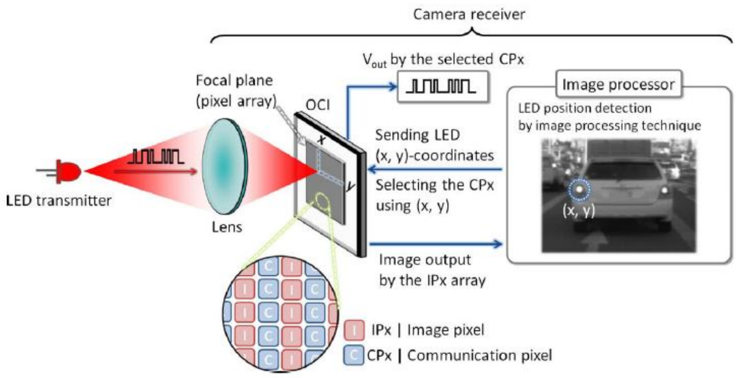

Figure 2.15 Basic operations of an image-sensor optical wireless communication system (Takai et al., 2013).

The authors provide a detailed description of the design, implementation(Takai et al., 2013), and evaluation findings of an optical communication image sensor (OCI), also to the formation and empirical performance analysis of the IS-OWC scheme using the OCI. In addition, they showcased the pioneering achievement of transmitting data at a rate of 20 megabits per second per pixel, while simultaneously achieving real-time detection of light-emitting diodes with a latency of 16.6 milliseconds.

Not only is VLC suitable for broadcast systems like road-to-vehicle or I2V communication systems, but it can also be used in V2V and V2I communication systems. In a vehicle-to-vehicle (V2V) scenario, a car positioned ahead of traffic signals receives traffic safety data and communicates it to the vehicle behind using the brake lights. They have the capability to construct a spontaneous network among one another and exchange information. Figure 2.16 depicts Illustration of a hypothetical situation. Similarly, utilizing an LED-based front headlight, the running automobile can request information from RSUs, providing a full duplex communication system.

For instance, in the I2V mode of vehicle communication systems, LED-based traffic lights excel at broadcast transmission. Continuous dissemination of traffic safety information may be achieved without any additional power consumption, improving traffic flow and lowering accident fatalities. The alteration frequency of a traffic light is undetectable by the human visual system. A photodetector receiver fitted on a vehicle detects the light that has been modulated, allowing the driver to obtain crucial safety information in advance. Advanced perspectives may use inter-vehicle communication techniques to exchange information among cars located near traffic control stations.

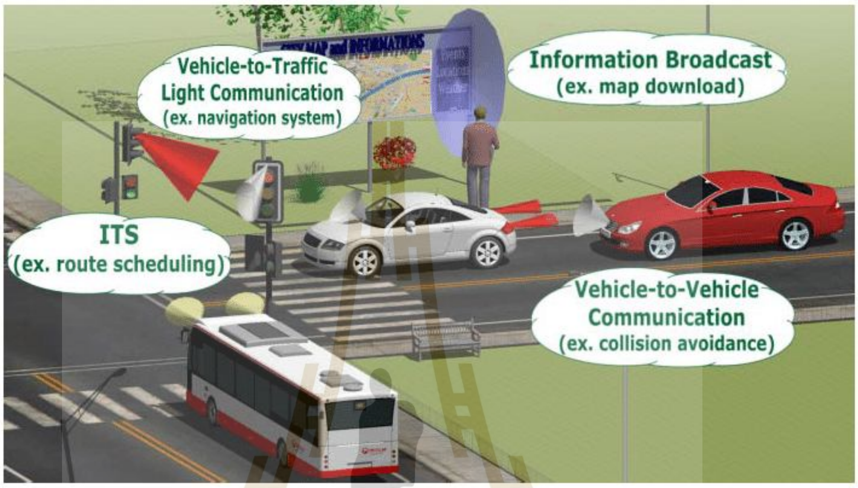

Figure 2.16 Outdoor VLC application examples (Lourenço et al., 2012b).

Figure 2.17 VLC usage scenario: road safety data is transmitted using the vehicle lighting systems, the street lighting system and the traffic lights.

Figure 2.17 demonstrates an instance where VLC is used in communication-oriented automobile safety applications (Căilean & Dimian, 2017). The intelligent traffic lights and street lighting system provide approaching vehicles with pertinent road safety information, including positional data, traffic light phase, time remaining until the next change, ongoing maintenance activities, and speed restrictions. The intelligent traffic lights and street lighting system facilitate the transmission of this information. Moreover, the vehicles have the capability to exchange information on their present condition, such as location, speed, rate of change of speed, engine operation, and other relevant factors.

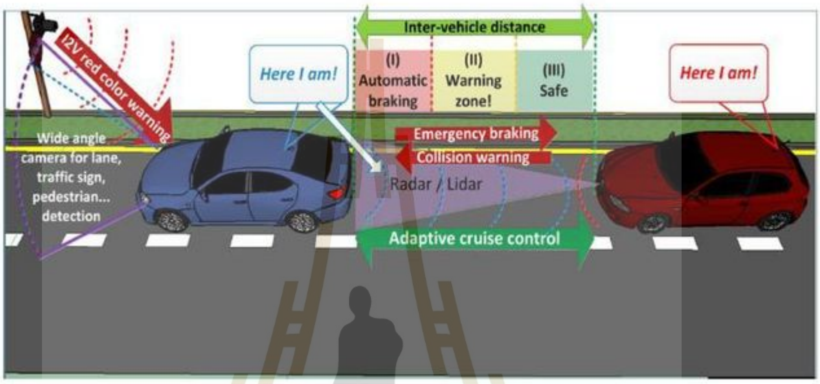

Figure 2.18 Sensors and wireless communication fusion for traffic safety applications (A.-M. Cailean et al., 2014).

According to (A.-M. Cailean et al., 2014), raising vehicle awareness is among the most effective approaches to reducing the frequency of bumps and the accompanying fatalities. Sensors embedded in the automobile can detect danger and aid the driver. Ultrasound sensors for parking assistance, cameras for traffic lanes, traffic flow, or walker recognition, and Lidar or Radar technologies for long-range obstacle detection and distance size are examples of such systems. Sensors, however, have limitations, and in certain cases, wireless connections can take driver assistance to the higher level. Wireless communications, as seen in Figure 2.18, allow cars to connect with one another by sending "Here I am!" note, as well as sharing sensor data. The system can take action in unsafe situations by utilizing the obtained data. It will, however, operate as a "safety net" rather than against the driver. Typically, the vehicle's action concludes before the driver's ability to respond. In addition to ensuring safety, communication may be used to enhance the efficiency of transportation systems by offering location services and identifying the most optimal alternative routes.

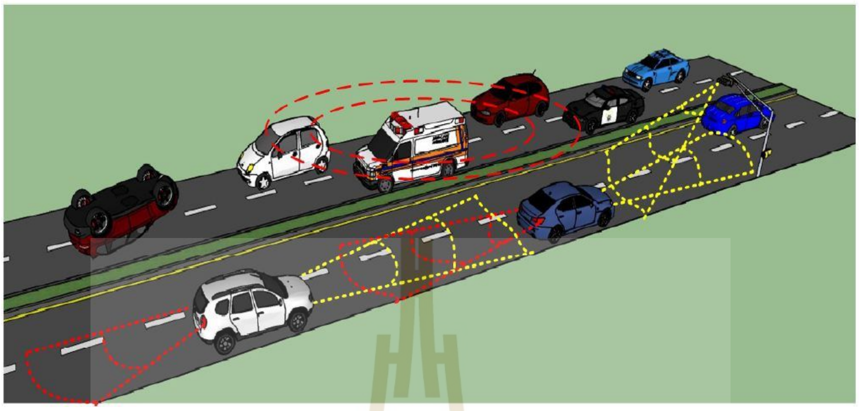

Figure 2.19 Visible light communication usage in a highway scenario (A.-M. Cailean et al., 2014).

Obtaining bidirectional connections among several transceivers in VLC is challenging (A.-M. Cailean et al., 2014). This reduces the amount of data sent over the network and avoids any conflicts or disruptions between different elements. When contemplating vehicle-to-vehicle (V2V) communication, information is sent from one vehicle to another. Figure 2.19 depicts a VLC use scenario in a highway setting. Adjacent vehicles capture the data using optical sensors and communicate it to the closest neighboring vehicles using front and rear lights. As a result, data is spread over the highway. Besides, the automobiles can connect with one another about their spontaneous status or other concerns that are necessary to improve traffic safety and security.

The optical V2V connection scheme is depicted in Figure 2.20. The LED transmitters in a leading vehicle (LV) make use of vehicle LED light sources like taillights, brake lights, and headlights. The camera receiver is situated in the following vehicle (FV). The LV autonomously collects its internal data, such as speed, and transmits it to the following vehicle via optical signals. At the same time, the camera receiver on the FV captures photographs and uses image processing algorithms to identify LED zones in the collected images. Figure 2.20 shows the LED placements, indicated by green rectangles. Subsequently, the recipient system observes the fluctuations in luminous intensity at the identified LED positions and captures the optical signals.

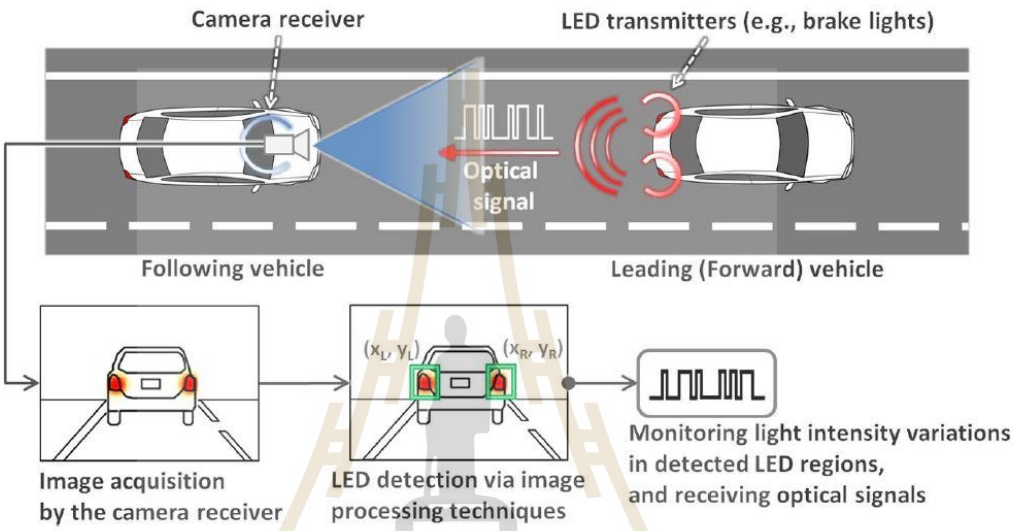

Figure 2.20 Illustration of the optical V2V communication system (Takai et al., 2014a).

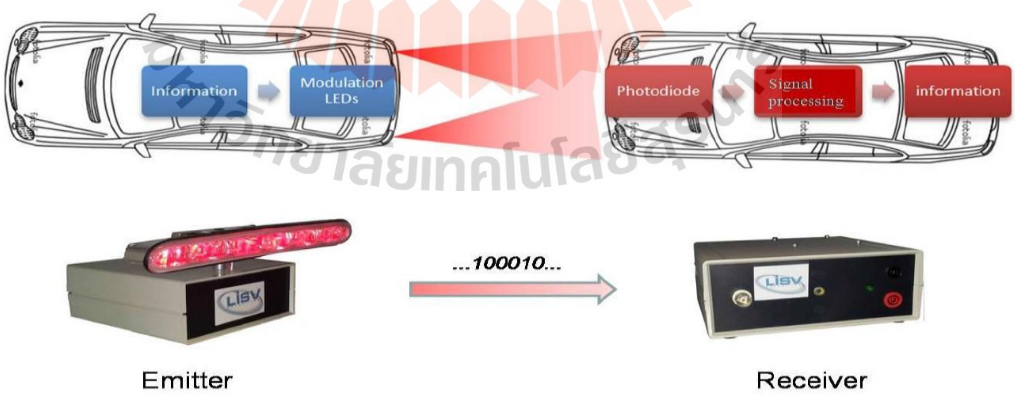

Figure 2.21 First prototype of transmission data system and the associated frame of digital data (A. Cailean et al., 2012).

A led-light communication prototype has been created. As seen in Figure 2.21, power modulation is employed to send digital data. The electronic device has not been inserted officially, but all of the components were picked due to its affordability and small size. With a microcontroller and an inexpensive digital power switch, the red rear light is current-modulated with OOK (On-Off Keying) amplitude modulation. As shown in Figure 2.21. As shown in Figure 2.21 (A. Cailean et al., 2012), a digital frame has been defined.

2.6.1 VLC for Intelligent Transportation System (ITS)

Every year, approximately 1.35 million people are killed in traffic accidents, approximately 50 million human are wounded. (*Global Status Report on Road Safety 2018*, 2018). According to researchers, the majority of occurrences are caused by the delayed reaction and incapacity of motor vehicle operators to promptly execute the necessary measures (Abualhoul, 2016). Ensuring the safety of individuals is assured by an Intelligent Transportation System (ITS) equipped with infrastructure-to-vehicle (I2V) and vehicle-to-vehicle (V2V) communication. ITS is dependent on honest, strong, to establish a reliable and protected means of communication between cars and infrastructure (traffic signals, billboards, and street lighting). Due to the existing communication is crowed RF-based communication (Arnon, 2014; Ghassemlooy et al., 2017). Every vehicle is equipped with headlights and taillights capable of transmitting data. Traffic lights, billboards, and street lights can serve as communication channels for disseminating crucial information about road, traffic, and weather conditions. These illumination sources can also be utilized to link people and IoE entities to the internet. C˘ailean et al. examined the issues that VLC faces in the context of vehicle communication (Belkhir & Elmeligi, 2018). The main factors considered for vehicle communications are improved agility, increased communication range, and faster data rates. The capacity of communication lines to withstand ambient or parasitic light is crucial in order to accomplish these objectives. The outside channel is subject to a wide range of ambient illumination conditions. It has been discovered that the distance measuring and localization capabilities of VLCs could be beneficial in applications involving communication between vehicles. Moreover, it is recommended that the creation of diverse systems incorporating Visible Light Communication (VLC) along with dedicated short-range communication (DSRC) or Cellular-V2X (or any other radio frequency-based scheme) could establish a reliable framework for vehicular communication. This might be attributed to the fact that each of these technologies can address the shortcomings of the others. This study presents an examination of Visible Light Communication (VLC) in relation to 5 GHz Dedicated Short-Range Communication (DSRC) within a hybrid framework. The findings suggest that enhancing a VLC system for vehicular communication involves exploring and incorporating innovative technologies like software-defined architecture, resource sharing, reconfigurable computing, and the integration of novel materials. Ucar et al. devised a secure autonomous platoon system, combining 802.11p and VLC (Ucar et al., 2018). The self-governing platoon functions using RF-based 802.11p, led by a platoon leader who directs fellow members to precisely adjust their speeds. SP-VLC, a communication protocol for hybrid vehicle convoys that blends 802.11p and VLC, addresses security vulnerabilities arising from the distinctive use of RF communication. They were developing a simulation platform to assess SP-VLC across various security flaw scenarios, focusing on vehicle mobility and platoon management. The simulation results validated the conclusions of (Căilean & Dimian, 2017), that an RF-VLC heterogeneous system offers several benefits compared to an RF-only system.

LED-operated roadside units (RSU) have been integrated into the modern ITS, (Kumar et al., 2012) it has proposed by Kumar et al.. VLC concepts are employed to transmit data from infrastructure to vehicle mode. To lessen the effect of noise as an ambient light, the utilization of a modulation approach that relies on a direct sequence spread spectrum (DSSS) and sequence inverse keying (SIK) is employed. A performance metric is the amount of data received by an automobile passing by RSU. The setup for the experiment involves a mobile receiver and a stationary emitter positioned 1.5 meters apart. Findings indicate that in daylight, the packet error rate (PER) exhibits a linear decrease with distance. Conversely, at night, the PER fluctuates based on the characteristics of local artificial lighting.

The VLC based V2V system was conducted by (Uysal et al., 2015). In his study, an investigation is conducted on a common V2V-VLC situation involving the use of left and right headlights to emit light. The dissipation pathways, likewise the line-of-sight route elements, are taken into account using the Lambertian profile. The results reveal that at a length of 70 m among automobiles, a data rate of 50 Mbps can be attained depending on the location of the headlamps.

In (Wang et al., 2017), the authors employed VLC-based ITS has been utilized to provide signals relating to decreasing speed, increasing speed, and vehicle braking to ITS infrastructure (e.g., RSUs) that can trigger relevant signals. For example, in a difficult environment, a vehicle can send a VLC signal to RSU, which can establish a green light or expressway to limit the frequency of emergency brakes and lane changes.

Yamazato et al. employ VLC with an image sensor-operated receiver for automotive applications (Yamazato et al., 2014). I2V and V2V were the two cases that were considered. A high-frame-rate CMOS image camera receives signals from a transmitter made of LED arrays in the first scenario, which involves roadside infrastructure. The second possibility involves the development of a unique CMOS sensor that can record optical data at fast speeds. The I2V system achieves 32 kilobits per second and the V2V system achieves 10 megabits per second throughout the testing.

The investigation conducted by (Dang & Yoo, 2017) Dang and Yoo in 2017 focused on establishing a handover mechanism for the V2I-VLC system, where infrastructure elements like street lighting could facilitate autonomous driving. The methodology employed a probabilistic algorithm based on distance to determine the optimal handover switching time. Given the swift movement of cars and the limited coverage of each streetlight, the challenge emerged during the car's passage through a series of LED-equipped streetlights, necessitating effective handover between LED groups. The devised handover technique and algorithm demonstrated significant improvements in signal quality, evolving positively with each transition to a different set of LEDs. In a parallel effort (Cheng et al., 2017), Cheng et al. (2017) aimed to compare the propagation characteristics of radio frequency (RF) and visible light communication (VLC), encompassing factors such as radiation pattern, path loss modeling, noise and interference, and channel time fluctuation.

2.7 Modulation techniques

The modulation in the VLC system is classified as single-carrier or multi-carrier. Light modulation in VLC is limited by two major factors. Firstly, the VLC system provided dimmer circuits on the light bulbs to control the intensity of light. Secondly, to protect human safety, the VLC modulation technique is allowed to prevent human damage. According to the literature, some instances of single-carrier modulation are On-off-keying (OOK), Pulse-Position modulation (PPM), and Pulse-width modulation (PWM). Eventually, color shift keying (CSK) modulation is a type of many colors coding that can be used to divide the visible spectrum. As previously stated, all modulation in the VLC system supports the dimming parameter.

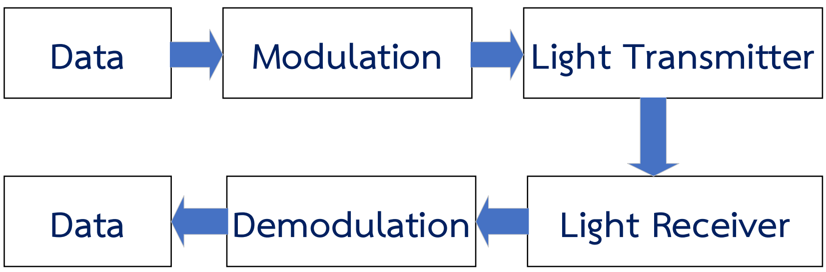

Figure 2.22 Simple block diagram of transmitting and receiving in VLC system.

2.7.1 On-off keying (OOK)

The OOK modulation technique is easiest for implementation in VLC system. There are changing the zero to one bit to turn on the LED light, and changing the one to zero bits to turn off the LED light. It can represent that the bit-1 is “on,” and bit-0 is “off”. The majority of studies has used white LED (WLED) OOK modulation for VLC. (Dahri et al., 2018). It can be produced by the blue emitter with the yellow phosphor. However, white LED has a limitation in speed response for a signal in a few megahertz (IEEE Standard, 2011). (Grubor et al., 2007) proposed to use Non-Return-to-Zero (NRZ) OOK with the white LED transmitter and there was demonstrated with the data rate of 10 Mbps. (IEEE Standard, 2011) used the bule filter to remove the slow response rate of the white LED achieving in data rate of 40 Mbps. The bule filtering with simple equalization at the receiver has proposed in (Park et al., 2007) and (Le Minh et al., 2008) the data rate achieved of 100 Mbps and 125Mbps respectively. In (Vucic et al., 2009) the avalanche photodiode at the receiver side was achieved the data rate up to 230 Mbps. The combination of RGB light frequency created the white LED. The white LED's main factor is that they do not have a low response time. In (Vučić et al., 2010) they modulated just the red LED in RGB white LED by remaining illumination whereas the data transmission. The results achieved the data rate of 477 Mbps, used the P-I-N photodiode at receiver. There were two methods for dimming support OOK that used in modulation scheme which was proposed by IEEE Standards in (Berman et al., 1991) as IEEE 802.15.7. The first method involves allocating various light intensity levels to the ON and OFF levels. The advantage of this technique is that it can achieve the appropriate dimming level without introducing an overhead bit. The data rate is the same as NRZ-OOK modulation. Similarly, with low dimming levels, the communication range decreases. The various light intensity levels are divided between the ON and OFF levels to accomplish the appropriate dimming rank. The profit of this technique is that it can achieve the appropriate dimming level without introducing an overhead bit. It maintains the same data rate as NRZ-OOK modulation. Similarly, with low dimming levels, the communication range decreases. The obvious negative is that utilizing reduced levels of light intensity for ON/OFF forces the LEDs to operate with low-power driving circuits. Other methods of acquiring rendering changes (changes in LED shade radiation) have been demonstrated (Fujimoto & Mochizuki, 2013). The second is the additional compensation periods. The intended level of dimming determines how long compensating periods should last. Specifically, the ON intervals are wished if the required dimming level is greater than 50%; otherwise, the OFF times are wished. Equation (2.27) shows how the authors calculated the dimming level (D) using a method based on the percentage of time spent actively transmitting data (γ) inside the transmission interval (T).

$$\gamma = \begin{cases} (2-2D)\times 100 & : D > 0.5 \\ 2D\times 100 & : D \leq 0.5 \end{cases} \tag{2.27}$$

The greatest communication efficiency (E_D) can be determined (Muthu & Gaines, 2003) using information theoretic entropy as equation (2.28) when the desired dimming level is D with OOK.

$$E_D = -D\log_2 D - (1-D)\log_2(1-D) \tag{2.28}$$

It suggests that communication system effectiveness is a triangle function of dimming level, with 50% being the optimal degree of dimming. Dimming levels between 0% and 100% cause a linear loss in efficiency. The adjustment periods utilized in dimming cause a decrease in the data rate. The range of communication and the ON/OFF modulations' intensity attributes are both unaltered. Inverse source coding was offered by (Kaur et al., n.d.) as a solution to this low data rate with compensating periods issue in order to maintain a high data rate while obtaining the required level of dimming.

2.7.2 Pulse modulation method

The OOK offers a simple and feasible implementation for VLC system. The limitation is its lower data rates, especially when maintaining different dimming levels. It is the inspiration for developing new pulse position modulation (PPM) and pulse width modulation (PWM) techniques. A successful PWM technique for achieving modulation and dimming. This system balances the pulse width according to the desired dimming level, and the pulses themselves get modulation in the form of a digital pulse. When the LED light is fully bright, data is being transmitted. Data rate can be allowed for and changed based on dimming requirements. In (Kwon, 2010), scientists noted that using the PWM frequency modulation approach, any dimming level from 0% to 100% can result in increased data rates. One of PWM's key benefits is that it performs dimming without altering light intensity, negating the need for color shifts or redefining the LED's on and off levels. (Kwon, 2010) shown the data rate up to 4.8 kbps. PWM and discrete multitone were intended to be combined for cooperative dimming control and communication in (Ntogari et al., 2011). DMT-based communication and PWM-based dimming are not coordinated on the emitter side. As displayed in Figure 2.23, the Quadrature Amplitude Modulation (QAM) is bit-streamed and transferred to symbols.

Pulse Position Modulation (PPM): Another modulation in visible light transmission is dependent on the pulse position. The PPM approach divides the symbol duration into t time intervals of equal length. Due to its simplicity and the fact that it is used in many early designs (Ntogari et al., 2011; Sugiyama et al., 2007) of optical wireless communication, the transmitted pulse can be recognized based on the position of the signal.

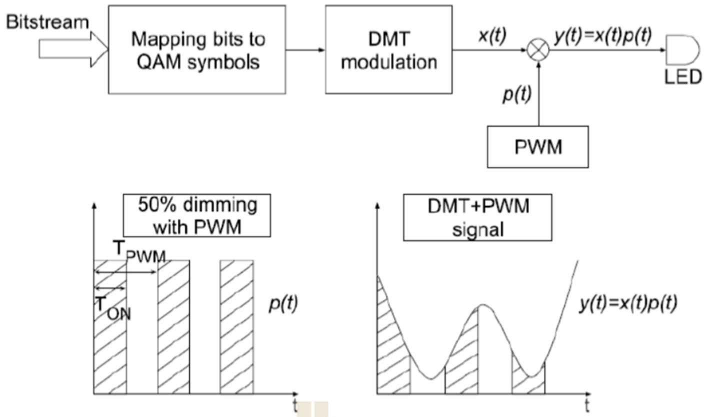

Figure 2.23 Transmitter block diagram of DMT transmitter with dimming control. An example of how 50% PWM-controlled dimming signal can be combined with a DMT signal (Dahri et al., 2018).

In prior work, PPM has been employed for infrared communication. The usage of rate adaptive transmission systems, where redundancy coding is utilized to subtly lower data throughput in the presence of bad channel conditions, has been advised in this work by (Georghiades, 1994). A rate variable penetration convolution coded PPM used in infrared communication systems has been presented by researchers in (Shiu & Kahn, 1999). It adopts modulation order with the channel situations through Convolution codes. Both rate adaptive approaches were applied for greater data rates. One is the punctured convolution coded PPM, while the other is the repeating one (F. Gfeller et al., 1996). Various variations of pulse position-based modulation have been proposed as a result of the restrictions of PPM's reduced spectrum performance and data throughput. Figure 2.24 shows the overlap PPM (OPPM), which allows for the transmission of multiple signals of varying durations through a single pulse (Georghiades, 1994). In (Ohtsuki, 1999), it was shown that OPPM is capable of a wide variety of dimming levels and larger data speeds in addition to having higher spectral efficiency. The alternative PPM variant, known as Multi-pulse PPM (MPPM), was suggested by (Bai et al., 2010). OPPM allows for several pulses to be communicated inside a single symbol length; however, as illustrated in Figure 2.24, the pulses within the symbol duration do not need to be constant. In contrast to OPPM, MPPM can achieve a better spectrum efficiency, as seen and demonstrated in (Georghiades, 1994).

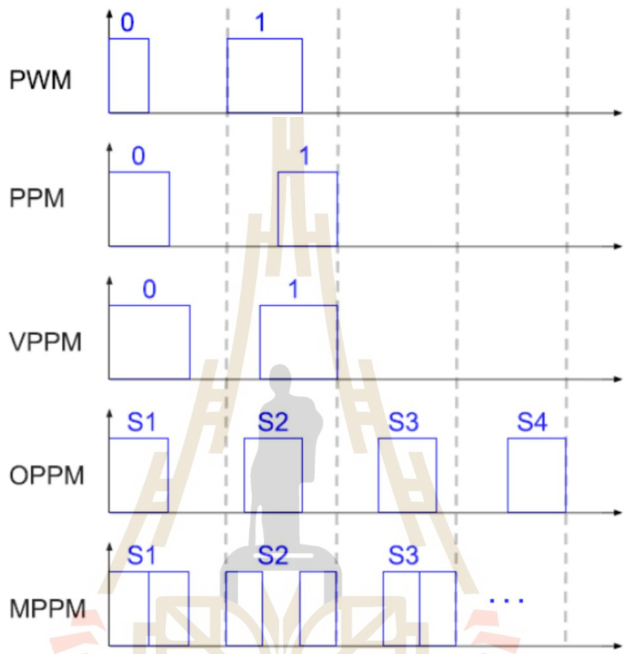

Figure 2.24 Schematic diagram showing the difference between Pulse Width Modulation (PWM), Pulse Position Modulation (PPM), Variable Pulse Position Modulation (VPPM), Overlapping Pulse Position Modulation (OPPM) and Multi-pulse Pulse Position Modulation (MPPM); Sn refers to the nth symbol (Dahri et al., 2018).

In (Sugiyama & Nosu, 1989), authors proposed using Overlapping MPPM (OMPPM), a hybrid of OPPM and MPPM techniques, to introduce variation in PPM. In this method, an optical signal is represented by many pulse positions. It was found that the OMPPM can boost MPPM's spectral efficiency without increasing data transfer capacity in the noiseless photon tallying channel. In (Ohtsuki et al., 1993), additional noisy channel performance study is shown. a reduced number of time slots and an increased quantity of pulses per symbol in (Ohtsuki et al., 1994b) OPPM, the cutoff rate performance is better. The effectiveness of direct detection is discussed in Trellis-coded OMPPM in the presence of background noise (Ohtsuki et al., 1994a).

2.7.3 Color shift keying (CSK)

To address circumstances where earlier modulation approaches were fading and having lower data rates, researchers introduced a converting data approach called color shift keying (CSK). White LED can be produced by combining several hues. As previously said, blue emitting and yellow phosphor can be used to generate white LEDs. However, white LED tolerates decreased transmission speed due to the yellow phosphor's response delay. Red, green, and blue (RGB) hues, which offer greater advantages for communication, can be combined to make white LED interactively (Khalid et al., 2012). The primary rationale for selecting CSK is the idea of using multi-color LEDs. The spectrum was divided into seven hues according to the IEEE 802.15.7 standard to determine distinct colors for transmission. The seven colors are shown on x-y chromaticity values according to CIE 1931 in Figure 2.25. The bits in Figure 2.25 determine each band of the seven colors, and the outside curve is the spectral region with wavelengths displayed in nm. Despite the fact that each light has its own power, the total power for all CSK light sources is constant. In order to maintain the required intensity of the center color of the color group, CSK dimming ensures that the average optical power from the LED is constant. Because of the amplitude altering, the flicker will not happen with CSK (Oh, 2013). CSK dimming controls and reduces brightness by altering the driving current for LEDs.

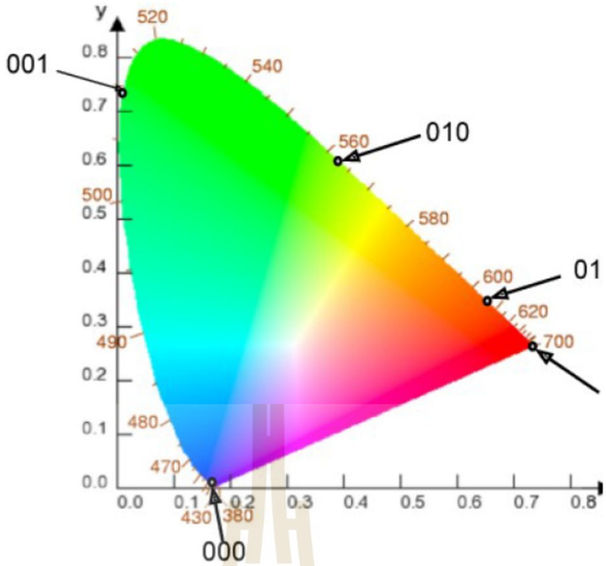

Figure 2.25 The seven color codes correspond to the centers of seven bands dividing the visible spectrum (Sugiyama & Nosu, 1989).

2.7.4 Binary phase-shift keying (BPSK)

The most basic type of phase shift keying, or PSK, is BPSK. BPSK employs two phases with a separation of 180 degrees. The points in the constellation are depicted along the real axis, specifically at 0 degrees and 180 degrees, and their precise locations are not especially important. Among the PSK modulation techniques, this modulation is the most resilient, as it necessitates the highest level of noise or distortion to cause the demodulator to make an incorrect decision. However, because it can only modulate at 1 bit per symbol, it cannot be used for high data-rate applications where bandwidth is constrained. In (Adiono et al., 2018), The authors developed BPSK to meet the demands of the VLC system and found that it performs effectively with an optical range of up to 40 cm while maintaining low complexity. BPSK modulation enabled the system to achieve a maximum bitrate of 13.4 kbps.

2.7.5 Quadrature phase-shift keying (QPSK)

Quadrature phase-shift keying (QPSK) on the constellation diagram, QPSK makes use of four evenly spaced points. Two bits per symbol can be encoded using QPSK with four phases, as indicated in the diagram with Gray coding to reduce BER. According to analysis, this can be used to either retain the bandwidth of the signal while doubling the data rate compared to a BPSK system, or to keep the data rate of BPSK while halving the bandwidth required. It is simpler to think about QPSK as two separately modulated quadrature carriers even though it can be considered as a quaternary modulation. According to this interpretation (Wani & Qadri, n.d.), the carrier's in-phase component is modulated using the even (or odd) bits. While the carrier's quadrature-phase component is modulated using the odd (or even) bits.

2.7.6 Multi-input multi-output (MIMO)

Multiple Input Single Output (MISO) is the name of a system that employs several antennas at the transmitter and just one antenna at the receiver. Alamouti STC (Space Time Coding) is a method used, at the transmitter with two antennas. The information is delivered by two antennas at two distinct periods sequentially when STC is used, allowing the transmitter to send signals (information) in both time and space. A base station (BS) often has many antennas, either SIMO or MISO. This allows all subscriber stations (SSs) covered by the BS to split the expense of providing either a receive diversity (in SIMO) or transmit diversity (in MISO). Multiple antennas are installed at the transmitter and receiver in order to increase the throughput of a radio connection. Multiple Input Multiple Output (MIMO) is the term used to describe this system. With each extra antenna, a MIMO system in a point-to-point (PTP) link that has a similar number of antennas at the transmitter and receiver can linearly increase its throughput (Wani & Qadri, n.d.).

2.7.7 Bit error rate (BER)

A crucial characteristic of the digital communication system is the bit error rate (BER). In the digital information transmission system, different types of modulation techniques are applied. The number of bits received from a data stream through a communication channel that may be impacted by noise, interference, distortion, or bit synchronization issues is known as BER (Wani & Qadri, n.d.). A simple calculation BER is shown as the equation (2.29) below.

$$BER = {}^{Bits\ error}\!\big/_{Total\ number\ of\ bits} \tag{2.29}$$

And Table 2.5 displays various modulation schemes.

Table 2.5 Calculation of BER for the different modulation schemes (Wani & Qadri, n.d.).

Modulation Schemes	Calculation BER	Remarks
NRZ-OOK	$BER_{NRZ-OOK} = 0.5erfc\left(\frac{1}{2\sqrt{2}}\sqrt{SNR}\right)$	Equation (2.30)
RZ-OOK	$BER_{RZ-OOK} = 0.5erfc\left(\frac{1}{2}\sqrt{SNR}\right)$	Equation (2.31)
L-PPM	$BER_{PPM} = 0.5erfc\left(\frac{1}{2\sqrt{2}}\sqrt{SNR\left({}^{L}\!/_{2}\right)\log_2 L}\right)$	Equation (2.32)
BPSK	$BER = 0.5erfc\left(\sqrt{\frac{E_b}{N_0}}\right)$	Equation (2.33)
QPSK	$BER = 0.5erfc\left(\sqrt{\frac{E_b}{2N_0}}\right)$	Equation (2.34)

Those modulation schemes used the Additive white gaussian noise (AWGN) to add noise for the channel system, it is added to the channel. The transmitted signal and the incoming signal are additive since they are equal. The received signal is distorted by noise because the spectral density has a lower power rent and a Gaussian probability dispersion.

2.8 Summary

This chapter provides an overview of the development of visible optical communications and the roots of the invention of optical telephony. LED bulb manufacturing technology has advanced significantly in recent times, enabling the production of a single LED light that can emit high-intensity light across a considerable distance while maintaining a favorable frequency response. LEDs possess a high degree of light intensity modulation in the high-frequency range, enabling its use for optical information transmission. Studying the impulse response signals of optical wireless communication channels is crucial for accurately analyzing and processing the electrical signals. As mentioned in this chapter, the VLC system for ITS communications has undergone continuous development. Various environments utilize VLC, including street illumination, underwater communication, hospital illumination, the Wi-Fi band, hazardous places, and defense and security. This research examines the effectiveness of various modulation techniques on VLC. Because of their ability to be dim, lights can offer a strong signal for transmission. As managing the dimming level of VLC sources is a crucial component of VLC, it is required to select a modulation technique that can reduce the effects of the dimming level and improve data rates. It is clear from the review and observations that MPPM offers dependable communication, satisfies power requirements, and ensures spectrum efficiency and data speeds in comparison to many other VLC-related methods. Additionally, BPSK always performs better in terms of BER. When compared to other modulation methods, CSK has higher data rates. In MIMO-OFDM, the more receivers, the lower the bit error rate. This chapter explores many concepts related to visible light communication and its use in data transmission systems, particularly in the context of nighttime infrastructure-to-vehicle communication. The research examines many interrelated theories that influence the amplitude of the impulse response signal in the communication channel of the I2V system. The article also explores the various digital modulation techniques used in optical communications.

CHAPTER III

MODELING OF OUTDOOR WIRELESS VISIBLE LIGHT COMMUNICATION FOR INFRASTRUCTURE TO VEHICLE SYSTEM

3.1 Introduction

The two primary transmission contexts for visible light communications (VLC) technologies are indoor and outdoor. Indoor VLC is a complex subject that offers the benefit of using two light sources (Ndjiongue et al., 1999). These can function as both lighting and transmitting antennas. This benefit is not consistently observed in outdoor VLC scenarios since the sun illuminates the surroundings and eliminates the need for an extra source of illumination during daylight hours. Due to this particular situation, many outdoor VLC applications that are used in daytime hours solely use light sources for communication. Outdoor VLC thus lacks attraction. However, these sources of light remain able to be used for lighting purposes and communication in applications that are deployed at night. For instance, they can act as both lighting fixtures and VLC transmitting antennas when nighttime street and park lighting is required. Both the front and rear lights of cars fall under this category. It should be noted that even in daylight, the light sources LEDs are still primarily utilized in the majority of outdoor VLC applications. During both daytime and nighttime, traffic panels and traffic information displays offer guidance, indicate locations, and serve communication purposes. Traffic lights are another example of how traffic control and communication is used both during the day and at night. This chapter we will discuss a modeling outdoor wireless visible light communication used in ITS framework.

3.2 Infrastructure to vehicle system configuration

Devices are increasingly sophisticated, and they have the ability to interact and exchange information with one another. Intelligent Transportation Systems (ITS) have created intelligent street lights to provide lighting and facilitate data transfer. A white LED bulb is a crucial lighting device for energy conservation as it serves as a replacement for fluorescent tubes and incandescent bulbs, providing efficient illumination. LEDs provide many benefits, including extended lifespan, reduced energy usage, compact dimensions, and efficient cooling. Future projections indicate that LED bulbs will replace traditional lamps in this context due to their many benefits. LEDs may serve as both lighting equipment and devices for data exchange. Figure 3.1 illustrates how LEDs in an infrastructure send traffic information to vehicles. The combination of both radio frequency (RF) and visible light communication (VLC) technologies is very compatible with intelligent transportation systems (ITS).

Figure 3.1 An infrastructure to vehicle communication concept.

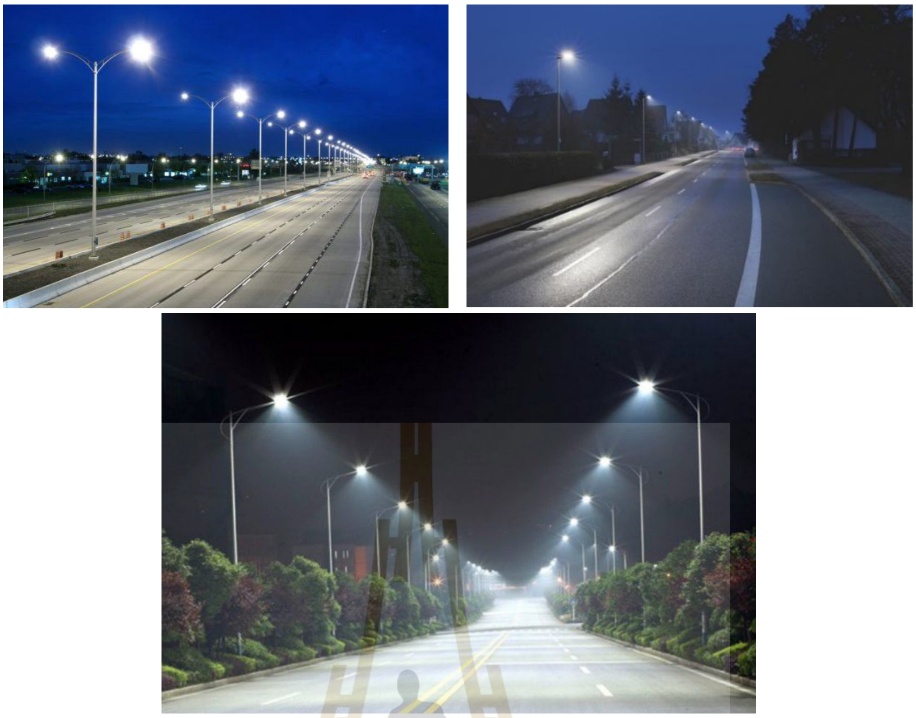

Figure 3.2 Road lighting at nighttime.

We have seen a white LED implemented in street lights for lighting on the road (as shown in Figure 3.2). Street light lighting is based on a white LED array. To examine the brightness of a streetlight's lighting post, it assumes that a street lamp consists of a 5x5 LED array, and the power of each LED is 1 watts. Moreover, white LED 1 Watt. It provides the illuminance of 100 – 120 lumens, employs a power supply of 3.0 – 3.4 voltages, and the current is 300 – 350 mA. LED provides an irradiance angle of 120 degrees. The color temperature available is 6000 – 6500 Kelvins (K), the light color is the daylight, and 3000 Kelvins is the warm light.

Figure 3.3 shows the LED array as a street light. The first picture is a commercial street light, and the second is a model we designed to be a 5x5 LED array. Finally, a single LED is the surface mount device (SMD). The power of a single LED is 1 watt. We designed each LED interval to be 1 cm.

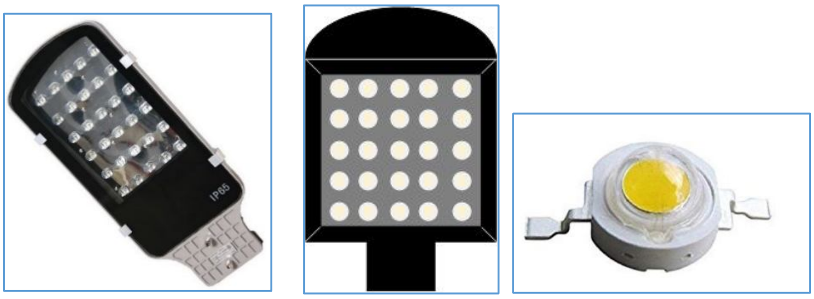

Figure 3.3 White LED array employing for street light as a lamp.

3.2.1 Illuminance of street light

We assume the physical parameters for developing the simulation in the Matlab program. The dimension of the road is 20 m x 20 m. Moreover, for the street light, a lamp is installed on the top, while the height of the transmitter from the road plane is 6 m. The receiver is placed on/in the vehicle's dashboard. The receiver's height from the road plane is 1.10 m, and if the receiver is on the vehicle roof, the receiver's height is 1.30 m.

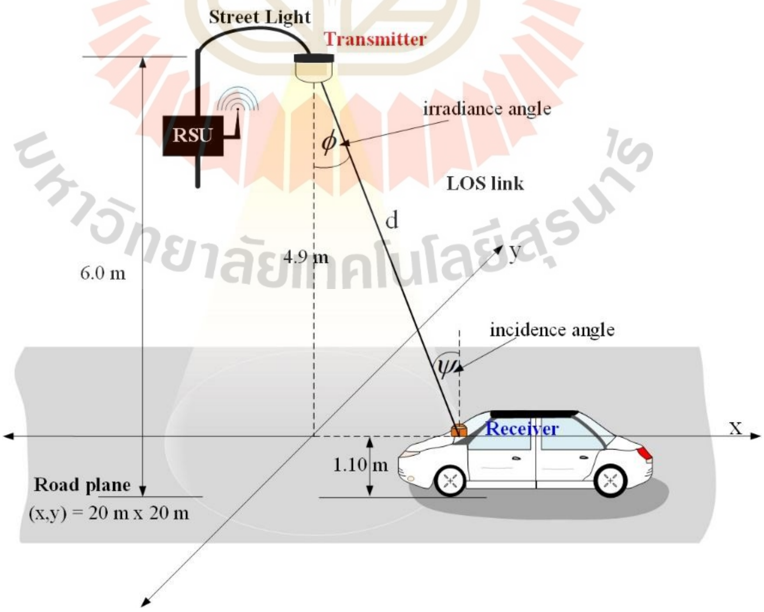

Figure 3.4 Geometry of an outdoor wireless VLC for infrastructure to vehicle.

Therefore, the distance between the transmitter and receiver (d) is 4.9 m and 4.7 m, where the receiver is on the dashboard or roof, respectively. The rest of the parameters are listed in Table 3.1. The geometry of the OWVLC system for I2V communication is shown in Figure 3.4.

The distribution of illuminance at a receiver plane is described here. It is assumed that the transmitter emits the light directly to the receiver position as the Lambertian radiation pattern (Kahn & Barry, 1997; Komine & Nakagawa, 2004). The light intensity emitted from the transmitter, which is an array of LEDs, is a cosine function dependent on the irradiance angle of emission with respect to the surface normal. The luminous intensity in angle ϕ is given as the equation (3.1)

$$I(\phi) = I(0)\cos^{m}(\phi) \tag{3.1}$$

Where $I(0)$ is the center luminous intensity of LED array, ϕ is the irradiance angle of a street light which is LED array. m is the order of Lambertian emission, it is provided by the cosine function of the semi-angle at half power of an illuminance of the LED transmitter $\phi_{1/2}$, as the equation (3.2).

$$m = \frac{-\ln(2)}{\ln\left(\cos\left(\phi_{1/2}\right)\right)} \tag{3.2}$$

We can simulate the illuminance of street light which is the LED array at the position of receiver plane as the horizontal (x, y, z), it is given by the equation (3.3).

$$E_{hor}(x,y,z) = \frac{I(\phi)}{d^{2}.\cos(\psi)} \tag{3.3}$$

Where d is the distance between the transmitter and receiver, ψ is the incidence angle of the light, and $I(\phi)$ the luminous intensity of the transmitter as equation (3.1). To study the distribution of illuminance of the street light that uses an array of LEDs to be the transmitter for the OWVLC-I2V system, we placed the street light at the center of the dimension of the road plane (x, y).

The illuminance performance of the street light is shown in Figure 3.5. We used the MATLAB program to study the luminous intensity of the street light, as the simulation parameters in Table 3.1 for the OWVLC-I2V system. The program calculates the direct illumination only for one street light by assuming that the center of luminous intensity is 3,000 lux. for a 5x5 LED array. Moreover, we depicted the level of brightness with 4 LED array lamps.

Table 3.1 Simulation parameters for OWVLC-I2V system.

Parameters	Values	Parameters	Values
LED array $(nLED \times nLED)$	5x5	Transmitted power (per LED)	1 watt
LED pitch	1 cm	Center illuminous intensity for an LED array = 5x5	3,000 lumens
Semi-angle at half power	70°	Photodetector area (A_r)	1 cm^2
Dimension of X is an along of the road	20 m	Refractive index at PD (n)	1.5
Dimension of Y is a cross of the road	20 m	Optical filter gain $T_s(\psi)$	1.0
Height of transmitter from ground (Z)	6 m	Field of view (FOV) (ψ_c)	120°
Height of receiver plane above the floor (a receiver placed in vehicle)	1.10 m	Vehicle speeds (As the same a receiver speeds)	90 km/hr 25 m/sec.
Number of lamps of street light $nLamp$	1	Time for vehicle moving through coverage area (20 m)	0.8 sec.
Position of Tx (x, y, z)	(10, 10, 6)	(d) is the distance between Tx and Rx	4.90 m

Figure 3.5 shows the distribution of illuminance using one and four street lights as the transmitter with a semi-angle at half power of 70°, respectively. In Figure 3.5 (b), the luminous flux maximum values of 125.0 lux is positioned near the midpoint, and in Figure 3.5 (c), the luminous flux maximum values of 1,798.0 lux is positioned near the midpoint, an average value of 512.42 lux. The distribution of illuminance for four transmitters will receive more illuminance if we have set a semi-angle at half power of 80°, the luminous flux maximum values of 1,816.0 lux, and an average value of 569.75 lux.

3.2.2 Optical power of street light

The optical power received distribution for at receiver plane in a LOS path, we do not consider the reflection path given by

$$P_r = P_t \frac{(m+1)}{2\pi d^2} \cos^m(\phi).T_s(\psi).g(\psi)\cos(\psi), \quad 0 \le \psi \le \psi_c \tag{3.4}$$

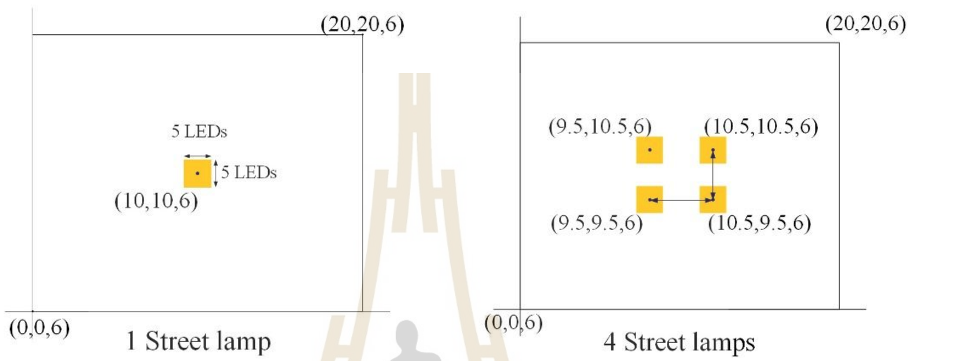

(a) Transmitter position 1 lamp (b) Transmitter position 4 lamps

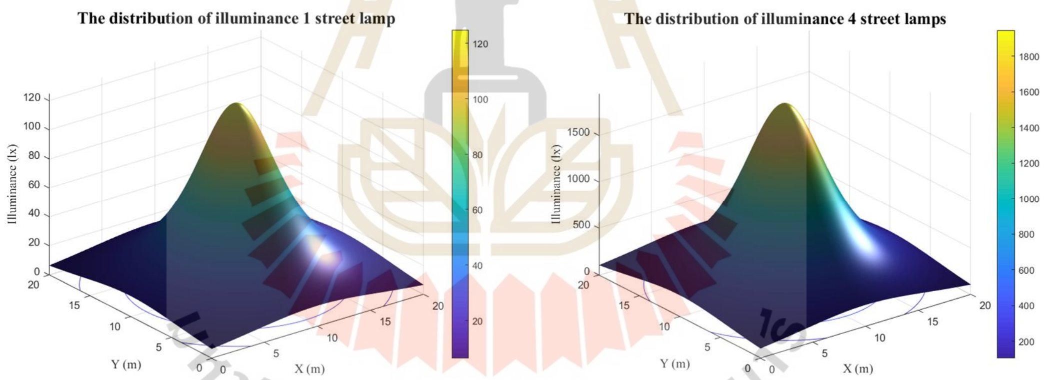

(c) 1 street lamp (d) 4 street lamps.

Figure 3.5 The distribution of illuminance street light, (a) Transmitter placed 1 lamp, (b) Transmitter placed 4 lamps, (c) 1 street lamp, and (d) 4 street lamps.

where ψ is an incidence angle with respect to the axis normal to the receiver surface, $g(\psi)$ is the concentrator gain at the receiver, ψ_c is the field of view (FOV) of detector, $T_s(\psi)$ is the filter transmission, and d is the distance between transmitter and receiver. The Lambertian order m is given by the equation (3.2).

The gain of the optical concentrator at the receiver is defined by

$$g(\psi)=\begin{cases}\dfrac{n^2}{\sin^2(\psi_c)}, & 0\le\psi\le\psi_c\\ 0, & \psi>\psi_c\end{cases} \tag{3.5}$$

The variable “ n ” represents the refractive index of the lens at the located where the light passes through and reaches the photodetector.

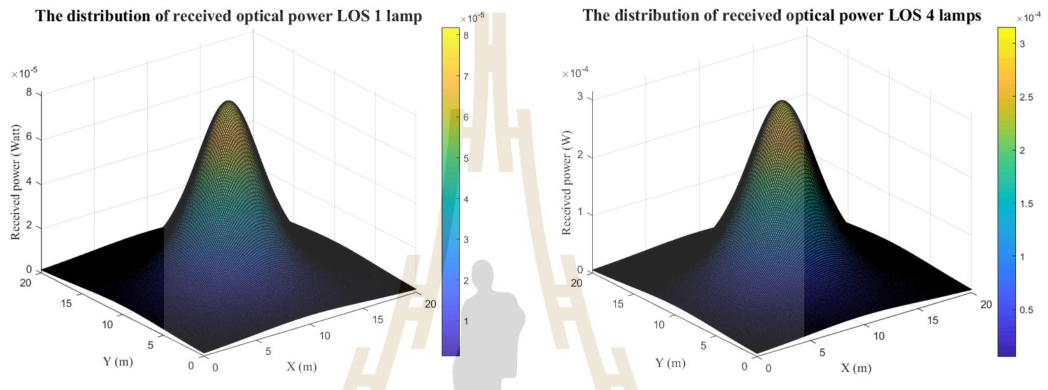

(a) (b)

Figure 3.6 The distribution of received optical power LOS in watt (a) 1 street light (b) 4 street light with the LED semi-angle at half power of 70 degrees.

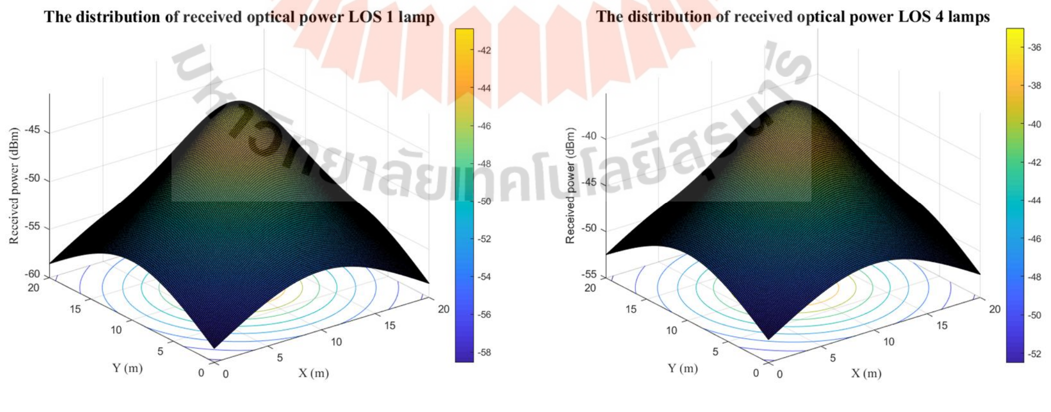

(a) (b)

Figure 3.7 The distribution of received optical power LOS in dBm (a) 1 street light (b) 4 street light with the LED semi-angle at half power of 70 degrees.

Figure 3.6 illustrates the distribution of received optical power for the LOS link measured in watts, as Figure 3.6 (a) the street light of 1 lamp and (b) the street light of 4 lamps. The optical power maximum values for Figure 3.6 (a) and (b) are 8.18x10^{-5} watts and 6.94x10^{-5} watts for one lamp and four lamps, respectively. Figure 3.7 illustrates the distribution of received optical power for the LOS link measured in dBm, as Figure 3.7 (a) the street light of 1 lamp and (b) the street light of 4 lamps. The optical power maximum values for Figure 3.7 (a) and (b) are -40.87 dBm and -36.16 dBm for one lamp and four lamps, respectively.

3.3 Channel modeling

The distribution of the radiation intensity pattern is modelled using a generalized Lambertian radiant intensity as equation (3.1) (Ghassemlooy et al., 2019; Komine & Nakagawa, 2004). The luminous intensity is used for expressing the brightness of an LED. The transmitted optical power indicates the total energy radiated from an LED. Luminous intensity is given in (Ghassemlooy et al., 2019), that is the luminous flux per solid angle. From the section 3.2, the transmitted optical power is $nLED \times nLED \times P_{LED}$ directly influenced by the strength of the sent optical signal.

$$P_t = nLED \times nLED \times P_{LED} \tag{3.6}$$

Take into account the direct current (DC) gain of the channel on direct pathways, also known as line-of-sight (LOS) paths. which is provided equation (3.7)

$$H_{LOS}(0) = \begin{cases} \dfrac{A_r(m+1)}{2\pi d^2}\cos^m(\phi)T_s(\psi)g(\psi)\cos(\psi), & 0 \le \psi \le \psi_c \\ 0, \quad eleswhere \end{cases} \tag{3.7}$$

where $T_s(\psi)$ is the optical filter transmission gain, $g(\psi)$ is the concentrator gain at the receiver , ψ_c is the field of view (FOV) of detector, A_r is the physical area of the photodetector in PD, ϕ is the irradiance angle of the transmitter, ψ is the incidence angle at the receiver. The received optical power P_r is expressed as the equation (3.4) or $P_r = P_t H_{los}(0)$. The propagation of light is based on the LOS link. We do not consider the channel DC gain on the reflection path. The channel response of light propagation from the transmitter to the receiver can be calculated as equation (3.8).

$$h_{LOS}(t) = \frac{A_r(m+1)}{2\pi d^2}\cos^m(\phi)T_s(\psi)g(\psi)\cos(\psi)\delta\left(t-\frac{d}{c}\right) \tag{3.8}$$

Where $h_{LOS}(t)$ is the impulse response of light propagation between the transmitter and the receiver, $\delta(.)$ is the Dirac function, and $\delta\left(t - d/c\right)$ represents the signal propagation delay. This function expression assumes that $\phi < 90^{\circ}$ and $\psi < FOV$ and $d \gg \sqrt{A_r}$. We show the signal propagation delay for the VLC-I2V system. Figure 3.8 shows the effect of light dispersion on the channel impulse response, Figure 3.8 (a) the real impulse response, its magnitude is 4.7624 x 10^{-4} and (b) the impulse response normalized to 1. In Figure 3.8, we placed the receiver at (0.5, 10.0, 6.0), It is located close to the boundary of the poor lighting condition in the road configuration. The LEDs have an impulse response of about 35.5 ns for light diffusion.

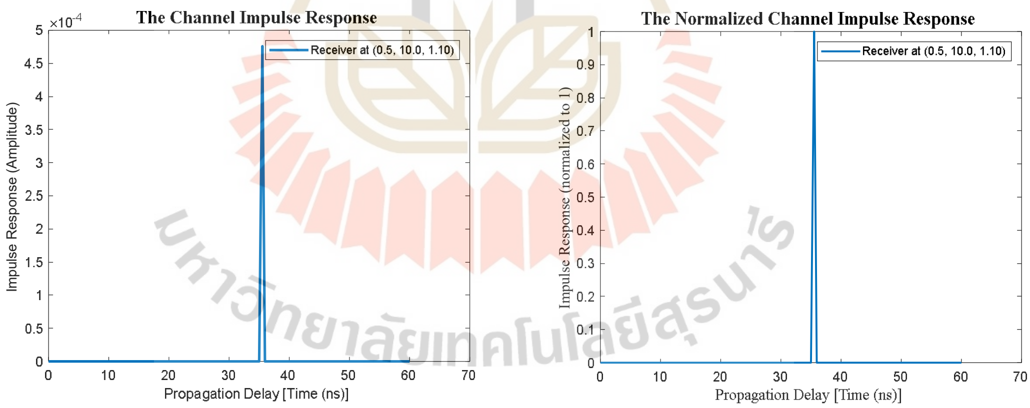

(a) (b)

Figure 3.8 The channel impulse response of LOS link with the receiver fixed near the edge.

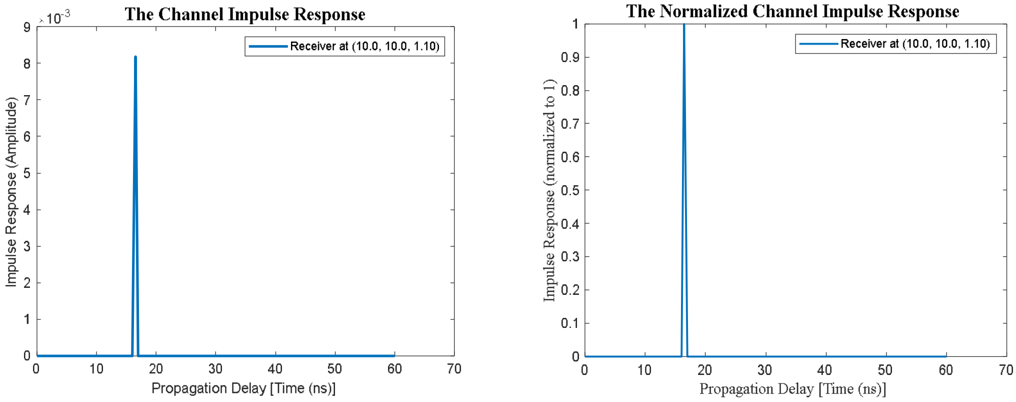

(a) (b)

Figure 3.9 The channel impulse response of LOS link with the receiver fixed close to the center.

Figure 3.9 (a) the real impulse response, its magnitude is 8.201 x 10^{-3} and (b) the impulse response normalized to 1. For Figure 3.9, we placed the receiver at (10.0, 10.0, 6.0), it is rather close to the center of the road setting dimension. The impulse response of LEDs light propagation is around 16.5 ns.

The photodetector is received the light then converted to the electrical current as $i = P_r * R_{PD}$. To study the SNR for the OWVLC-I2V system, the SNR can be expressed in terms of the received optical power (P_r), the photodetector responsivity (R) (Ampere/Watt), and noise variance that is (Ghassemlooy et al., 2019)

$$SNR = \frac{(R_{PD} P_r)^2}{\sigma_{shot}^2 + \sigma_{amp}^2} \tag{3.9}$$

where the shot noise and amplifier noise variances are given by (Zeng et al., 2008)

$$\sigma_{shot}^2 = 2qB_n \left(R_{PD} P_r + P_n \right) \tag{3.10}$$

$$\sigma_{amp}^2 = i_{amplifier}^2 B_a \tag{3.11}$$

where B_n is noise bandwidth $B_n = I_2 R_b$, R_b is the data rate, B_a is the amplifier bandwidth, q is the electron mass, P_n is the noise power of the ambient light, i_{amp}^2 is the amplifier noise density and I_2 is the noise bandwidth factor. The total noise is given by

$$\sigma_{total}^2 = 2qR_{PD}B_n\left(P_r + P_n\right) + i_{amp}^2 B_a \tag{3.12}$$

The SNR distribution is illustrated in dB as Figure 3.10. We designed the parameters of SNR as following these B_n is $R_b\left(20Mbps\right)\times I_2\left(0.562\right)$, $B_a = 50MHz$, $R_{PD} = 0.55$, $q = 1.6\times10^{-19}$, $i_{amp}^2 = 50\,pA/\sqrt{Hz}$, $P_n = 0.07\times10^{-6}$, and $R = 0.55\,A/W$. The bit error rate can be calculated from the SNR as $BER = Q\sqrt{SNR}$, where $Q(x) = \frac{1}{2}\int_x^\infty e^{-y^2/2}\,dy$.

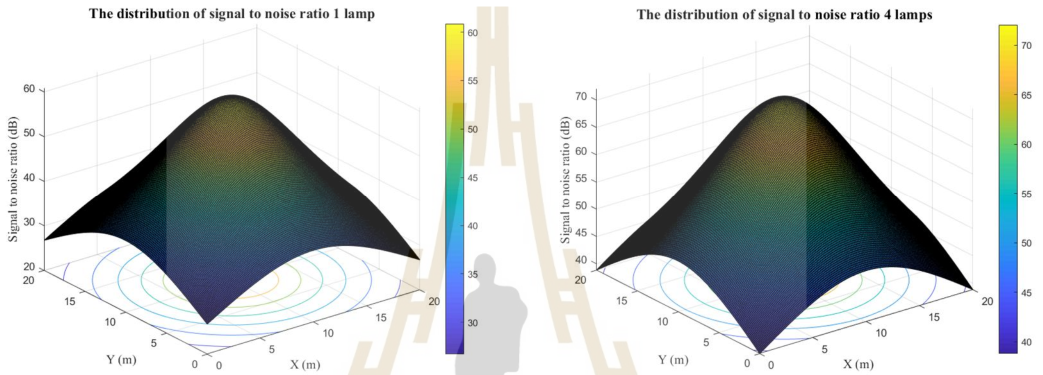

(a) (b)

Figure 3.10 The signal to noise ratio distribution for an optical bandwidth at data rate 20 Mbps, (a) 1 street lamp (b) 4 street lamps.

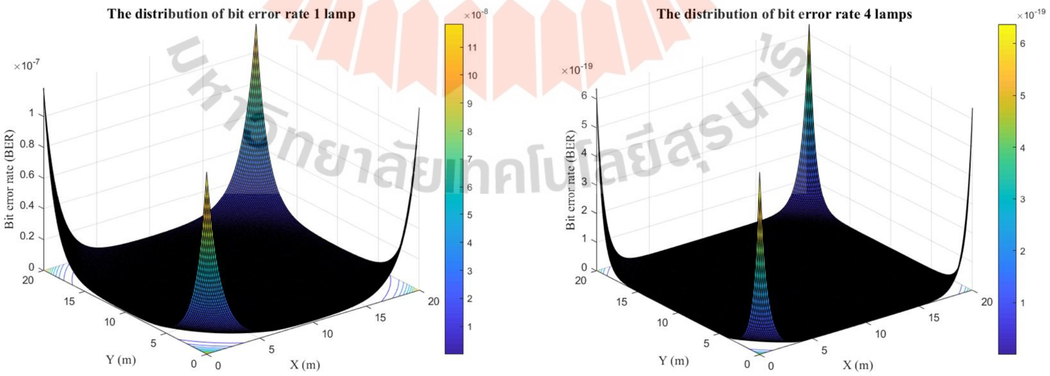

(a) (b)

Figure 3.11 The distribution of BER for the communication areas, (a) 1 street lamp (b) 4 street lamps.

Figure 3.11 illustrates the performance of bit error rate for OWVLC-I2V system by as Figure 3.11 (a) the 1 street lamp and (b) the 4 street lamps have been used for our simulation system. The performance of BER is related to the SNR that we received, it seems at around the edge or the corners that higher BER related to the low SNR.

3.3.1 The channel model for the VLC-I2V SISO System

We designed the I2V communication system using visible light communication. Furthermore, we have considered while the receiver is installed on/in the car's dashboard and the vehicle moves through the coverage areas. The areas 20 m x 20 m are the road dimensions for our communication areas in the I2V system. We assume the vehicle speed is 90 km/hr, and the coverage area is 20 meters. Then, the vehicle could take the time of 0.85 seconds to pass the communication areas. We study the channel response of I2V while the vehicle moves through the communication area on the road. The data rate is 20 Mbps, and the distance down the road is 20 meters. We divided the channel LOS link into three positions: the number of LOS for studying the channel response and the vehicle speed of 90 km/hr. Table 3.2 shows the parameters related to the transmitted data and the vehicle speed for the I2V system.

We applied the channel DC gain on the direct paths as in equation (3.8) to the OWVLC-I2V system configuration. The LOS link occurs by the number of LOS path positions that can be written as an infinite sum:

$$h^{v}_{LOS}\left(t,R_x\right)=\sum_{nLOS=1}^{NLOS} h^{v}_{nLOS}\left(t,R_x\right) \tag{3.13}$$

where v is the vehicle speed, $nLOS$ is the total amount of LOS link positions, R_x is the amount of receiver, Consequently, the transmitter has a greater number of lights, thus necessitating a modification of equation (3.13) to

$$h^{v}_{LOS}\left(t,R_x\right)=\sum_{nLOS=1}^{NLOS}\sum_{nLamp=1}^{NLamp} h^{v}_{nLOS,nLamp}\left(t,R_x\right) \tag{3.14}$$

Table 3.2 The relation between the number of LOS link and the data rate per position.

Vehicle speed	Time over area	Coverage area	Number LOS links	Data rate	Data received	Data rate / position
90 km/hr 25 m/sec.	0.8 sec.	20 m	3	10 Mbps	8 Mb	2.6 Mb/pos.
				20 Mbps	16 Mb	5.3 Mb/pos.
90 km/hr 25 m/sec.	0.8 sec.	20 m	5	10 Mbps	8 Mb	1.6 Mb/pos.
				20 Mbps	16 Mb	3.2 Mb/pos.
90 km/hr 25 m/sec.	0.8 sec.	20 m	7	10 Mbps	8 Mb	1.14 Mb/pos.
				20 Mbps	16 Mb	2.2 Mb/pos.

Table 3.2 shows the relationship between the number of LOS links and the data rate per position while the receiver passes over the communication area. For example, if the vehicle speed is 90 km/hr (or 25 m/s), moving over the coverage area of 20 meters, then time over the area is taken of 0.8 seconds, we divided the channel response into three positions, which is the number of LOS path $(nLOS)$ (as shown in Figure 3.12). Furthermore, the range that we divided is equally as the same range. The data rate is 20 Mbps, the data per position is around 5.3 Mb, and the total received data is 16 Mb.

Figure 3.13 shows the channel impulse response of the channel model LOS link while the vehicle is moving. The receiver positions are at (6.6, 10.0, 1.10), (13.2, 10.0, 1.10) and (19.8, 10.0, 1.10). The peak channel impulse response occurs at different position because the distance of the transmitter and the receiver is changed. Furthermore, the total transmitted data is depended on the velocity of the vehicle inside the designated communication zone, because of limited time. The total transmitted data is given as

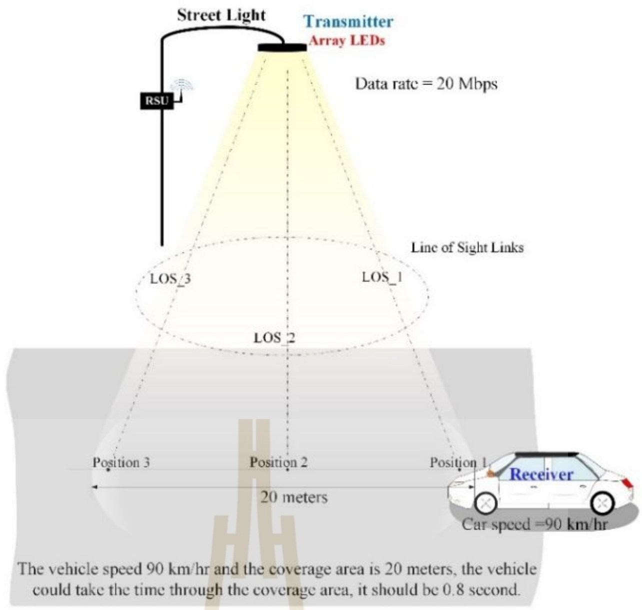

Figure 3.12 The channel model of LOS link, nLOS = 3.

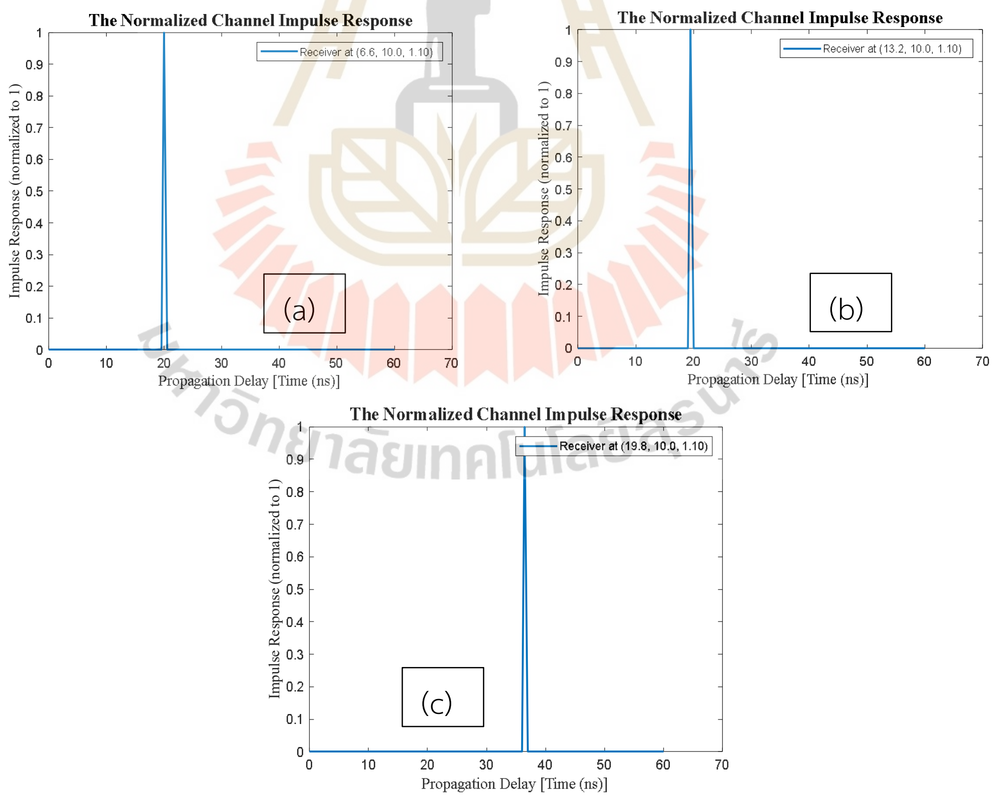

Figure 3.13 The channel impulse response of 3 LOS links.

$$D_{tx} = (t_{over}) \times D_R \tag{3.15}$$

where D_R is input bit (bps), D_{tx} is the total transmitted data during the vehicle through communication areas (20 m), and t_{over} is time of vehicle through the communication areas. Therefore, the Table 3.2 shows the bit input of 10 Mbps and 20 Mbps and the different number of LOS link 3, 5 and 7, at the vehicle speed 90 km/hr the data rate per position of LOS links is displayed in the Table 3.2.

In Figure 3.14, the LOS link is divided to 5 positions which are the quantity of LOS paths $(nLOS)$. Furthermore, the range is equally as the same range as shown in Figure 3.14. The data rate is 20 Mbps and the data per position is around 3.2 Mbps and the total received data is 16 Mbps.

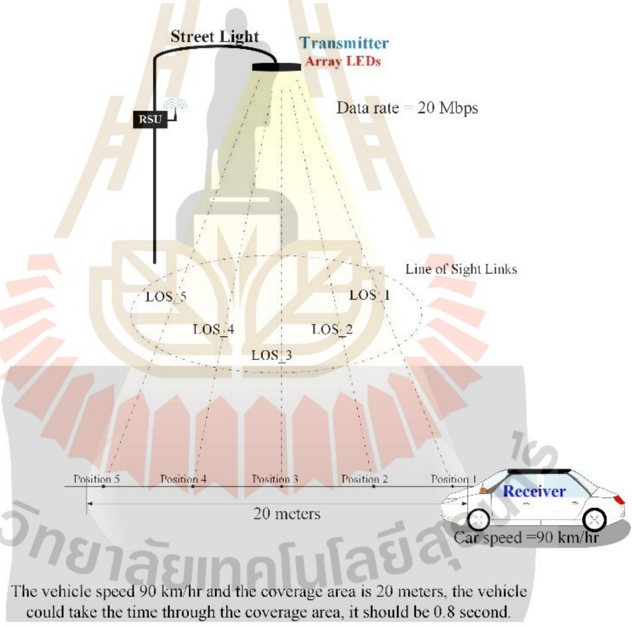

Figure 3.14 The channel model of LOS link, nLOS = 5.

The impulse response of 5 LOS links is shown in Figure 3.15. The receivers are at (4.0, 10.0, 1.10), (8.0, 10.0, 1.10), (12.0, 10.0, 1.10), (16.0, 10.0, 1.10), and (20.0, 10.0, 1.10). Each receiver position provides the differences of the channel impulse response. It is shown that the light propagation arrived at the receiver. Also, the received optical power in each position is so different that we must study the average received optical power. Moreover, the relation of vehicle speed to both the channel impulse response and the received optical power is investigated.

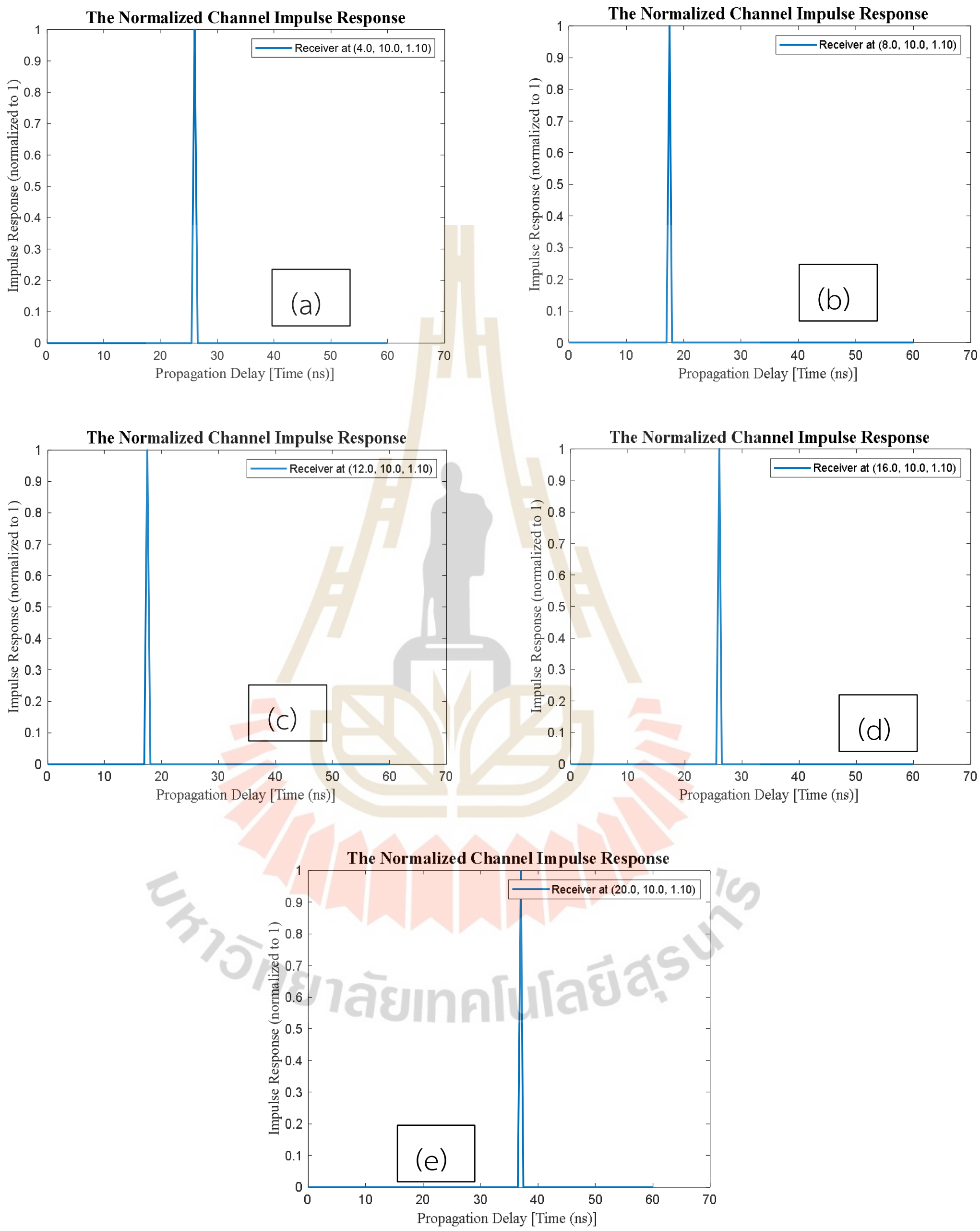

Figure 3.15 The channel impulse response of 5 LOS links.

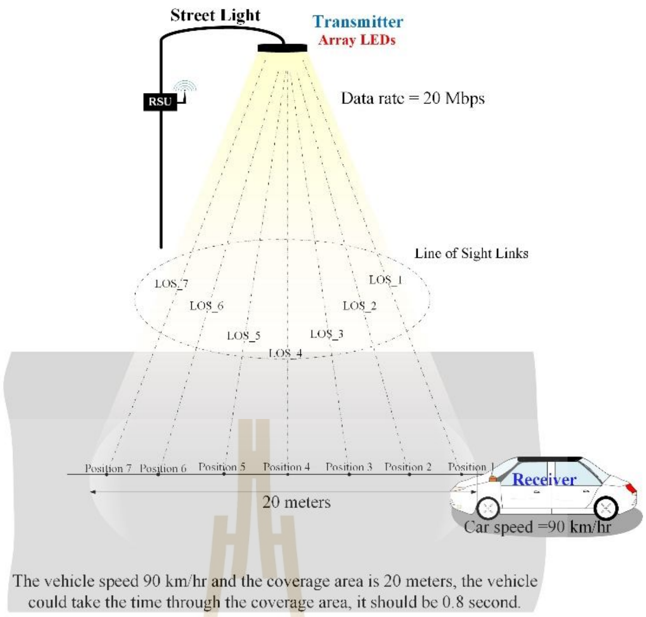

Figure 3.16 The channel model of LOS link, nLOS = 7.

The number of LOS links is 7 positions which are at (2.85, 10.0, 1.10), (5.70, 10.0, 1.10), (8.55, 10.0, 1.10), (11.40, 10.0, 1.10), (14.25, 10.0, 1.10), (17.10, 10.0, 1.10), and (19.95, 10.0, 1.10) along the road as the communication area (as see in Figure 3.16). The results are shown in Figure 3.17 (a) - (g). The data rate per position is approximately 2.2 Mb per position when the vehicle speed is 90 km/hr.

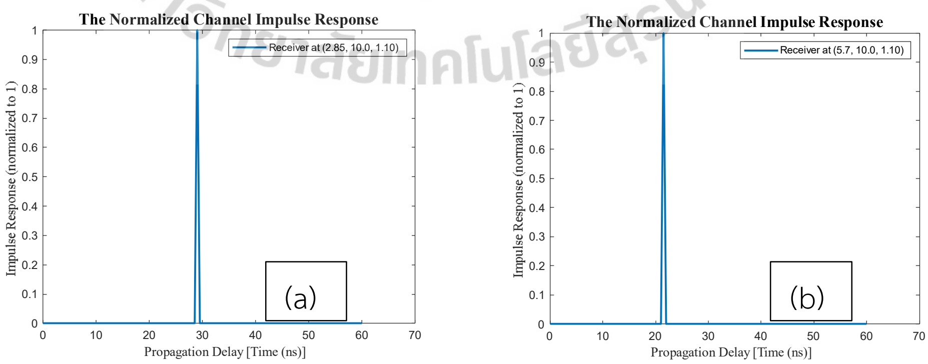

Figure 3.17 The channel impulse response of 7 LOS links.

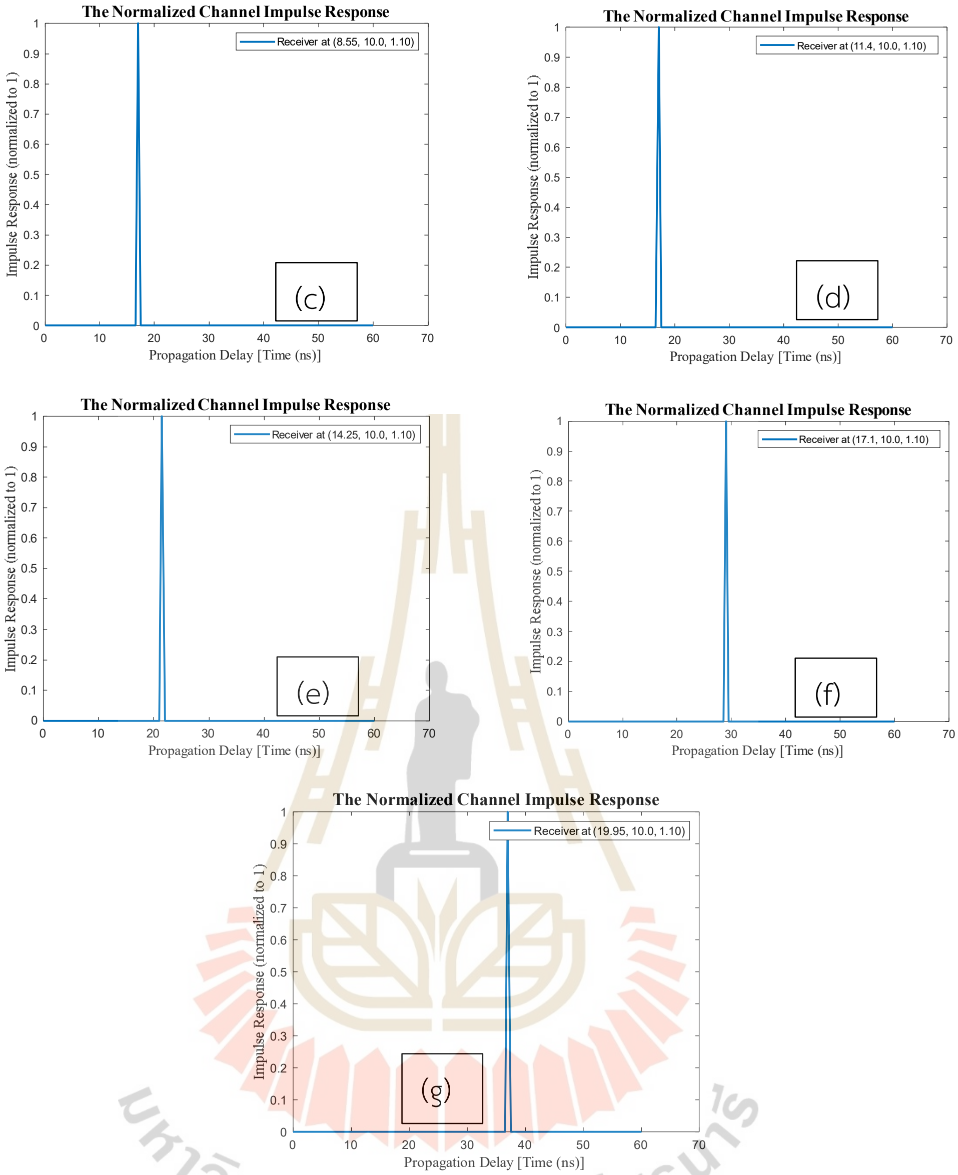

Figure 3.17 The channel impulse response of 7 LOS links (continued).

From Figure 3.13, 3.15 and 3.17, the results of determining the impulse response signal of the I2V communication channel are shown. The impulse response signal represents the signal generated on the communication channel of the system. It shows the occurrence of impulse response signals at various positions throughout the communication area coverage.

3.3.2 The channel model for VLC-I2V MISO System

The following part outlines the channel design for VLC-I2V system using multiple input single output (MISO). The purpose of this setup is to analyze the channel impulse response by introducing additional transmitters and positioning the receiver at the communication area's periphery. Four lamps were incorporated as additional transmitters. Transmitters are placed at Tx1(9.5, 9.5, 6), Tx2(10.5, 9.5, 6), Tx3(9.5, 10.5, 6), and Tx4(10.5, 10.5, 6) as shown in Figure 3.18. The rest of all parameters are shown in Table 3.2. To study the CIRs, the receivers are positioned at two different locations that are Rx(19.95, 0.5, 1.10) and Rx(19.0, 5.0, 1.10). The receiver positions are fixed. To illustrate the channel impulse response of VLC-I2V system using MISO technique. Figure 3.19 shows the channel impulse response of MISO technique of both receiver positions. The propagation of lights from Tx1, Tx2, Tx3 and Tx4 are arrived at the photodetector.

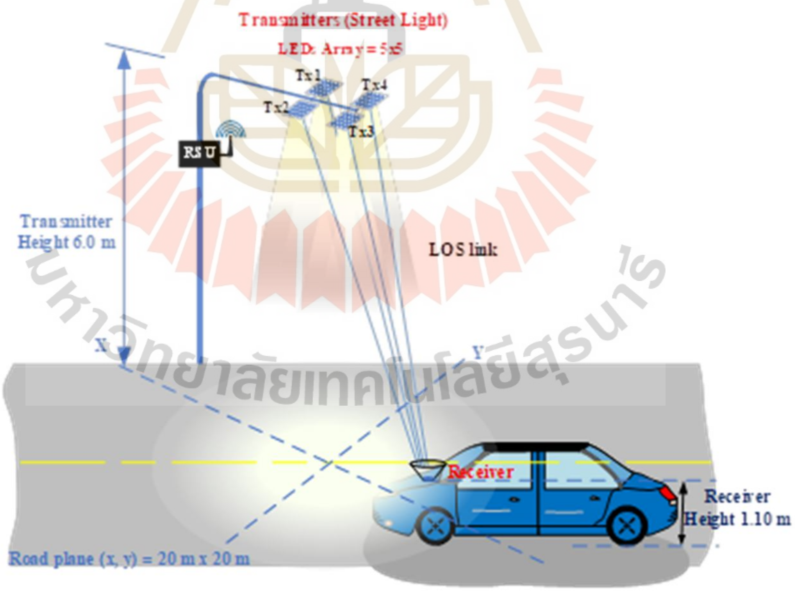

Figure 3.18 Geometry of the VLC-I2V MISO system

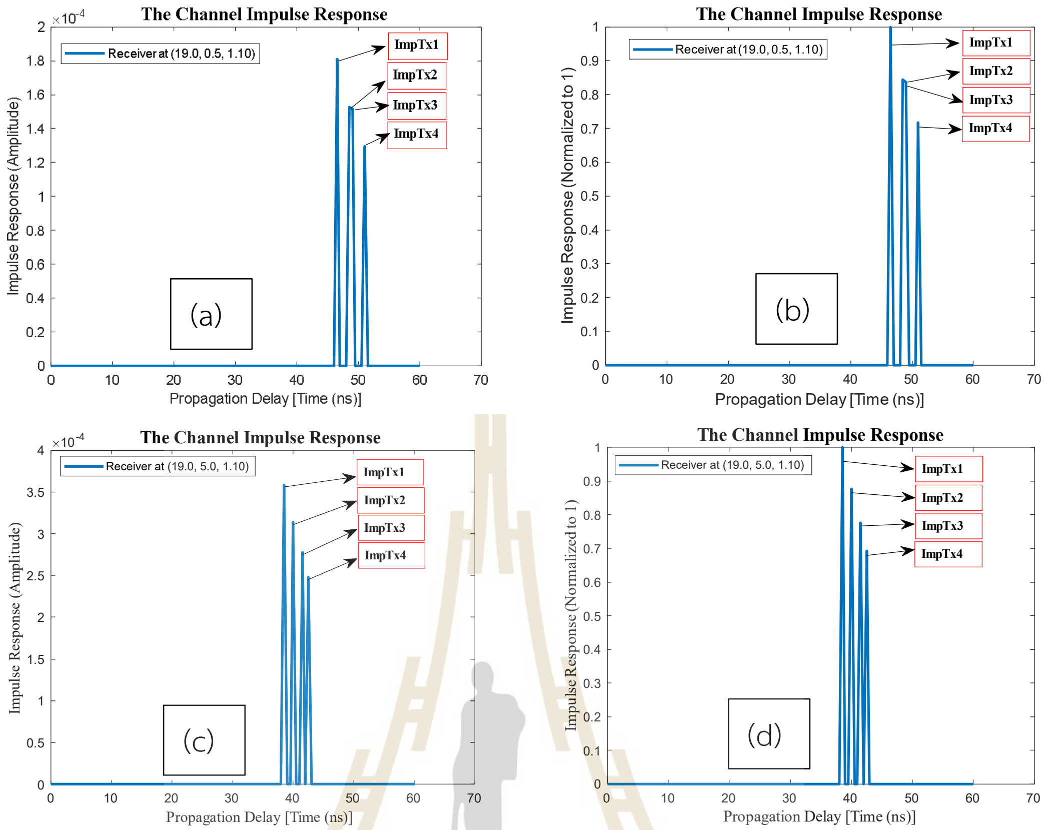

Figure 3.19 The channel impulse response of VLC-I2V system using MISO, (a) receiver position 1 at (19.0, 0.5, 1.10), (b) normalized to 1, (c) receiver position 2 at (19.0, 5.0, 1.10), (d) normalized to 1.

3.4 Receiver design for VLC-I2V SISO system

This section describes the modeling of the receiver design for I2V communication system based on visible light communication. To understand all the I2V system and the data transmitted through the LED response and the channel impulse response. The receiver designing is illustrated as the Figure 3.20. The data input a_k is the random binary bit 1 and 0, the number of binary bits is L bits. The data input is modulated with OOK scheme. Then, the signal is convoluted with the LED response $h_{LED}(t)$ (Zeng et al., 2008) and the optical channel impulse response $h_{CIR}(t)$ respectively. Therefore, the signal input is transmitted with the LED street light in case of our study. The receiver is combination with the equalizer, low-pass filter

(LPF), sampling the analog to digital signal and the threshold detector to decode the binary output data.

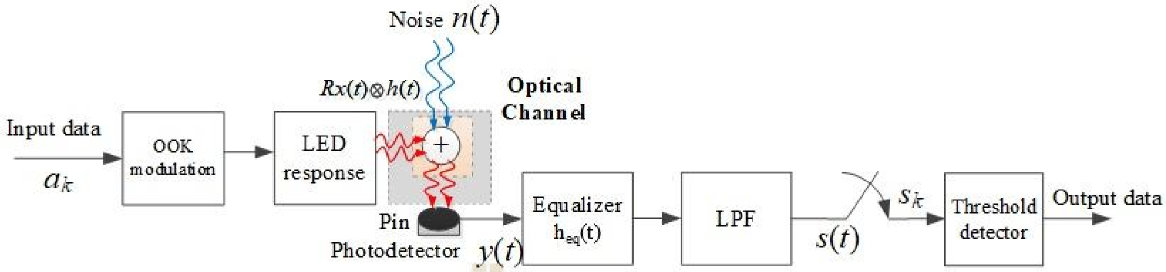

Figure 3.20 Block diagram of OWVLC-I2V SISO system.

$$y(t)=\left[x(t)\otimes h_{LED}(t)\otimes h_{CIR}(t)\right]+n(t) \tag{3.16}$$

where $h_{LED}(t)$ is the impulse response of LED and given as (Zeng et al., 2008), $x(t)$ represents the input data, $h_{CIR}(t)$ denotes the channel impulse response, $n(t)$ is the noise signal and $y(t)$ denotes the received signal from PD which conversed the optical signal to electrical signal.

3.5 External interference considerations

In the context of OWVLC-I2V system, “external interference” refers to any unwanted signals or influences that disrupt the transmission or reception of data through light. OWVLC-I2V system utilizes light LEDs, to transmit data by modulating the intensity of light signals. However, various factors can introduce interference, potentially degrading the system’s performance. Figure 3.21 shows some common sources of external interference in OWVLC-I2V systems.

Figure 3.21 Model of external optical interference in OWVLC-I2V system.

From Figure 3.21, A, B, and C are the ambient lights, (A) is indoor lighting from the building nearby, can interfere with the signal being transmitted. This interference can lead to inaccuracies in data reception or reduced signal-to-noise ratio. And next interference is lighting from another street light (B) that two light overlapping each other. Both interferences from A and B are not considered because It has little light intensity. (C) is the light from the headlighting of vehicle traveling the opposite direction. (D) is atmospheric conditions; environmental factors such as rain, gloomy, cloudy, fog, haze, or atmospheric turbulence can scatter or attenuate light signals, impacting the reliability and range of OWVLC-I2V transmissions. As mentioned above, this is optical interference from factors outside the designed OWVLC-I2V system. From reviewing past literature, it was found that there were attempts to study external interference in the VLC system, such as (Galal et al., 2018; Moreira et al., 1995), an interference model was deduced to determine the overall noise power due to these light sources. Therefore, the system takes into account the direct light emitted by street lights onto vehicles. Many studies reviewed do not consider external noise signals in this way as well. The study clearly states that it will be conducted in a specific, point-by-point manner. In this thesis, the effects of external noise signals are not considered as well.

3.6 Summary

In Chapter 3, we designed the outdoor wireless visible light communication system for infrastructure-to-vehicle communication applications. By simulating the transmitter which is an LED street lamp to study the channel impulse response signals. In case of the single-input single-output (SISO) and multiple-input single-output (MISO) were studied in this chapter. Also, we studied multiple-input single-output (MIMO) in the next chapter. The scenario of the OWVLC-I2V system was equipped by the transmitter and the receiver. All parameters were designed in this chapter for all to evaluate the CIRs. The communication link is designed in three cases 3 links, 5 links, and 7 links for the coverage communication area. To assume the automobile crosses the illuminated zone and to find the channel impulse response of each links. Finally, we showed the receiver designed for the OWVLC-I2V system in section 3.4. To showcase the data transfer of the Outdoor Wireless Visible Light Communication (OWVLC) system from input to output in a Single-Input Single-Output (SISO) configuration.

CHAPTER IV
A RECEIVER DESIGN FOR THE OWVLC-I2V SYSTEM USING MIMO TECHNIQUE

4.1 Introduction

This chapter proposed an optical wireless visible light communication for infrastructure to vehicle using MIMO technique. We designed the OWVLC-I2V system continuously from the chapter 3 (SISO). The concept is that the transmitter added of four street lamps and the receivers of four photodetectors. An illuminance on the road at nighttime has more an illumination. Furthermore, the traffic information broadcasted with the lighting system cooperated with the Roadside Unit (RSU) of the intelligent transportation system (ITS). We investigate the channel impulse response of OWVLC-I2V system while the vehicle on the move. Moreover, we illustrated the I2V system configuration and the receiver designed based on VLC system. All the result of this chapter is based on the signal processing simulation by Matlab programing.

Visible Light Communication (VLC) is a wireless communication technology that uses light in the visible spectrum to transmit data. Multiple-Input Multiple-Output (MIMO) is a technique used in wireless communication systems to improve performance by using multiple antennas at both the transmitter and receiver. In general, MIMO techniques can improve the throughput and reliability of VLC systems by exploiting spatial diversity. This means that by using multiple antennas, the system can mitigate the effects of fading and increase the overall data rate. The distance over which VLC with MIMO can effectively operate depends on various factors including the specific implementation, environmental conditions, the quality of the components used, and interference. There isn't a fixed or standard distance that applies universally, as it can vary greatly depending on these factors. For OWVLC-I2V system using MIMO technique, we have considered by divided into four topics. For a specific OWVLC-I2V with MIMO system, the achievable distance would need to be determined through testing and evaluation in the particular deployment scenario. Factors such as the number of transmitter used, modulation scheme, optical power, receiver sensitivity, and environmental conditions all play a role in determining the effective communication distance. The transmitter dimensions were determined by street light illumination standards (Eldeeb et al., 2023 & Lee et al., 2013) combined with research on visible light communication (Zeng et al., 2009). The first procedure in Figure 4.1 is the transmitter placement for MIMO system, it was continued from the previous chapter. We placed the transmitter to achieve the standard of streetlight luminance. (Lee et al., 2013) used height of streetlight of 10 meters and roadway width 12 meters.

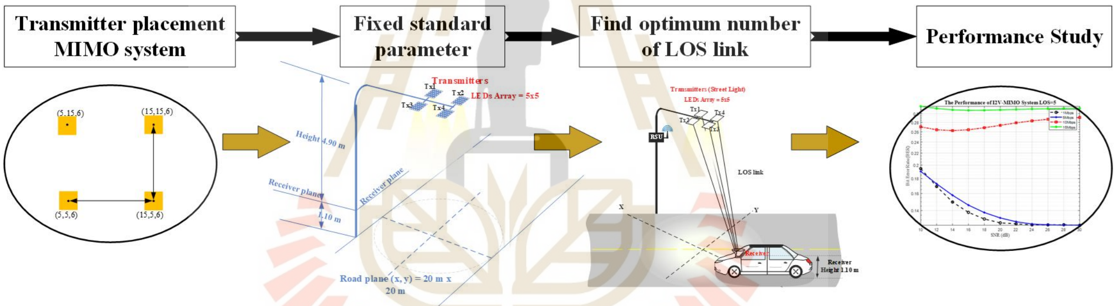

Figure 4.1 Standard parameter relationships for OWVLC-I2V system design using the MIMO technique.

The third block diagram, as shown in Figure 4.1, shows the process of finding the optimum number of LOS links in the OWVLC-I2V system using the MIMO technique. We have assumed the vehicle moved through the coverage communication area. The main ideal is to determine the channel impulse response signal throughout the period the vehicle moves past the communication area.

Finally, we have studied the performance of the OWVLC-I2V system using the MIMO technique in terms of bit error rate related to the signal-to-noise ratio (Zeng et al., 2009) and the throughput versus the vehicle speed related to the total received data in our transceiver, as mentioned in the next section.

4.2 Configuration of VLC-I2V system using MIMO technique

This chapter specifically examines the development of an outdoor wireless visible light communication system for infrastructure to vehicle communication using multiple-input multiple-output (MIMO) scheme. Recently, a large capacity transmission is required in optical wireless communications as well. MIMO have attracted much attention in RF and VLC wireless communications (Takase & Ohtsuki, 2004; Zeng et al., 2009). We realize that using MIMO can gain more transmission data without increasing the transmit power but add more transmitters or multiple antennas (as RF communication). This proposed to obtain the throughput more than the SISO system. However, we will receive the interference from another transmitter meanly the bit error rate will increase. We use the optical transmitter LEDs array N = 4 and the optical receiver photodetector M = 4, employ an optical wireless (OW) channel. In Figure 4.2 shows the model of VLC-I2V system using MIMO. It is considered at nighttime and the receiver on the move that installed in/on the vehicle. To investigate the CIRs, in this case the LOS link has been considered. There is a time difference in the LOS component that needs to be accounted for in the simulation.

Table 4.1 The simulation parameters for OWVLC-I2V system using MIMO.

Parameters	Values	Parameters	Values
Dimension road plane (x,y)	20 m. x 20 m.	Array LED (25 LEDs)	5 x 5
LED power	1 W.	Field of view (FOV)	120^{o}
A street light (1 lamp)	25 LEDs	Refractive lens	1
Receiver plane height	1.10 m.	Photodiode responsibility (R_{PD})	0.55
Height street lamp (z)	6 m.	Detector physical area	1 cm^2
Number of transmitters Tx1, Tx2, Tx3, and Tx4	4	Number of receivers Rx1, Rx2, Rx3, and Rx4	4

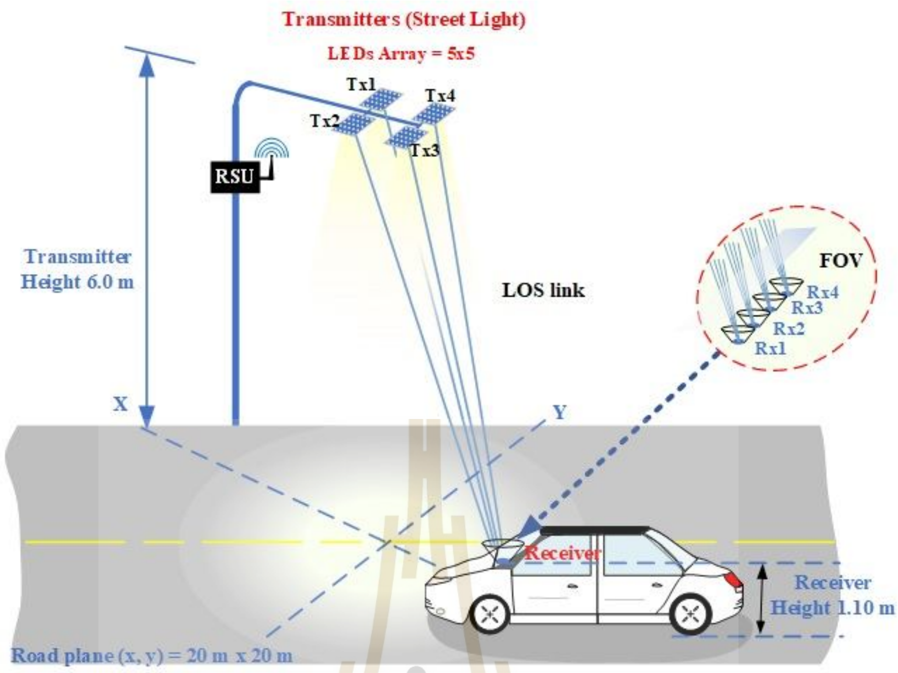

Figure 4.2 The Model of OWVLC-I2V system using MIMO.

All simulation parameters are displayed in Table 4.1. The transmitters are 4 LED array of the street lights, it is a pole of street light and each LED array is 5 x 5 (25 LEDs). The road dimension (wide and long) is 20 meters wide and 20 meters long. The transmitter height is 6 meters. Semi-angle at half power of LED or incident angle of 70°. The distance of the receiver from the road plane is 1.10 meters. (then, the vertical distance from transmitter to receiver plane is 4.9 meters). The field of view (FOV) of photodetector (PD) is 120°.

4.2.1 Illuminance of street light with 4 array LED

This section is the illuminance of street light with 4 array LED that distribute illuminance on the road dimension (20 m. long and 20 m. wide). It differs from previous section 3.2.1 because we placed the transmitter at the difference position as shown in Figure 4.3. For the distribution illuminance of MIMO system, we can use the equation (3.3) to express the transmitter arranged as Figure 4.3 (a) and (b) respectively.

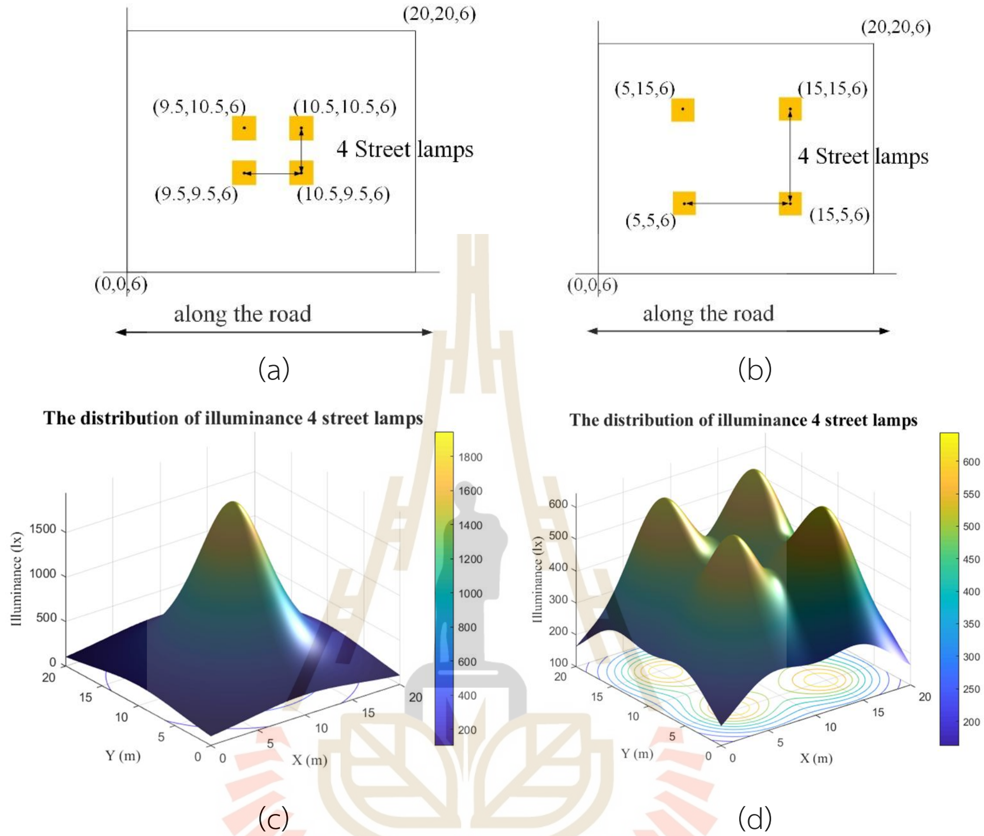

Figure 4.3 The distribution of illuminance street light as 4 transmitters (lux).

Figure 4.3 illustrates the illuminance characteristics of the streetlight, we used Matlab programing to investigate the luminous intensity of the streetlight. As the simulation parameters in Table 4.1 for OWVLC-I2V MIMO scheme. The software computes the direct illumination of 4 lamps of street light. We assumed that the focal point of luminous intensity is 3,000 lux. per array LED. Figure 4.3 (c) transmitter places Figure 4.3 (a), and also Figure 4.3 (d) transmitter places as Figure 4.3 (b). According to the Figure 4.3 (c), the maximum of illuminous is 1943.30 lx, minimum is 104.48 lx, an average is 511.33 lx. Figure 4.3 (d) the maximum of illuminous is 644.09 lx, minimum is 162.26 lx, an average is 431.13 lx.

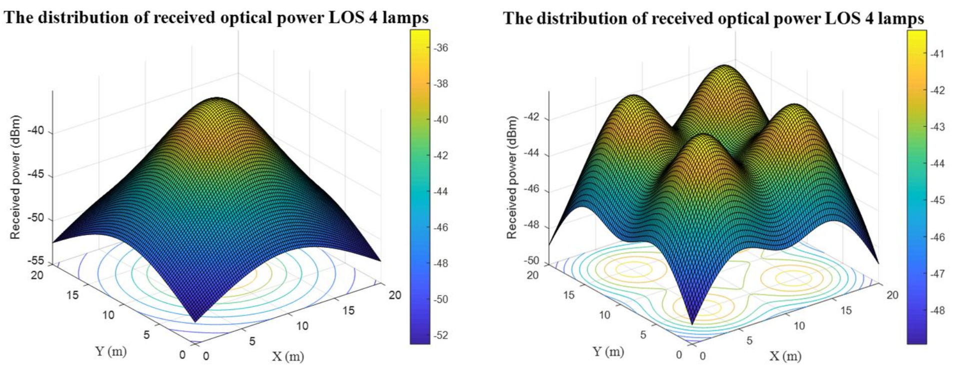

(a) (b)

Figure 4.4 The distribution of received optical power LOS in dBm, (a) and (b) are transmitter at different placed.

4.2.2 Optical power of street light with 4 array LED

According to the equation (3.4), The distribution of received optical power in the line-of-sight (LOS) connection of a visible light communication (VLC) system can be calculated using multiple-input multiple-output (MIMO) technique. Figure 4.4 illustrates the distribution of received optical power for LOS link measured in dBm, as Figure 4.4 (a) and (b) the street light of 4 lamps are placed as Figure 4.3 (a) and (b) respectively. The optical power maximum value for Figure 4.4 (a) and (b) are -35.01 dBm, -40.38 dBm.

Figure 4.5 depicts a plot with identical values to those in Figure 4.4 (a) and (b). The analysis reveals that the power distribution in Figure 4.5 (a) does not extend to the boundary of the road dimension. However, Figure 4.5 (b) demonstrates significantly greater coverage with the same 4 lamps as Figure 4.5 (a) due to a more strategically organized transmitter placement.

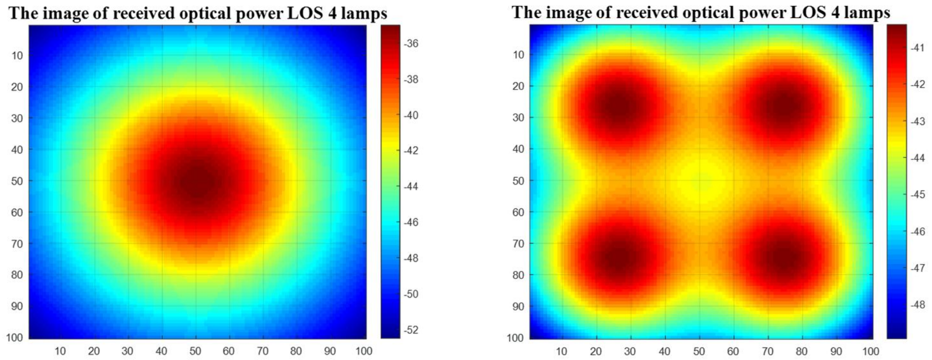

(a) (b)

Figure 4.5 The image of received optical power LOS in dBm, (a) and (b) are transmitter at different placed.

4.3 Study channel model of VLC-I2V system using MIMO technique

There are many MIMO system for employed with the VLC system (Zeng et al., 2009). The receiver will capture the optical signal from several line-of-sight connections emanating from various directions. The line-of-sight (LOS) impulse response for the multiple-input multiple-output (MIMO) optical wireless channel $h_{ij}^{v,LOS}(t)$ from the $K-LED$ in the transmitter i^{th} to the receiver j^{th}

$$h_{ij}^{v,LOS}(t)=\begin{cases}\displaystyle\sum_{k=1}^{K}\frac{A_{rj}(m+1)}{2\pi d_{ijk}^{2}}\cos^{m}(\phi_{ijk})T_{s}(\psi_{ijk})g(\psi_{ijk})\cos(\psi_{ijk}), & 0\le\psi_{ijk}\le\psi_{c}\\ 0, & elsewhere\end{cases} \tag{4.1}$$

where d_{ijk}^{2} is the distance from the i^{th} transmitter to the j^{th} receiver, A_{rj} is the collection area of the j^{th} receiver, ϕ_{ijk} is the irradiance angle of transmitter, ψ_{ijk} is the angle of incidence on the receiver, ψ_{c} is the receiver field of view (FOV). m is the Lambertian number given as equation (3.2), g is the concentrator gain at the receiver and T_s is the filter transmission. Figure 4.6 displays the channel impulse response of a Visible Light Communication (VLC) - Internet to Vehicle (I2V) Multiple-Input Multiple-Output (MIMO) system. This image considers the line-of-sight (LOS) situation at three distinct places while the receiver is in motion.

4.3.1 The channel model for the VLC-I2V MIMO system with three links

As demonstrated in Figure 4.6, we divided the communication link into three positions to study the channel impulse response of the VLC-I2V MIMO system. The first position (Pos#1) was when the vehicle arrived at the possible communication areas. The second position (Pos#2) was the center area of street lighting. And the third position (Pos#3) was the bound of the communication area. The model is depicted in Figure 4.6. All the links that can represent the channel impulse response for the VLC-I2V system are the data transmission from the street light to the vehicle moving through this area. Therefore, the impulse channel response characteristics at each position will have an impact on the functionality of data communication within the scheme. In such a way that there is minimal link break in areas that can be illuminated for the VLC-I2V communication system.

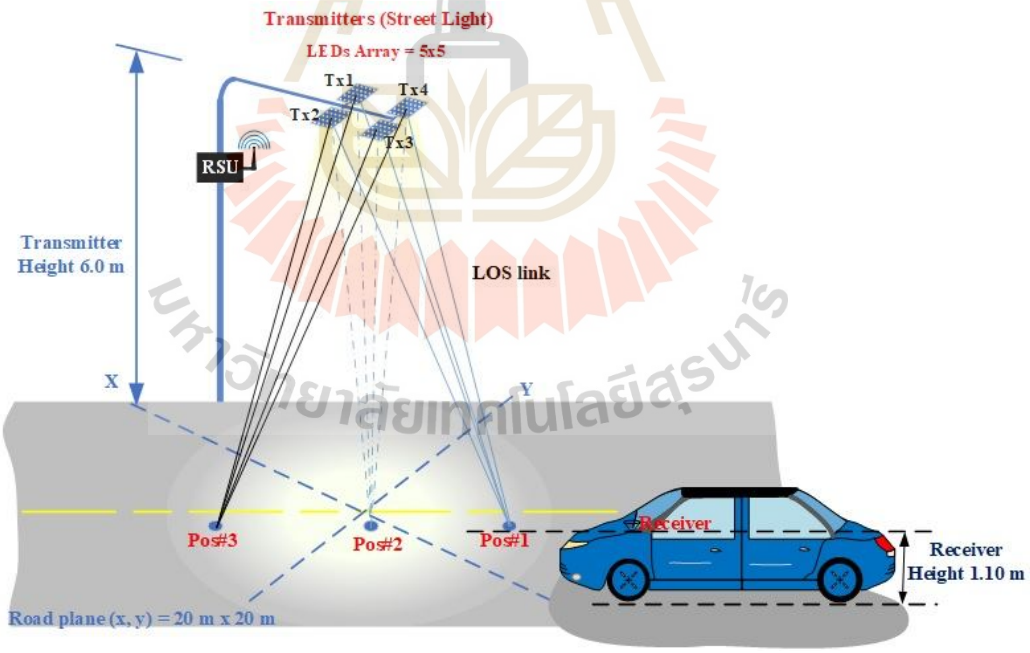

Figure 4.6 The channel modeling of LOS link, nLOS = 3 for the OWVLC-I2V MIMO system.

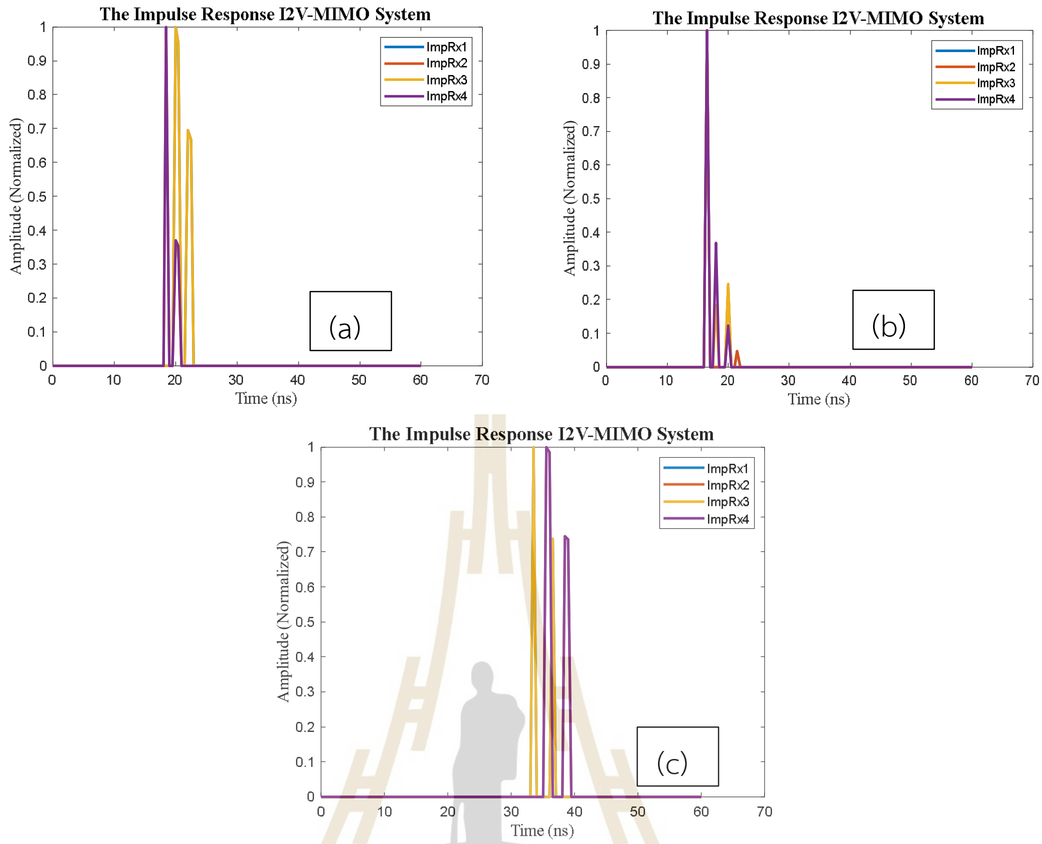

Figure 4.7 The channel impulse response of OWVLC-I2V using MIMO, LOS = 3.

Figure 4.7 shows the experimental results of the channel impulse response signal. The resulting three impulse signals correspond to the position of the designed communications link as shown in Figure 4.6. The numerical simulation according to equation (4.1) produces the impulse signal. At each designed position, we observed different signal characteristics in the impulse signal. Researchers found that the impulse signal exhibits different signal characteristics in each designed position. The first receiver detected the light signal sent by the four transmitters as the impulse signal. Therefore, the peak of the signal is an indicator of which transmitter it is coming from. The amplitude of the received impulse signal determines whether the received light is cancelled or overlapped. As a result, the total signal may not be complete from all four transmitters if we consider only one receiver. Figure 4.7 (a) to (c) shows the impulse response signals of the three designed communication links, illustrating that the total signal may not be complete from all four transmitters when considering only one receiver.

4.3.2 The channel model for the VLC-I2V MIMO system with five links

The difference from the previous topic is the increased number of communication links. The quantity of connections in this topic has been designed to be five. If the number of links increases, the system's communication efficiency will improve by reducing data errors and increasing the amount of data sent. As shown in Figure 4.8, we divided the communication link into five positions to study the channel impulse response of the VLC-I2V MIMO system. The first position is once the vehicle comes inside the possible range for communication, and all the way to the last position is the bound of the communication area. The model is depicted in Figure 4.8. All the links that can represent the channel impulse response for the VLC-I2V system are the data transmission from the street light to the vehicle moving through this area. Therefore, the impulse channel response characteristics at each position will affect the efficiency of data communication in the system. In such a way that there is a moderate link in areas that can be illuminated for the VLC-I2V communication system.

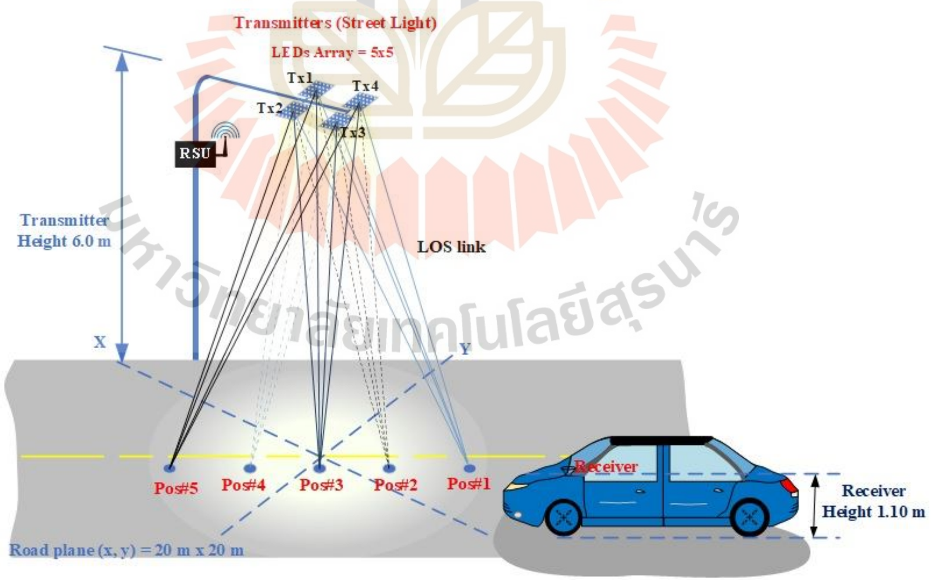

Figure 4.8 The channel modeling of LOS link, nLOS = 5 for the OWVLC-I2V MIMO system.

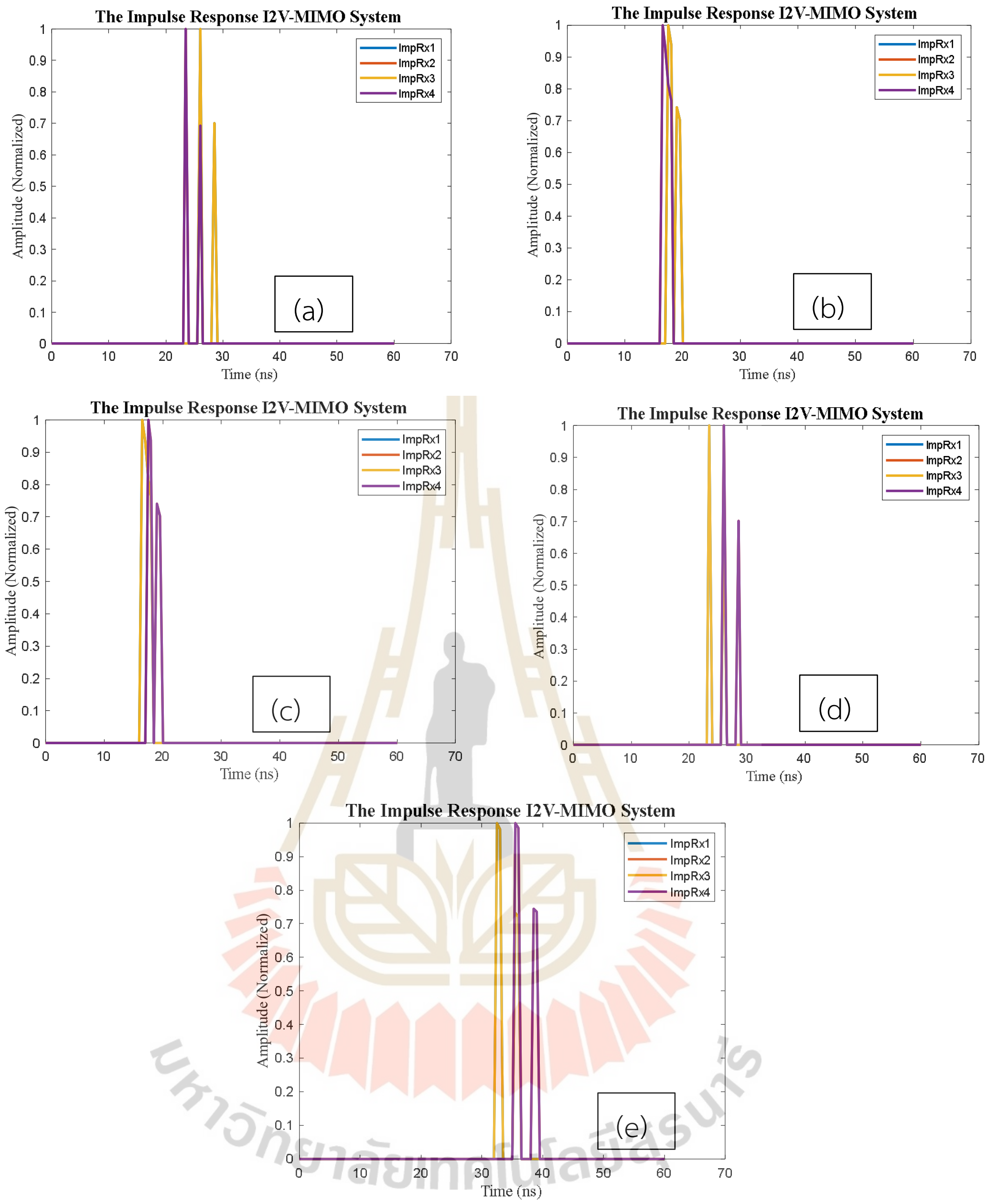

Figure 4.9 The channel impulse response of OWVLC-I2V using MIMO, LOS = 5.

Figure 4.9 shows the experimental results of the channel impulse response signal. The resulting five impulse signals correspond to the position of the designed communications link as displayed in Figure 4.8. Therefore, the impulse signals in Figure 4.9 (c) and (d) correspond to link positions in Figure 4.8, positions 3 (Pos#3) and 4 (Pos#4), respectively. The researcher designed the number of links to increase from three to five in order to hypothesize that the communication system would have higher efficiency. This chapter has shown the differences in impulse response signals at each position. The next chapter will cover the effectiveness of data communication.

4.3.3 The channel model for the VLC-I2V MIMO system with seven links

As displayed in Figure 4.10, we divided the communication link into seven positions to study the CIRs of the VLC-I2V MIMO scheme. The first position (Pos#1) is once the vehicle approaches the potential communication zone, and all the way to the last position (Pos#7) is the bound of the communication area. The model is depicted in Figure 4.10. All the links that can represent the CIRs for the VLC-I2V MIMO scheme are the data transmission from the street light to the vehicle moving through this area. Therefore, the impulse channel response characteristics at each position will impact the effectiveness of data transmission within the system. In such a way that there is the most link in areas that can be illuminated for the VLC-I2V communication system for comparison with LOS_3 and LOS_5 links.

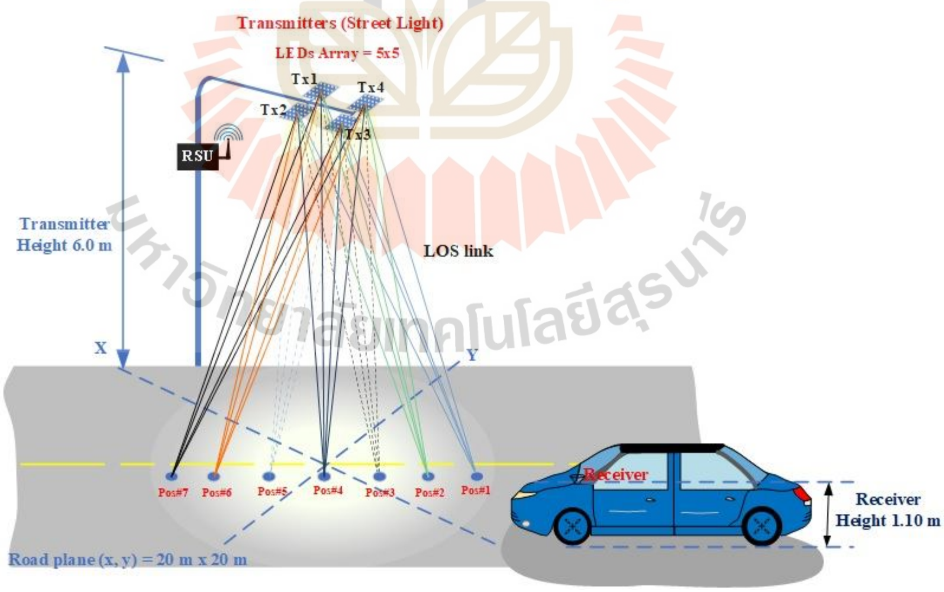

Figure 4.10 The channel modeling of LOS link, nLOS = 7 for the OWVLC-I2V MIMO system.

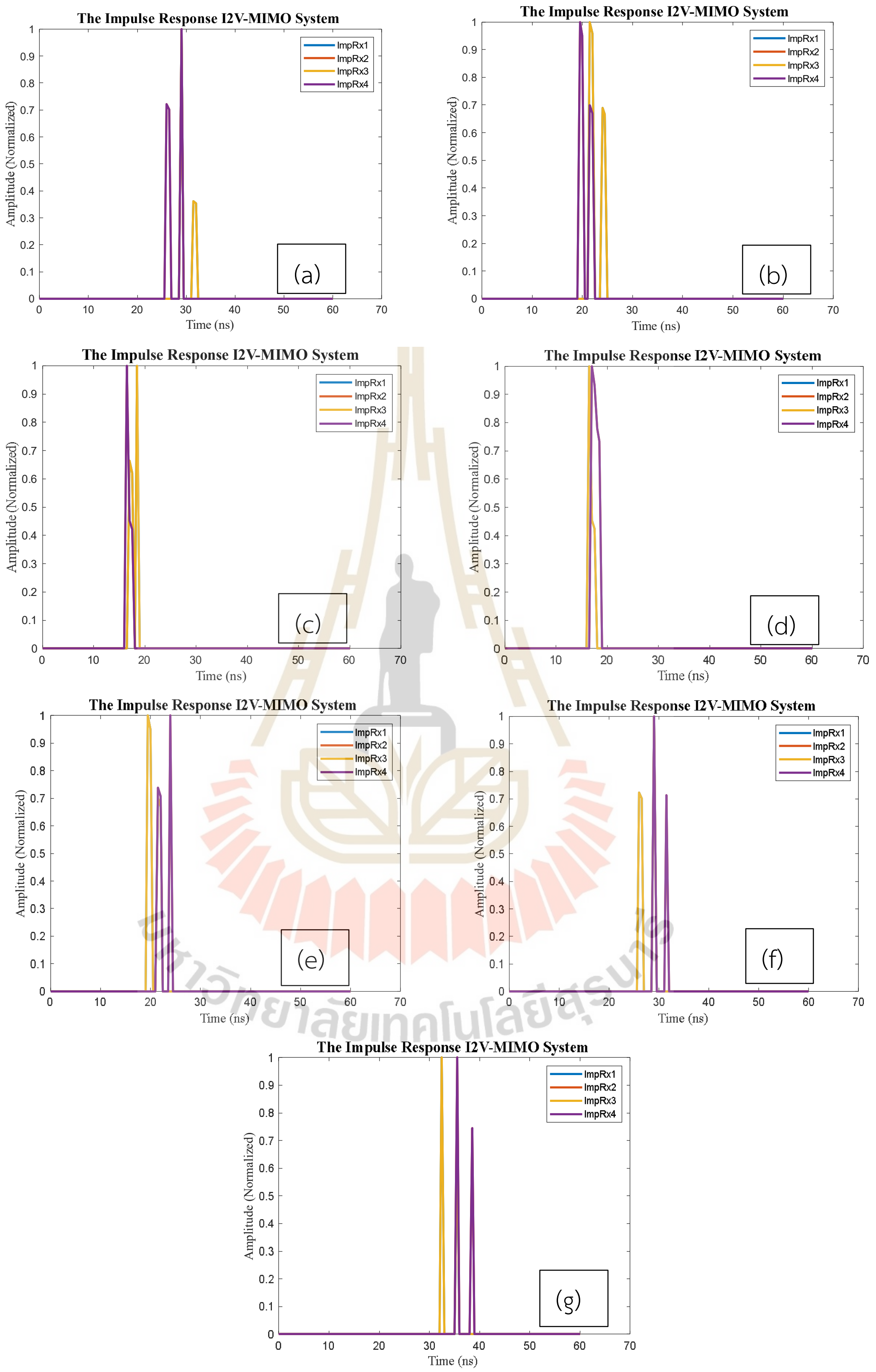

Figure 4.11 The channel impulse response of OWVLC-I2V using MIMO, LOS = 7.

Figure 4.11 is the result of a numerical simulation based on equation (4.1). There are seven link positions throughout the communication area that vehicles move through. To study the impulse response signal of the communication pathway. The results shown in Figure 4.11 (a) to (g) relate to the designed LOS link position in Figure 4.10 with reference to the position of the vehicle-mounted receiver. Studies have shown that the finer the link positions, the better we can understand the behavior of the CIRs signals. The researchers showed that the CIRs signal of a communication channel varies over the entire range of the streetlight illumination area as vehicles move through it. The impulse signals that have already been studied will determine the response of the data signals sent through this channel, as discussed in the next section.

4.4 Receiver design for VLC-I2V MIMO system

In this topic, the researcher utilized the MIMO technique to design the receiver circuit for the OWVLC-I2V system. By means of numerical simulation from the input signal through modulation into the channel. To simulate data transmission in the channel. The receiver decodes the signal to retrieve the input data. As displayed in Figure 4.12, this is the schematic representation of the MIMO system's receiver circuit. We designed the MIMO system as a four-input, four-output system. We can construct a channel impulse response matrix based on equation (4.1). Therefore, a 4x4 MIMO system forms an NxM matrix, where N is the amount of inputs or transmitters, and M is the amount of outputs or receivers. Therefore, it forms a channel matrix of size NxM. The matrix is created by the direct current (DC) gains between each transmitter and receiver, as stated in equation (4.2).

$$H_{NLOS}^{v} = \begin{bmatrix} h_{11} & h_{12} & \cdots & h_{1M} \\ h_{21} & h_{22} & \cdots & h_{2M} \\ \vdots & \vdots & \ddots & \vdots \\ h_{N1} & h_{42} & \cdots & h_{NM} \end{bmatrix}_{r \times t} \tag{4.2}$$

where $NLOS$ denotes the number of LOS link position for example as Figure 4.9 $NLOS = 5$, v represents the vehicle speed, The receiver comprises an optical concentrator as well as a photodetector and amplifier. At the receiver, utilizing the inverse of the H matrix allows for the derivation of the estimated input signals.

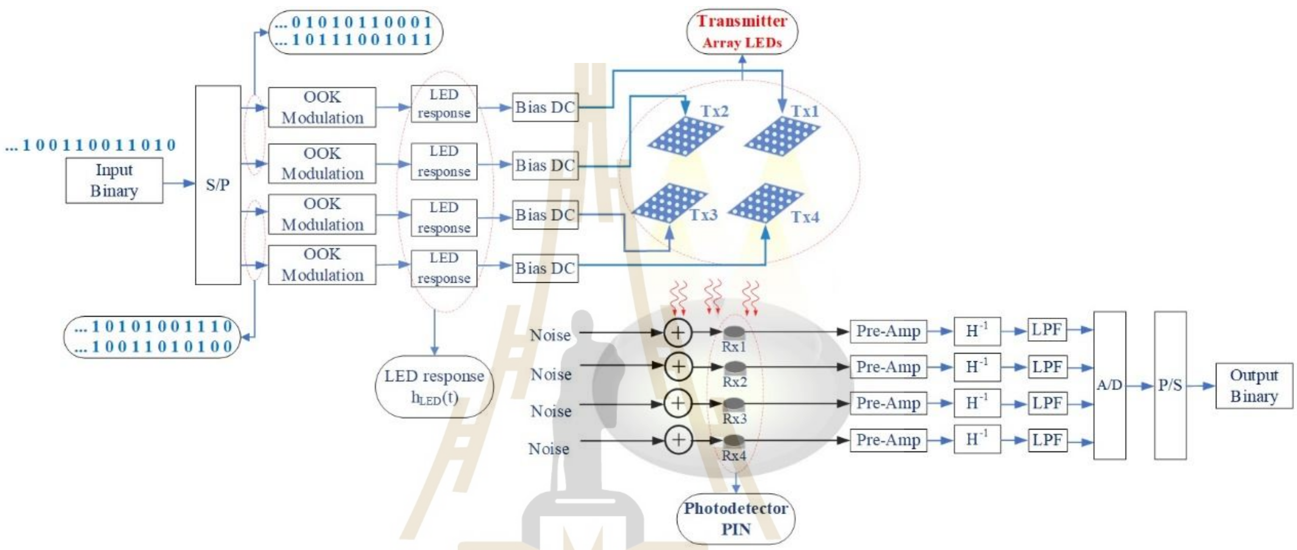

Figure 4.12 Block diagram of OWVLC-I2V system using MIMO technique.

Figure 4.12 illustrates an OWLVC-I2V system that utilizes the MIMO approach. This section introduces a Multiple-Input Multiple-Output (MIMO) system with four transmitters and four receivers. The input binary data is generated and there are converted the serial data into four parallel data stream, for example in this case of serial to parallel S/P its 4 parallel input streams. Then, each stream signal is modulated by OOK modulation. At the receiver, four photodetectors receive the light signal from four transmitters through line-of-sight (LOS) links. We have taken into account five links to indicate the duration of vehicle movement. Multiple light-emitting diodes (LEDs) are configured within a single fixture in the MIMO transmitters. The study examines the performance of bit error rate (BER) at various locations within the street lighting region in relation to the position of the receiver. We will also graph the bit error rate (BER) as a function of the received optical power. as in Figure 4.12. The optical wireless channel with IM/DD can be expressed as

The input binary is converted from serial to parallel (S/P). In the receiver the optical receive signal $Y_j(t)$ Therefore, we can write the output current $Y_j(t)$ as

$$Y = R_{PD} X H_{LOS}^{v} + n \tag{4.3}$$

where $X_i(t)$ represents the input signal i^{th} of the transmitter, N dimensional transmitted optical signal vector, Y represents the received optical signal there are M dimensional received optical signal, R_{PD} is the Photodiode responsibility, n represents the noise signal vector, and H_{LOS}^{v} represents the MIMO channel matrix, and the inverse of H matrix will be instead the received signal equalization.

4.5 Summary

In Chapter 4, the researcher designs a OWVLC-I2V system using MIMO technique that continues from Chapter 3 by increasing the number of transmitters and receivers. Study the operation of the VLC-I2V system, from the transmission device to the source of light distribution. The power distribution of light propagating from the transmitter to the receiver. As well as numerically calculating the impulse response signals of the channels in the system by designing the communication link position to simulate the situation of vehicles moving through the communication area. The result is a channel impulse response signal, which is important in the analysis of electrical signals in I2V communication systems. The last topic is the design of the receiver circuit of the VLC-I2V system used for simulating the data transmission system. Used for analyzing the electrical signals of the system and the receiver that must decode the data back. The bit error rate of transmitted data indicates system performance and the amount of received data, with the results presented in the next chapter.

CHAPTER V

SIMULATION RESULTS AND DISCUSSION

5.1 Introduction

In Chapter 5, the researcher shows the results of the experiment using the OWVLC-I2V system. These are experimental results from the SISO-based system designs described in Chapter 3 and the MIMO-based systems discussed in Chapter 4. Both are the result of the channel impulse response signals in the I2V system. The channel impulse response signals studied in Chapters 3 and 4 are used to model the data transmission of the OWVLC-I2V scheme. The first experiment is the OWVLC-I2V scheme employing SISO approach. Simulates the movement of the receiver mounted on a vehicle by dividing the communication link throughout the communication area. The LOS link between the transmitter and receiver is divided into 3 links, 5 links, and 7 links. The second experiment is the OWVLC-I2V system using MIMO technique. In Chapter 3 and 4, we have seen the numerically calculated channel impulse response. Of course, we need to compare the performance of the two systems. For example, Bit error rate, the total received data relates to the vehicle acceleration and the information throughput for both systems.

5.2 Experimental results of VLC-I2V system using SISO technique

This section discusses the performance of the VLC-I2V system using the SISO technique to compare the performance of both the SISO and MIMO expressed for the VLC-I2V system in the next section. In the simulation, all parameters are in the SISO system. We consider only changing the channel impulse response (CIR) because the SISO and MIMO systems both have different CIRs. The first efficiency of the VLC-I2V system using the SISO technique is the total amount of data received that is shown in Figure 5.1.

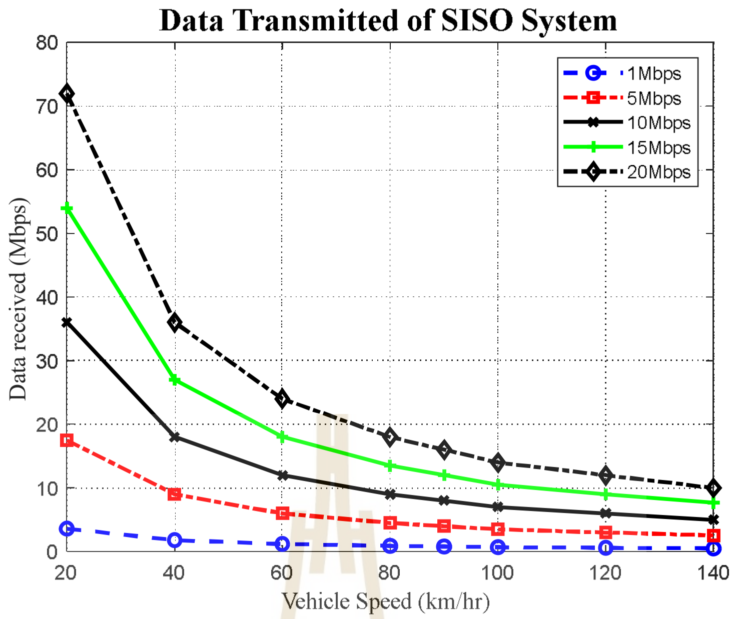

Figure 5.1 The total received data of VLC-I2V SISO system.

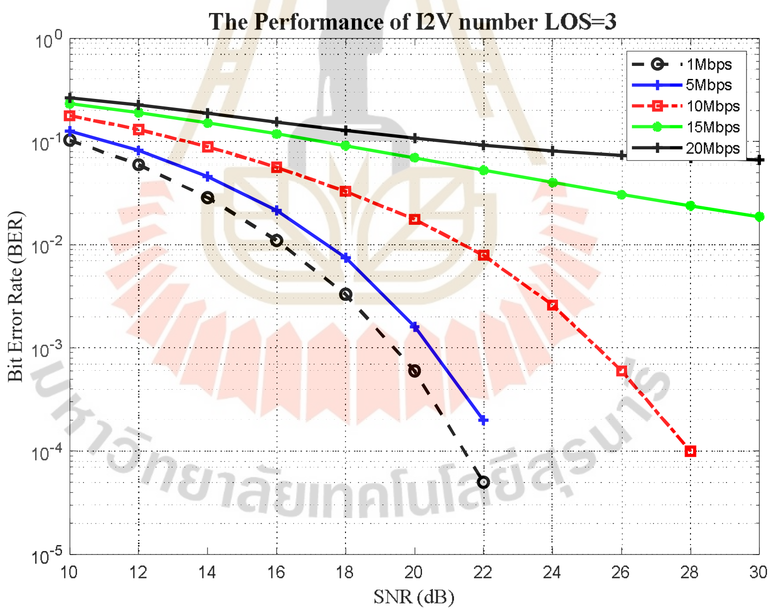

Figure 5.2 The performance of VLC-I2V SISO with the number of LOS = 3.

The experiment of the VLC-I2V SISO system is to simulate the data rate related with the number of LOS link that occurred from the vehicle on the move. For example, the vehicle speed is 90 km/hr, the number of LOS is 3, 5, and 7 links. The result shows that the achievement of VLC-I2V SISO scheme is similarly all the LOS link 3, 5 and 7 as see in Figure 5.2, 5.3, and 5.4 respectively. However, the bit error rate achieves 10^{-4} at the data rate 1, 5, 10 Mbps. Then, the higher the data transmission rate, the bit error in data decoding exceeds 10^{-4}. It relies on other factors that can decode data correctly when the data transmission rate increases.

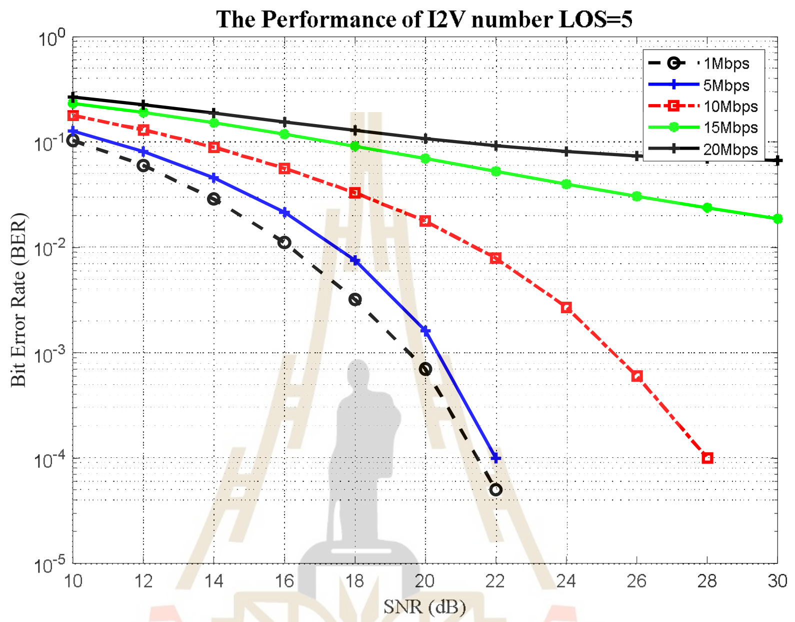

Figure 5.3 The performance of VLC-I2V SISO with the number of LOS = 5.

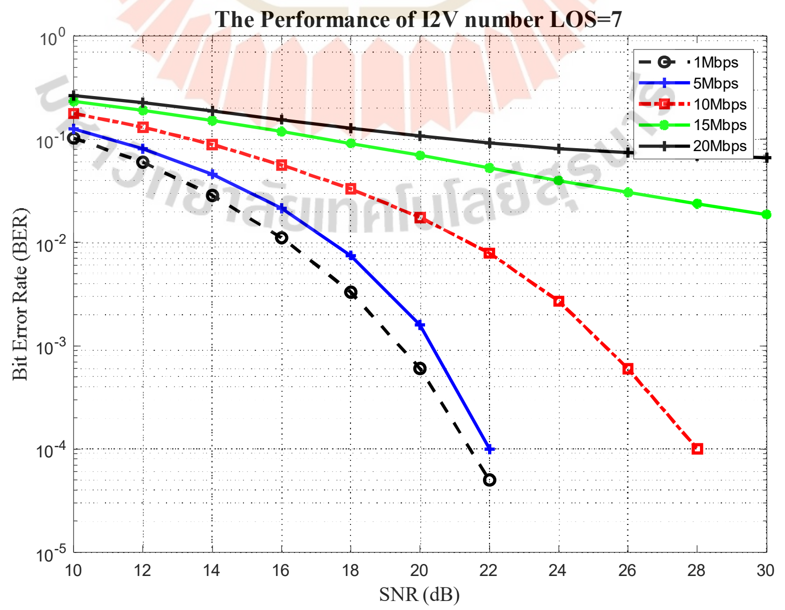

Figure 5.4 The performance of VLC-I2V SISO with the number of LOS = 7.

According to the performance of VLC-I2V SISO system as Figure 5.2, 5.3, and 5.4, we can calculate the throughput of VLC-I2V SISO system. For example, SNR = 16 dB, the vehicle speed from 20 to 140 km/hr. The throughput can be expressed as

$$Throughput_{SISO} = \left[V_{speed} \times D_{tx} \times (1 - BER) \right] \tag{5.1}$$

V_{speed} is the vehicle speed (m/s), BER is bit error rate, D_{tx} is the data transmitted (bps). Finally, Figure 5.5 shows the throughput decreased when the vehicle is at high speed.

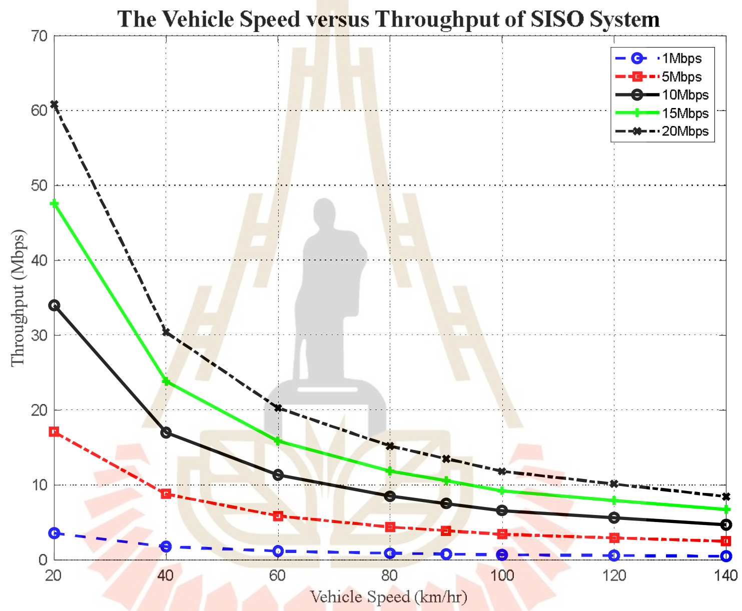

Figure 5.5 Throughput versus vehicle speed of VLC-I2V SISO system.

5.3 Experimental results of VLC-I2V system using MIMO technique

This section discusses the performance of the VLC-I2V system using the MIMO technique to compare the performance of both the SISO and MIMO expressed for the VLC-I2V system. In the simulation, all parameters are similar to those in the SISO system. We consider only changing the CIRs because the SISO and MIMO systems both have different CIRs. The first efficiency of the VLC-I2V system using the MIMO technique is the total amount of data received, according to Figure 5.6.

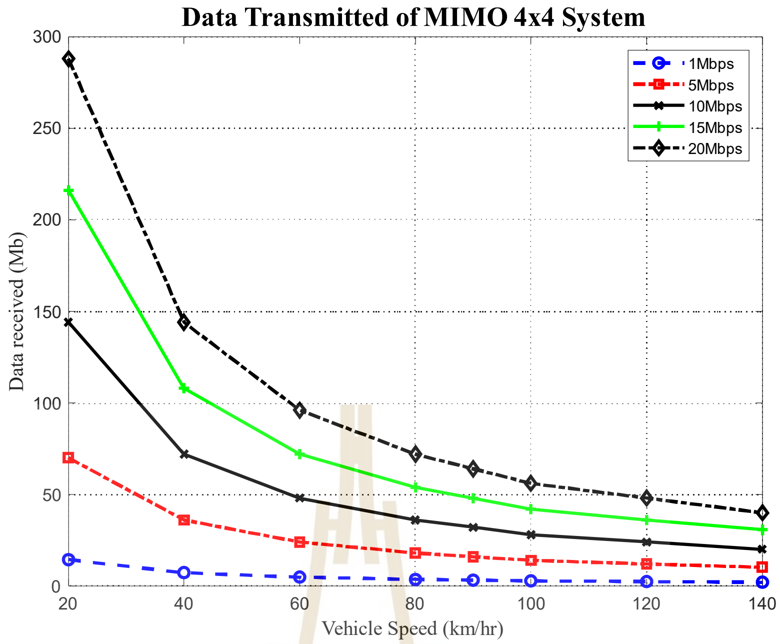

Figure 5.6 The total data received of VLC-I2V MIMO system.

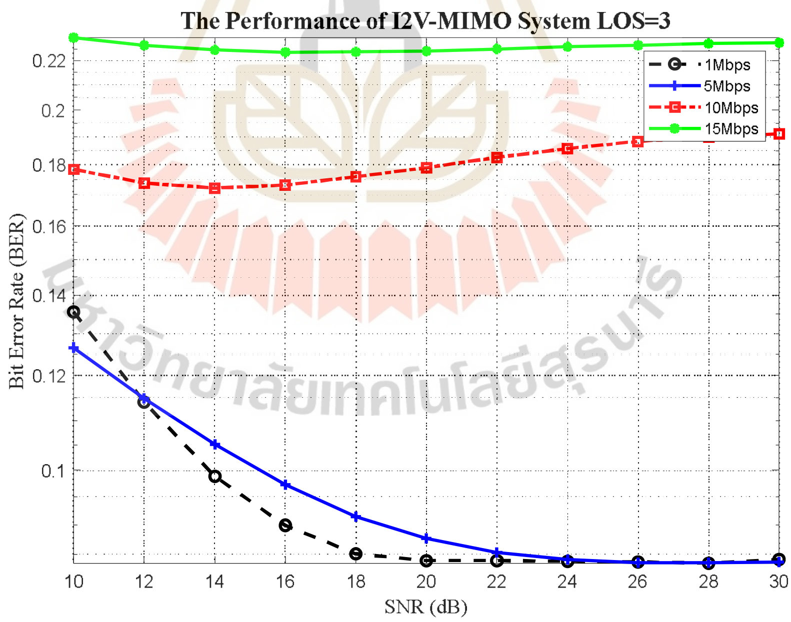

Figure 5.7 The performance of VLC-I2V MIMO with the number of LOS = 3.

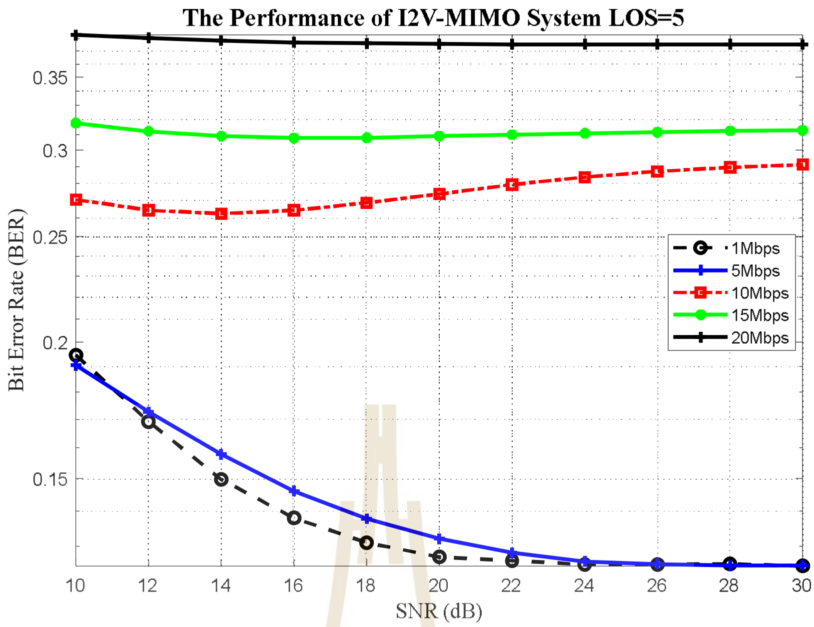

Figure 5.8 The performance of VLC-I2V MIMO with the number of LOS = 5.

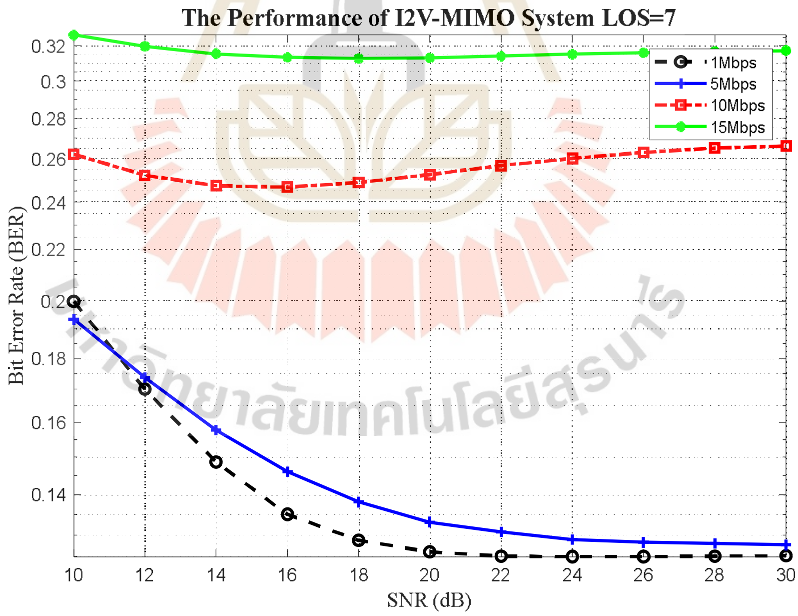

Figure 5.9 The performance of VLC-I2V MIMO with the number of LOS = 7.

According to the performance of VLC-I2V MIMO system as Figure 5.7, we can calculate the throughput of VLC-I2V MIMO system. For example, SNR = 16 dB, the vehicle speed from 20 to 140 km/hr. The throughput can be expressed as

$$Throughput_{MIMO} = \left[V_{speed} \times D_{tx} \times (1 - BER)\right] \times 4_{Tx} \tag{5.2}$$

V_{speed} is the vehicle speed (m/s), BER is bit error rate, D_{tx} is the data transmitted (bps). In general, the data transmission rate is sufficiently strong to match the power of the noise and the system's ability to separate the interfering from each other, If the interferent cannot be separated from each other. Existing or interfering signals in this system are grouped with the normal signals or added as noise. It turns out that instead of increasing the SNR to make the signal-to-noise ratio better and with higher power, it actually causes the noise in the system to increase instead. Finally, Figure 5.10 shows the throughput decreased when the vehicle is high speed.

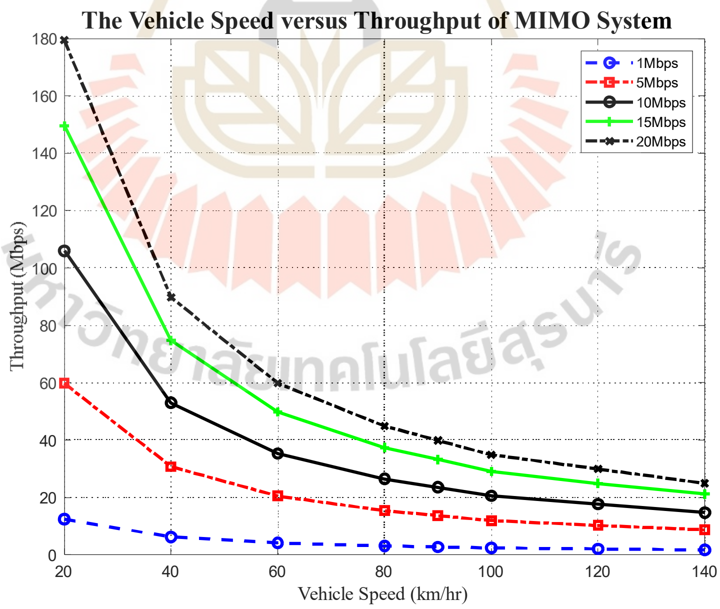

Figure 5.10 Throughput versus vehicle speed of VLC-I2V MIMO system.

Figures 5.11 and 5.12 show the comparison of throughput versus vehicle speed between SISO and MIMO techniques. There is a significant disparity in throughput when the vehicle speed is as low as 20 km/hr. Moreover, there is a subtle disparity in the elevated velocity of the vehicle, which reaches 140 km/hr. Both 10 Mbps and 20 Mbps are expressed in Figure 5.11, 5.12 respectively.

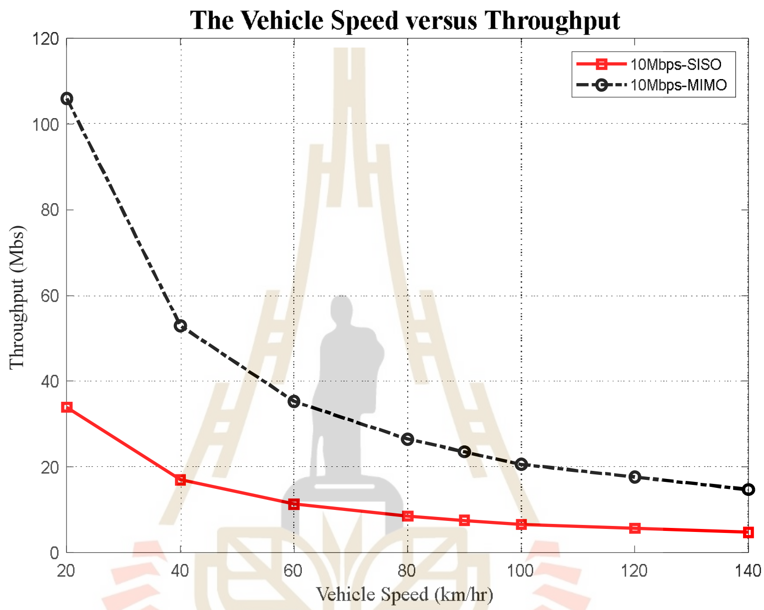

Figure 5.11 Comparison of throughput versus vehicle speed of SISO and MIMO system at 10 Mbps.

5.4 Summary

The results of an experiment were presented in Chapter 5. The experiment was about transmission data into an OWVLC-I2V system with different channel impulse response signal properties during the time the receiver moves through the communication coverage area. The transmitter was an LED bulb, which in the future will replace fluorescent and incandescent bulbs. Results of experiment 1: Analysis of electrical signals through the OWVLC-I2V system using SISO technique all the way to the receiver, which was discussed in the block diagram of the receiver circuit in chapter

3. And, results of experiment 2: the OWVLC-I2V system using MIMO technique shown the block diagram of the receiver circuit in chapter 4. And finally, there were experimental results comparing the amount of data received between systems using SISO and MIMO. The researchers found that, according to the experimental results, it is important to decode the information generated by electrical signals that change according to the channel's impulse response signal, or the channel changes according to the movement of the receiver mounted on the vehicle.

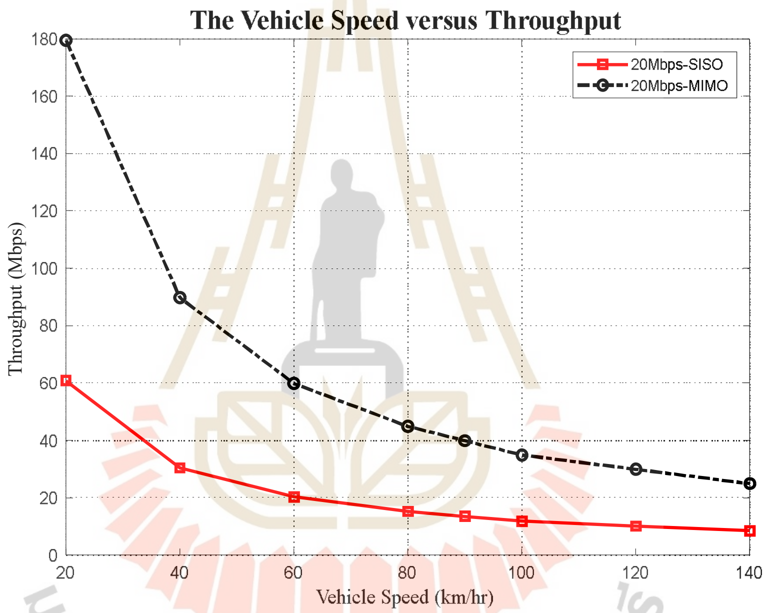

Figure 5.12 Comparison of throughput versus vehicle speed of SISO and MIMO system at 20 Mbps.

CHAPTER VI
CONCLUSIONS

6.1 Conclusions

The Intelligent Transportation System (ITS) utilizes information and communication technology to effectively manage transportation and traffic. ITS aims to enhance the efficiency of road systems, public transportation, and traffic safety, while reducing accidents and congestion. The benefits of Intelligent Transportation Systems (ITS) include the provision of warning signs to alert drivers in advance of accident locations, enabling them to avoid accidents and choose other routes. Additionally, ITS allows for the adjustment of speed limits before reaching regulated areas. Vehicular communication can utilize visible light communication technology, leveraging the automobile lights and the current traffic signal equipment. Intelligent Transportation Systems (ITS) utilize outdoor wireless visible light communication to transmit data from infrastructure to vehicles. We have examined the channel impulse response of a single-input single-output (SISO) system for I2V communication. The systems examined in this thesis partially depict the channel impulse response of both SISO and MIMO techniques while the receiver is in motion. It is possible that some of these systems establish a connection between the speed of the vehicle and the data received, as well as the throughput. This warrants additional effort to enhance the data rate beyond what our current configuration system allows.

6.2 Future works

In this thesis, the researcher simulates a system based on electrical signal processing with a computer program. In the future, it will be a very good thing to apply it to the implementation of work. Whether it is a transmission circuit whose important part is the circuit to drive a street light bulb that is an LED light bulb with a data signal included.

If the receiver circuit is MIMO, the receiver circuit will be even more complicated. This presents a potential research issue regarding the connection between infrastructure and cars (I2V) using visible light communication systems.

Furthermore, the crucial objective is to enhance the bit error rate (BER) of the Visible Light Communication (VLC) - Infrastructure to Vehicle (I2V) Multiple-Input Multiple-Output (MIMO) system. As demonstrated in the preceding chapter, the MIMO system's performance falls short of achieving a bit error rate (BER) of 10^{-4}. Researchers have the ability to create many scenarios that closely resemble the real-life I2V communication system. It is advisable to take into account additional scenarios for OWVLC-I2V systems during the night, including ambient light, artificial light, and other sources of light that may disrupt the I2V system. Several issues need to be addressed in the OWVLC-I2V system, such as strong noise interference, long-distance communication, coverage area limitations, and daytime communication limitations. We will consider these issues for future studies.

REFERENCES

Abualhoul, M. (2016). Visible light and radio communication for cooperative autonomous driving: Applied to vehicle convoy [PhD Thesis]. MINES ParisTech.

Adiono, T., Pradana, A., & Fuada, S. (2018). A Low-complexity of VLC System using BPSK. International Journal of Recent Contributions from Engineering, Science & IT (iJES), 6(1), 99–106.

Al Naboulsi, M. C., Sizun, H., & de Fornel, F. (2004). Wavelength selection for the free space optical telecommunication technology. Reliability of Optical Fiber Components, Devices, Systems, and Networks II, 5465, 168–179.

Arnon, S. (2014). Optimised optical wireless car-to-traffic-light communication. Transactions on Emerging Telecommunications Technologies, 25(6), 660–665. doi:https://doi.org/10.1002/ett.2817

Bai, B., Xu, Z., & Fan, Y. (2010). Joint LED dimming and high capacity visible light communication by overlapping PPM. The 19th Annual Wireless and Optical Communications Conference (WOCC 2010), 1–5.

Barry, J. R., Kahn, J. M., Krause, W. J., Lee, E. A., & Messerschmitt, D. G. (1993). Simulation of multipath impulse response for indoor wireless optical channels. IEEE Journal on Selected Areas in Communications, 11(3), 367–379.

Belkhir, L., & Elmeligi, A. (2018). Assessing ICT global emissions footprint: Trends to 2040 & recommendations. Journal of Cleaner Production, 177, 448–463. doi:https://doi.org/10.1016/j.jclepro.2017.12.239

Bell, A. G. (1881). On the production and reproduction of sound by light. Proc. Am. Assoc. Adv. Sci., 29, 115–136.

Berman, S. M., Greenhouse, D. S., Bailey, I. L., Clear, R. D., & Raasch, T. W. (1991). Human electroretinogram responses to video displays, fluorescent lighting, and other high frequency sources. Optometry and Vision Science, 68(8), 645–662.

Bouchet, O., El Tabach, M., Wolf, M., O'Brien, D. C., Faulkner, G. E., Walewski, J. W., Randel, S., Franke, M., Nerreter, S., & Langer, K.-D. (2008). Hybrid wireless optics (HWO): Building the next-generation home network. 2008 6th International Symposium on Communication Systems, Networks and Digital Signal Processing, 283–287.

Cailean, A., Cagneau, B., Chassagne, L., Topsu, S., Alayli, Y., & Blosseville, J.-M. (2012). Visible light communications: Application to cooperation between vehicles and road infrastructures. 2012 IEEE Intelligent Vehicles Symposium, 1055–1059.

Căilean, A.-M., Cagneau, B., Chassagne, L., Dimian, M., & Popa, V. (2015). Novel receiver sensor for visible light communications in automotive applications. IEEE Sensors Journal, 15(8), 4632–4639.

Cailean, A.-M., Cagneau, B., Chassagne, L., Popa, V., & Dimian, M. (2014). A survey on the usage of DSRC and VLC in communication-based vehicle safety applications. 2014 IEEE 21st Symposium on Communications and Vehicular Technology in the Benelux (SCVT), 69–74. doi:https://doi.org/10.1109/SCVT.2014.7046710

Cailean, A.-M., Cagneau, B., Chassagne, L., Topsu, S., Alayli, Y., & Dimian, M. (2013). Visible light communications cooperative architecture for the intelligent transportation system. 2013 IEEE 20th Symposium on Communications and Vehicular Technology in the Benelux (SCVT), 1–5.

Căilean, A.-M., & Dimian, M. (2017). Current challenges for visible light communications usage in vehicle applications: A survey. IEEE Communications Surveys & Tutorials, 19(4), 2681–2703.

Carruthers, J. B., & Carroll, S. M. (2005). Statistical impulse response models for indoor optical wireless channels. International Journal of Communication Systems, 18(3), 267–284.

Cheng, L., Viriyasitavat, W., Boban, M., & Tsai, H.-M. (2017). Comparison of radio frequency and visible light propagation channels for vehicular communications. IEEE Access, 6, 2634–2644.

Corsini, R., Pelliccia, R., Cossu, G., Khalid, A. M., Ghibaudi, M., Petracca, M., Pagano, P., & Ciaramella, E. (2012). Free space optical communication in the visible bandwidth for V2V safety critical protocols. 2012 8th International Wireless Communications and Mobile Computing Conference (IWCMC), 1097–1102.

Dahri, F. A., Ali, S., & Jawaid, M. M. (2018). A Review of Modulation Schemes for Visible Light Communication.

Dang, Q.-H., & Yoo, M. (2017). Handover Procedure and Algorithm in Vehicle to Infrastructure Visible Light Communication. IEEE Access, 5, 26466–26475. doi:https://doi.org/10.1109/ACCESS.2017.2771199

Fujimoto, N., & Mochizuki, H. (2013). 477 Mbit/s visible light transmission based on OOK-NRZ modulation using a single commercially available visible LED and a practical LED driver with a pre-emphasis circuit. National Fiber Optic Engineers Conference, JTh2A-73.

Galal, M., Ng, W. P., Abd El Aziz, A., & Binns, R. (2018). Characterisation and Interference Model of Contemporary Artificial Light Sources Noise on a VLC channel. In 2018 11th International Symposium on Communication Systems, Networks & Digital Signal Processing (CSNDSP) (pp. 1-6). IEEE.

Georghiades, C. N. (1994). Modulation and coding for throughput-efficient optical systems. IEEE Transactions on Information Theory, 40(5), 1313–1326.

Gfeller, F., Hirt, W., de Lange, M., & Weiss, B. (1996). Wireless infrared transmission: How to reach all office space. Proceedings of Vehicular Technology Conference-VTC, 3, 1535–1539.

Gfeller, F. R., & Bapst, U. (1979). Wireless in-house data communication via diffuse infrared radiation. Proceedings of the IEEE, 67(11), 1474–1486.

Ghassemlooy, Z., Alves, L. N., Zvanovec, S., & Khalighi, M.-A. (2017). Visible Light Communications: Theory and Applications. CRC Press.

Ghassemlooy, Z., Popoola, W., & Rajbhandari, S. (2019). Optical wireless communications: System and channel modelling with Matlab®. CRC press.

Global status report on road safety 2018. (2018). https://www.who.int/publications-detail-redirect/9789241565684

Goto, Y., Takai, I., Yamazato, T., Okada, H., Fujii, T., Kawahito, S., Arai, S., Yendo, T., & Kamakura, K. (2016). A new automotive VLC system using optical communication image sensor. IEEE Photonics Journal, 8(3), 1–17.

Grubor, J., Lee, S. C. J., Langer, K.-D., & Koonen, T. (2007). Wireless High-Speed Data Transmission with Phosphorescent White- Light LEOs. 1–2.

IEEE Standard. (2011). 802.15.7-2011—IEEE Standard for Local and Metropolitan Area Networks—Part 15.7: Short-Range Wireless Optical Communication Using Visible Light. IEEE Standard 802.15.7-2011. doi:https://doi.org/10.1109/IEEESTD.2011.6016195

Ji, P., Tsai, H.-M., Wang, C., & Liu, F. (2014). Vehicular visible light communications with LED taillight and rolling shutter camera. 2014 IEEE 79th Vehicular Technology Conference (VTC Spring), 1–6.

Kahn, J. M., & Barry, J. R. (1997). Wireless infrared communications. Proceedings of the IEEE, 85(2), 265–298.

Kaur, S., Liu, W., & Castor, D. (n.d.). VLC dimming support IEEE 802.15-09-0641-00-0007.

Khalid, A., Cossu, G., Corsini, R., Choudhury, P., & Ciaramella, E. (2012). 1-Gb/s transmission over a phosphorescent white LED by using rate-adaptive discrete multitone modulation. IEEE Photonics Journal, 4(5), 1465–1473.

Khalighi, M. A., & Uysal, M. (2014). Survey on free space optical communication: A communication theory perspective. IEEE Communications Surveys & Tutorials, 16(4), 2231–2258.

Komine, T. (2005). Visible light wireless communications and its fundamental study. Keio University, PhD Thesis, Japan, 90, 217–219.

Komine, T., & Nakagawa, M. (2004). Fundamental analysis for visible-light communication system using LED lights. IEEE Transactions on Consumer Electronics, 50(1), 100–107.

Kumar, N., Lourenço, N., Terra, D., Alves, L. N., & Aguiar, R. L. (2012). Visible light communications in intelligent transportation systems. 2012 IEEE Intelligent Vehicles Symposium, 748–753.

Kwon, J. K. (2010). Inverse source coding for dimming in visible light communications using NRZ-OOK on reliable links. IEEE Photonics Technology Letters, 22(19), 1455–1457.

Lambert, J. H. (1760). Photometria sive de mensura et gradibus luminis, colorum et umbrae. sumptibus vidvae E. Klett, typis CP Detleffsen.

Le Minh, H., O'Brien, D., Faulkner, G., Zeng, L., Lee, K., Jung, D., & Oh, Y. (2008). High-speed visible light communications using multiple-resonant equalization. IEEE Photonics Technology Letters, 20(14), 1243–1245.

Lourenço, N., Terra, D., Kumar, N., Alves, L. N., & Aguiar, R. L. (2012). Visible light communication system for outdoor applications. 2012 8th International Symposium on Communication Systems, Networks & Digital Signal Processing (CSNDSP), 1–6.

Moreira, A. J., Valadas, R. T., & de Oliveira Duarte, A. M. (1995). Characterisation and modelling of artificial light interference in optical wireless communication systems. In Proceedings of 6th International Symposium on Personal, Indoor and Mobile Radio Communications (Vol. 1, pp. 326-331). IEEE.

Muthu, S., & Gaines, J. (2003). Red, green and blue LED-based white light source: Implementation challenges and control design. 38th IAS Annual Meeting on Conference Record of the Industry Applications Conference, 2003., 1, 515–522.

Ntogari, G., Kamalakis, T., Walewski, J., & Sphicopoulos, T. (2011). Combining illumination dimming based on pulse-width modulation with visible-light communications based on discrete multitone. Journal of Optical Communications and Networking, 3(1), 56–65.

O'Brien, D. C., Katz, M., Wang, P., Kalliojarvi, K., Arnon, S., Matsumoto, M., Green, R. J., & Jivkova, S. (2005). Short-range optical wireless communications. Wireless World Research Forum, 1–22.

Oh, M. (2013). A flicker mitigation modulation scheme for visible light communications. 2013 15th International Conference on Advanced Communications Technology (ICACT), 933–936.

Ohtsuki, T. (1999). Rate adaptive indoor infrared wireless communication systems using repeated and punctured convolutional codes. 1999 IEEE International Conference on Communications (Cat. No. 99CH36311), 1, 609–613.

Ohtsuki, T., Sasase, I., & Mori, S. (1993). Overlapping multi-pulse pulse position modulation in optical direct detection channel. Proceedings of ICC'93-IEEE International Conference on Communications, 2, 1123–1127.

Ohtsuki, T., Sasase, I., & Mori, S. (1994a). Capacity and cutoff rate of overlapping multi-pulse pulse position modulation (OMPPM) in optical direct-detection channel: Quantum-limited case. IEICE TRANSACTIONS on Fundamentals of Electronics, Communications and Computer Sciences, 77(8), 1298–1308.

Ohtsuki, T., Sasase, I., & Mori, S. (1994b). Performance analysis of overlapping multi-pulse pulse position modulation (OMPPM) in noisy photon counting channel. Proceedings of 1994 IEEE International Symposium on Information Theory, 80.

Okada, S., Yendo, T., Yamazato, T., Fujii, T., Tanimoto, M., & Kimura, Y. (2009). On-vehicle receiver for distant visible light road-to-vehicle communication. 2009 IEEE Intelligent Vehicles Symposium, 1033–1038.

Optical wireless communications. (2021). In Wikipedia. https://en.wikipedia.org/w/index.php?title=Optical_wireless_communications&oldid=1028441051

Papadimitratos, P., De La Fortelle, A., Evenssen, K., Brignolo, R., & Cosenza, S. (2009). Vehicular communication systems: Enabling technologies, applications, and future outlook on intelligent transportation. IEEE Communications Magazine, 47(11), 84–95.

Park, S., Jung, D., Shin, H., Shin, D., Hyun, Y., Lee, K., & Oh, Y. (2007). Information broadcasting system based on visible light signboard. Proc. Wireless Opt. Commun, 30, 311–313.

Roberts, R. D. (2013a). A MIMO protocol for camera communications (CamCom) using undersampled frequency shift ON-OFF keying (UFSOOK). 2013 IEEE Globecom Workshops (GC Wkshps), 1052–1057.

Roberts, R. D. (2013b). Undersampled frequency shift ON-OFF keying (UFSOOK) for camera communications (CamCom). 2013 22nd Wireless and Optical Communication Conference, 645–648.

Saito, T., Haruyama, S., & Nakagawa, M. (2008). A new tracking method using image sensor and photo diode for visible light road-to-vehicle communication. 2008 10th International Conference on Advanced Communication Technology, 1, 673–678.

Shiu, D., & Kahn, J. M. (1999). Differential pulse-position modulation for power-efficient optical communication. IEEE Transactions on Communications, 47(8), 1201–1210.

Sugiyama, H., Haruyama, S., & Nakagawa, M. (2007). Brightness control methods for illumination and visible-light communication systems. 2007 Third International Conference on Wireless and Mobile Communications (ICWMC'07), 78–78.

Sugiyama, H., & Nosu, K. (1989). MPPM: A method for improving the band-utilization efficiency in optical PPM. Journal of Lightwave Technology, 7(3), 465–472.

Takai, I., Harada, T., Andoh, M., Yasutomi, K., Kagawa, K., & Kawahito, S. (2014). Optical vehicle-to-vehicle communication system using LED transmitter and camera receiver. IEEE Photonics Journal, 6(5), 1–14.

Takai, I., Ito, S., Yasutomi, K., Kagawa, K., Andoh, M., & Kawahito, S. (2013). LED and CMOS image sensor based optical wireless communication system for automotive applications. IEEE Photonics Journal, 5(5), 6801418–6801418.

Terra, D., Kumar, N., Lourenço, N., Alves, L. N., & Aguiar, R. L. (2011). Design, development and performance analysis of DSSS-based transceiver for VLC. 2011 IEEE EUROCON-International Conference on Computer as a Tool, 1–4.

Tonguz, O. K., Wisitpongphan, N., Parikh, J. S., Bai, F., Mudalige, P., & Sadekar, V. K. (2006). On the broadcast storm problem in ad hoc wireless networks. 2006 3Rd International Conference on Broadband Communications, Networks and Systems, 1–11.

Ucar, S., Ergen, S. C., & Ozkasap, O. (2018). IEEE 802.11 p and visible light hybrid communication based secure autonomous platoon. IEEE Transactions on Vehicular Technology, 67(9), 8667–8681.

Uysal, M., Ghassemlooy, Z., Bekkali, A., Kadri, A., & Menouar, H. (2015). Visible Light Communication for Vehicular Networking: Performance Study of a V2V System Using a Measured Headlamp Beam Pattern Model. IEEE Vehicular Technology Magazine, 10(4), 45–53. https://doi.org/10.1109/MVT.2015.2481561

Vucic, J., Kottke, C., Nerreter, S., Habel, K., Buttner, A., Langer, K.-D., & Walewski, J. (2009). 125 Mbit/s over 5 m wireless distance by use of OOK-modulated phosphorescent white LEDs. 2009 35th European Conference on Optical Communication, 1–2.

Vučić, J., Kottke, C., Nerreter, S., Habel, K., Büttner, A., Langer, K.-D., & Walewski, J. W. (2010). 230 Mbit/s via a wireless visible-light link based on OOK modulation of phosphorescent white LEDs. 2010 Conference on Optical Fiber Communication (OFC/NFOEC), Collocated National Fiber Optic Engineers Conference, 1–3.

Wang, N., Liu, C., Lu, Y., & Shen, J. (2017). A visible light communication (VLC) based intelligent transportation system for lorry fleet. 2017 16th International Conference on Optical Communications and Networks (ICOCN), 1–3.

Wani, T., & Qadri, S. A. A. (n.d.). An insight into the modulation schemes for visible light communication.

Yamazato, T., Takai, I., Okada, H., Fujii, T., Yendo, T., Arai, S., Andoh, M., Harada, T., Yasutomi, K., Kagawa, K., & Kawahito, S. (2014). Image-sensor-based visible light communication for automotive applications. IEEE Communications Magazine, 52(7), 88–97. https://doi.org/10.1109/MCOM.2014.6852088

Zeshan, A., & Baykas, T. (2019). Performance analysis of VLC based on 802.11 ac frame structure. IEEE Communications Letters, 23(9), 1560–1563.

APPENDIX

PUBLICATIONS

List of Publications

International Journal Paper

A. Kaewpukdee and P. Uthansakul, "Characteristic of line-of-sight in infrastructure-to-vehicle visible light communication using mimo technique," Computers, Materials & Continua, vol. 74, no.1, pp. 1025–1048, 2023.

National Conference Paper

Adisorn Kaewpukdee, Peerapong Uthansakul and Jesada Sartthong, "Modelling of Outdoor Wireless Visible Light Communication for Street Lamp to Vehicle Application," Electrical Engineering Conference (EECON-43), Pitsanulok, Thailand, 28-30 October 2020.

Computers, Materials & Continua
DOI: 10.32604/cmc.2023.032569
Article

Tech Science Press

Characteristic of Line-of-Sight in Infrastructure-to-Vehicle Visible Light Communication Using MIMO Technique

Adisorn Kaewpukdee and Peerapong Uthansakul*

School of Telecommunication Engineering, Suranaree University of Technology, Nakhon Ratchasima, 30000, Thailand
*Corresponding Author: Peerapong Uthansakul. Email: uthansakul@sut.ac.th
Received: 22 May 2022; Accepted: 28 June 2022

Abstract: Visible Light Communication (VLC) technology is aggressive research for the next generation of communication. Currently, Radio Frequency (RF) communication has crowed spectrum. An Intelligent Transportation System (ITS) has been improved in the communication network for Vehicle-to-Vehicle (V2 V), Vehicle-to-Infrastructure (V2I), and Infrastructure-to-Vehicle (I2 V) by using the visible light spectrum instead of the RF spectrum. This article studies the characterization of Line-of-Sight (LOS) optical performance in an Outdoor Wireless Visible Light Communication (OWVLC) system employing a Multiple-Input Multiple-Output (MIMO) technique for I2 V communications in ITS regulations. We design the new configuration of the OWVLC-I2 V system, which is an alternative approach to communication for I2 V system at nighttime. The results show the Channel Impulse Response (CIR) of the LOS links in visible light communication for I2 V system in ITS by investigating the receiver on the vehicle moving along the coverage communication area. Furthermore, the OWVLC-I2 V system using the MIMO technique depicts the performance of throughput and Bit Error Rate (BER) *vs.* vehicle speed while the vehicle passes a street light.

Keywords: Infrastructure to vehicle communication; intelligent transportation system; visible light communication; channel impulse response

1 Introduction

Every year, the number of deaths steadily increases, and vehicles using transportation infrastructure are also rising. A car accident is one of the leading causes of death [1]. Among death on road, accidents are often happened by the youths aged from 15 to 29 years, reported by the World Health Organization (WHO). The scientific community, the automotive industry, and government agencies collaborate to improve vehicle and road safety in this sector. There are research projects aimed at assisting people in preventing injuries and fatalities. The safety and reliability of transportation system can be significantly improved [2]. It combines Vehicle-to-Vehicle (V2 V) and Infrastructure-to-Vehicle (I2 V/V2I) communications to allow real-time data exchange between vehicles and traffic infrastructure. Since it is not influenced by broadcast storm phenomena [3,4], Visible Light Communication (VLC) technology has the potential to significantly improve vehicle network capacity, especially in high traffic congestion. The Intelligent Transportation System (ITS) [5] considers using cutting-edge collaborative technology to reduce injuries and fatalities. The ITS aims to increase transportation system performance and minimize Carbon dioxide (CO_2) emissions by providing real-time access to relevant traffic information through I2 V/V2I and V2 V communications. The ITS constantly gathers analyses and distributes traffic data to improve vehicle visibility. Moreover, this knowledge aids in effectively managing transportation networks, increasing performance, and reducing traffic congestion. The transportation systems automatically use the information provided to adapt to different traffic situations. As a result, widespread adoption of ITS is crucial. On the other hand, several intelligent vehicle deployments and regional intelligence networks are required to assure system dependability and to gather and send more data effectively. Moreover, the ITS primary challenge is to keep operating costs as low as possible while ensuring reliability. The benefit of integrating transportation intelligence is efficient traffic analysis and management, which reduces traffic congestion and provides alternative routes based on traffic conditions, saving time, money, and pollution.

Existing VLC prototypes have a low error contact distance of up to 100 m in the case of camera-based systems [6–9] and 40–60 m in the case of photodiode-based systems [10–12]. As a result, the contact gap must be increased to be used in the automotive industry. The work presented in [13] has given a brief demonstration of the technological features for the most suitable I2 V/V2 V prototypes. The authors of [6] have described the nature, function, and valuation results of Optical Communication Image (OCI) sensor and demonstrated the advanced results and experimental performances of Image Sensor base Optical Wireless Communication (IS-OWC) method using the OCI. They have also shown the results of the world's first 20 Mbps per pixel communication with 16.6 ms real-time Light-Emitting Diode (LED) detection. The VLC is not only suitable for broadcasting systems such as road communication systems or I2 V communication systems, but it is also valuable for V2 V and V2I communication systems. In V2 V cases, the vehicle in front of the traffic light receives traffic security information and transmits it to the vehicle through the brake light. They may also set up ad hoc networks for their vehicles and exchange data with the others. Similarly, a running vehicle may use its LED headlights to request data from the Roadside Unit (RSU), resulting in a full-duplex communication system [12]. The RSUs, such as LED traffic lights, are suitable for in-vehicle broadcast communications systems that work in the I2 V mode. Traffic safety information can be transmitted continuously without extra fuel, resulting in smoother traffic and fewer injuries. The light emitted by traffic lights (which make an LED array) is tuned to a frequency that the human eye cannot perceive. The modulated light is then detected by the vehicle's receiver photodetector (PD), providing the driver with valuable safety knowledge ahead of time. A more advanced viewpoint may employ inter-vehicle communication methods to send data between vehicles stopped near traffic control poles. The work presented in [13] has provided an example explaining the use of VLC in a vehicle safety application using communication. Using intelligent traffic lights and street lighting systems, approaching vehicles can now receive road safety information (e.g., location information, traffic light mileage and time before the next change, maintenance work, and speed limit). Furthermore, vehicles can share status information (e.g., location, velocity, acceleration, and engine state). In [2], one of the most effective ways to reduce the number of collisions and associated victims is to increase vehicle awareness. Embedded sensors can sense the environment and assist drivers in dangerous situations. As mentioned, it includes ultrasound sensors used for parking aids, cameras used for traffic lanes and traffic lights, radar or lidar technology used to detect remote obstacles and measure distances. However, the sensors are limited, and in these conditions, wireless communication can provide an additional level of assistance to the driver. In [2], wireless communication allows vehicles to communicate with each other by texting and sharing information collected by sensors. By using the data collected, it can be carried out in risky situations. Nevertheless, it will not resist the driver, but it is more like a preventer of collisions. In most cases, the car's activity ends before the driver responds. Besides safety, wireless communication improves the transportation system efficiency by providing the most suitable alternative locations and routes. The Multiple-Input Multiple-Output (MIMO) is widely used in Radio Frequency (RF) communication systems [14], where dispersion and interference generate decorrelated channels. Given a certain amount of total transmission power, MIMO channels have a greater capacity than their Single Input Single Output (SISO) counterparts. A small amount of research has been done on optical MIMO. Most optical channels use intensity modulation and direct detection. Optical MIMO is no decorrelation in most instances, and it is only in long air routes that turbulence and scattering are likely to produce as shown in [15]. The work presented in [16] has demonstrated a MIMO method to modeling an indoor system, while [17] investigated the capacity of a MIMO system and presented a low-speed demonstration. The authors of [18] have described work on space-time coding for MIMO. Preliminary experiments with a basic MIMO link have been described in [19]. There has been also a substantial body of work on the optical coupling of source and sensor arrays [20]. Several hundred Mbps up to 1 Gbps by simulation used MIMO optical wireless communication system [21]. MIMO enables the alignment needed for such a connection to be accomplished in electronic devices since light from a transmitter does not have to hit a single receiver exactly. MIMO methods may be used to understand the channel matrix, allowing the crosstalk between the channels generated by each source and detector to be quantified.

Figure 1: Concept of an infrastructure-to-vehicle communication using a VLC system

The rest of this article is organized as follows. The second topic discusses visible light communication for intelligent transportation systems. We divide the article into subheading, which are an infrastructure-to-vehicle configuration, street light illumination and power distribution, and channel modeling of the Outdoor Wireless Visible Light Communication Infrastructure-to-Vehicle (OWVLC-I2 V) using MIMO techniques. Fig. 1 shows the concept of I2V communication on the road at night. The numerical simulations of the characteristic channel impulse response are described in the Section 3. The performance of OWVLC-I2 V system using MIMO technique will be illustrated in Section 4. Finally, the conclusion is discussed in Section 5.

2 Visible Light Communication for Intelligent Transportation System

Annually, nearly 1.35 million people die in traffic collisions [1], and an estimated 50 million people are injured. According to experts, many accidents are triggered by the sluggish reaction and failure of car drivers to take the necessary action at the appropriate time [22]. An ITS with V2 V and I2 V connectivity ensures people protection. ITS relies on vehicles and infrastructure interacting in a truthful, robust, and secure manner (traffic lights, billboards and street lights). Since RF-based network is already overcrowded [23,24], all vehicles are outfitted with headlights and taillights that can transmit data. Traffic lights, billboards, and street lights may also broadcast important information about lanes, traffic, and weather conditions. These lighting sources can also connect users and the Internet of Everything (IoE). Cailean et al. [2] have addressed the difficulties that VLC faces in vehicular communication. The primary requirements for vehicular communications are enhanced mobility, expanded contact range, and faster data speeds. The ability of communication channels to avoid ambient or parasitic light is critical to achieving these goals. The outdoor channel is illuminated by various types of ambient lighting. VLC distance measuring and localization capabilities have been found to be helpful in vehicular communication applications. Furthermore, it is suggested that the development of disparate systems comprised of VLC and dedicated short-range communication (DSRC) or Cellular-V2X (or any other RF-based scheme) could result in a dependable system for vehicular communication because each of these technologies can compensate for the shortcomings of the others. A survey of VLC relating to 5 GHz DSRC in a hybrid preparation is produced. It is concluded that VLC systems for vehicular communication can be enhanced by researching and incorporating emerging technologies such as software-defined architecture, resource sharing, reconfigurable computing, and the introduction of new materials. Ucar et al. [25] have created a stable autonomous platoon system that is a combination of 802.11p and VLC. The autonomous platoon operates on RF-based 802.11p and is led by a platoon leader who monitors other members to precisely change the speeds. An IEEE 802.11p and VLC-based hybrid security protocol for platoon communication, namely (SP-VLC) [25] is a hybrid vehicular platoon communication protocol based on 802.11p and VLC. This protocol is intended to fix security flaws caused by the specific use of RF communication. It has been developed a simulation platform for vehicle mobility and platoon management. SP-VLC is tested in a few security flaw situations. The simulation results confirmed the findings in [13] that the RF-VLC heterogeneous system has many advantages over the RF-only system.

Emerging LED-based RSU have been used in current ITS. Kumar et al. [26] have suggested using VLC principles to broadcast information in infrastructure to vehicle (I2 V) mode. A Direct Sequence Spread Spectrum (DSSS) and Sequence Inverse Keying (SIK) are used to make noise less of an ambient light. An output metric is the sum of data obtained through a car passing by RSU. The experimental setup consists of a movable receiver and a stationary emitter separated by 1.5 m. The results show that during the day, the Packet Error Rate (PER) degrades linearly with distance, while at night, the PER differs due to the local existence of artificial light. The authors of [27] have carried out the VLC-based V2 V scheme. Uysal et al. [27] have considered a standard V2 V-VLC scenario with left and right headlamps emitting light. The Lambertian profile is used to consider the diffusion paths as well as the Line-of-Sight (LOS) path components. The results have shown that at a distance of 70 m between vehicles, a data rate of 50 Mbps can be reached depending on the position of the headlamps. The authors used VLC-based ITS for accident avoidance in [28]. VLC was used to send signals related to increasing speed, decreasing speed, and vehicle braking to ITS infrastructure (e.g., RSUs) that can cause appropriate signals. For example, in a complex setting, a vehicle can send a VLC signal to RSU, which can set a green signal or express path to minimize the number of emergency braking and lane changes. Yamazato et al. [8] have used VLC with an imaging sensor-based receiver for automotive applications. There were two scenarios I2 V and V2 V. The first scenario includes a transmitter made of LED arrays that radiates signals to roadside devices, while the receiver is a high frame rate Complementary Metal–Oxide Semiconductor (CMOS) imaging camera. In the second scenario, a special CMOS sensor capable of receiving high-speed optical signals has been produced. In the experiment, I2 V and V2 V reached data rates of 32 kb/s and 10 Mb/s, respectively. The analysis of [29] has intended a handover procedure of the V2I-VLC system, infrastructure such as street lighting could allow automatic car driving. This technique used a probabilistic algorithm based on distance to determine the handover switching time. As we all know, a car moves quickly, and each street light has a limited coverage area. The vehicle passes through a cluster of LED-powered street lights. The transition between each LED group is a major issue. The handover procedure and algorithm generated high signal quality, which was appreciated when it came time to turn to another group of LEDs. The aim of [30] was to compare RF and VLC propagation characteristics, such as radiation pattern, path loss modeling, noise and interference, and channel time variation. In other related works, [31] this research finds three contextual variables that aid real-time tiredness detection—their experimental shown that the proposed recognition approach outperforms single-fatigue feature and single-source fusion-based methods. In [32–34], Fair Power Allocation (FPA) scheme can enhance the fairness of Non-Orthogonal Multiple Access (NOMA) in VLC-based IoT networks for the intravehicular communication system. Moreover, [35–42] the I2 V communication systems were popular in traffic lights, street lights, headlights, and taillight. The transmitter used the array of White LEDs (WLEDs), and the receiver was the PD installed on the vehicle's front hood in [36,39,40]. In contrast, others [38,41,42] placed the receiver on the top of the car, which is better for PD to receive the light. Also, in recent years there has been so much research [43–46]. The Non-LOS have been studied in [43], and the V2 V-VLC-based system model under shadowing is proposed in [44]. Furthermore, [45,46] suggested that Vehicular-Visible Light Communication (V-VLC) can improve outage performance. These deployment methodologies may be a favored solution for ITS to satisfy ultra-high reliability and ultra-low latency connectivity for Beyond 5G (B5G) vehicular networks.

2.1 Infrastructure-to-Vehicle (I2 V) Configuration

Several devices are becoming more sophisticated, and they can interact with one another. Smart street lights have been built in ITS for illumination and data communication. A White LED bulb is a lighting system critical for energy savings because LED lamps provide complete fluorescent tubes and incandescent bulb lighting. LEDs have many benefits, including a long lifetime, low power consumption, small size, cool operation, etc. As a result, future trends expect that LED lamps will be used as a substitute for traditional lamps in this course because they provide more benefits. In addition to lighting, they discovered that LEDs could be used as a data communication system. Fig. 2 illustrates a situation in which LEDs in infrastructure are used to relay traffic information to a vehicle. For ITS, the integration of both RF and VLC technologies is comfortable. White LEDs are being utilized in street lights to give the lighting on the road. Consider a street lamp to be a 5 × 5 LED array while investigating the illumination of a lighting pole street light. Each LED has a 1 W power rating and provides an illuminance of 135–320 lumens [47], a power supply voltage of 2.90–3.25 V, and a 350–700 mA current. LEDs have an irradiance angle of 120 degrees, and the color temperature offered varies from 4500 to 10000 Kelvins. The light is white color, and the temperature is 3000 Kelvins. In a commercial, the LED array is shown as a street light. The Surface Mount Device (SMD) LEDs are made up of only one LED. A single LED has a watt of power, and the LED interval is 1 cm in length.

Fig. 2 defines the geometry of the OWVLC for the I2 V communication system and the physical parameters for developing the simulation in the Matlab program. The dimension of the road is 20 m × 20 m, and the street light is installed on the top, while the height of the transmitter from the road plane is 6 m. As shown in Fig. 3, four street lamp array LEDs are placed in different positions. The receiver is placed on the vehicle dashboard. The height of the receiver from the road plane is 1.10 m. Therefore, the distance between the transmitter and the receiver (d) is 4.9 m. The rest of the parameters are listed in Tab. 1.

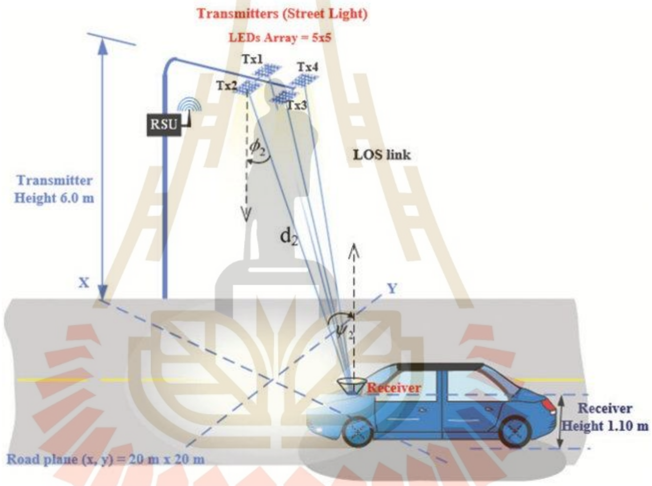

Figure 2: Geometry of the OWVLC-I2 V using MIMO technique

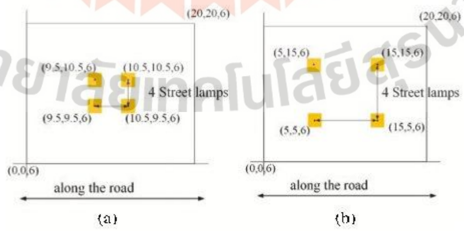

Figure 3: Street lamp transmitter position

Table 1: Simulation parameters for the OWVLC-I2 V system

Parameters	Values
LED array (nLED × nLED)	5 × 5
LED pitch	1 cm
Transmitted power (per LED)	1 watt
Center illuminous intensity for LED array	3,000 lumens
Semi-angle at half power	70 degrees
Photodetector area (A_r)	1 cm²
Reflective index at PD (n)	1.5
Optical filter gain (T_s)	1.0
Field of view (FOV)	120 degrees
Dimension of X is an along of the road	20 m
Dimension of Y is a cross of the road	20 m
Height of transmitter from the ground (Z)	6 m
Height of receiver plane above the floor (a receiver placed on vehicle)	1.10 m
Vehicle speeds (as the same as the receiver speeds)	90 km/hr or (25 m/sec.)
Number of lamps of street light (nLamp)	4 lamps
Position of Tx (x, y, z)	as Figs. 3a and 3b
(d) is the distance between Tx and Rx	4.90 m
Time for vehicle moving through coverage area (20 m)	0.8 s

2.2 *Street Light Illumination and Power Distribution*

The distribution of illuminance at a receiver plane is described in this section. It is assumed that the transmitter emits the light directly to the receiver position as the Lambertian radiation pattern [47,48]. The light intensity emitted from the transmitter, which is an array LEDs, is a cosine function dependence on the irradiance angle of emission with respect to the surface normal. The luminous intensity in angle ϕ is given as the Eq. (1).

$$I(\phi) = I(0)\cos^m(\phi) \tag{1}$$

where $I(0)$ is the center luminous intensity of LED array, ϕ is the irradiance angle of a street light which is an LED array. m is the order of Lambertian emission, it is provided by the cosine function of the semi-angle at half power of an illuminance of the LED transmitter $\phi_{1/2}$, as the Eq. (2).

$$m = -\ln(2) / \ln\left(\cos\left(\phi_{1/2}\right)\right) \tag{2}$$

The illuminance of street light is simulated by the LED array at the position of receiver plane as the horizontal (x, y, z), it is given by the Eq. (3).

$$E_{hor}(x, y, z) = \frac{I(\phi)}{d^2 . \cos(\psi)} \tag{3}$$

where d is the distance between the transmitter and receiver, ψ is an incidence angle that the light and $I(\phi)$ the illuminous intensity of the transmitter as Eq. (1). To study the illuminance distribution of the street light that using LEDs array to be the transmitter for the OWVLC-I2 V system, The street light placed at the center of the dimension of road plane (x, y).

The illuminance performance of the street light is shown in Fig. 4. The simulation is carried out using Matlab program to study the illuminous intensity of the street light and as the simulation parameters in Tab. 1. For the OWVLC-I2 V system, the program calculates the direct illumination only for 1 lamp of street light by assuming that the center of luminous intensity is 3,000 lux. for 5 × 5 LEDs array. Moreover, we illustrated the illuminance by four lamps LED array. Fig. 4. shows the distribution of illuminance using one and four street lights as the transmitter with a semi-angle at half power of 70°, respectively. As Fig. 4a, the illuminous flux maximum value of 125.0 lx is right at the center and for Fig. 4b the illuminous flux maximum value of 1798.0 lx is right at the center giving an average value of 512.42 lx. The distribution of illuminance for four transmitters will receive higher illuminance if we set a semi-angle at half power of 80°, the illuminous flux maximum value of 1816.0 lx and an average value of 569.75 lx.

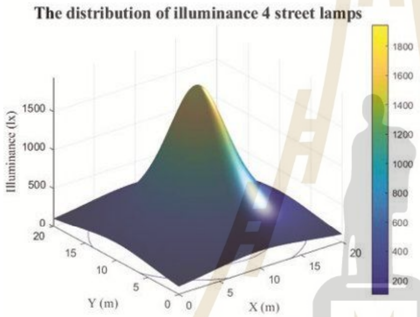

(a) Four street lamps LED array close placed.

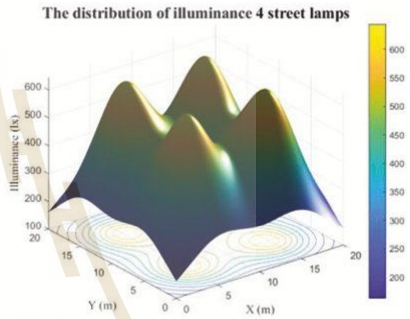

(b) Four street lamps LED array far placed.

Figure 4: The distribution of illuminance street lamp by difference transmitter position

As the optical power received distribution for at receiver plane in a LOS path, the reflection path is neglected, and the power received is given by

$$P_{r,LOS} = P_t \frac{(m+1)}{2\pi d^2} \cos^m(\phi)\, T_s(\psi)\, g(\psi) \cos(\psi),\ 0 \le \psi \le \psi_c \tag{4}$$

where ψ is an incidence angle with respect to the axis normal to the receiver surface, $g(\psi)$ is the concentrator gain at the receiver, ψ_c is the field of view (FOV) of detector, $T_s(\psi)$ is the filter transmission, and d is the distance between transmitter and receiver. The Lambertian order m is given by Eq. (2). The gain of the optical concentrator at the receiver is defined by

$$g(\psi) = \begin{cases} \dfrac{n^2}{\sin^2(\psi_c)}, & 0 \le \psi \le \psi_c \\ 0, & \psi > \psi_c \end{cases} \tag{5}$$

where n is the refractive index when the light passed the lens at a photodetector. The concentrator gain will be zero when an incidence angle is more than FOV at the photodetector. The power received distribution performance of the street light is shown in Fig. 5, simulated by Matlab program to study the received power of the street light and as the simulation parameters shown in Tab. 1.

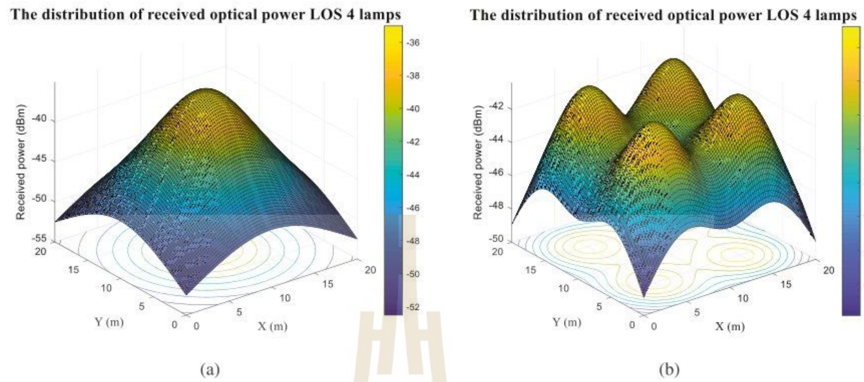

Figure 5: The distribution of received optical power LOS, (a) and (b) are transmitter at different places

According to Eq. (4), we can compute the distribution of received optical power at the LOS link of the OWVLC-I2 V system using the MIMO technique. Fig. 5 depicts the distribution of received optical power for a LOS link measured in dBm, as shown in Figs. 5a and 5b, where four street lights are placed as shown in Figs. 3a and 3b, respectively. The optical power maximum values for Figs. 5a and 5b are −35.01 dBm and −40.38 dBm. Fig. 5 shows another plot with the same value as in Figs. 5a and 5b. It is seen that the distribution of received power of Fig. 5a uncovers the edge of the road dimension, but Fig. 5b can greatly cover with the same four lamps of Fig. 5a because of the transmitter placement. Another plot with the same value as shown in Figs. 5a and 5b. It is seen that the distribution of received power in Fig. 6a does not cover the edge of the road dimension, but Fig. 6b can greatly cover with the same four lamps of Fig. 6a because of the transmitter placement.

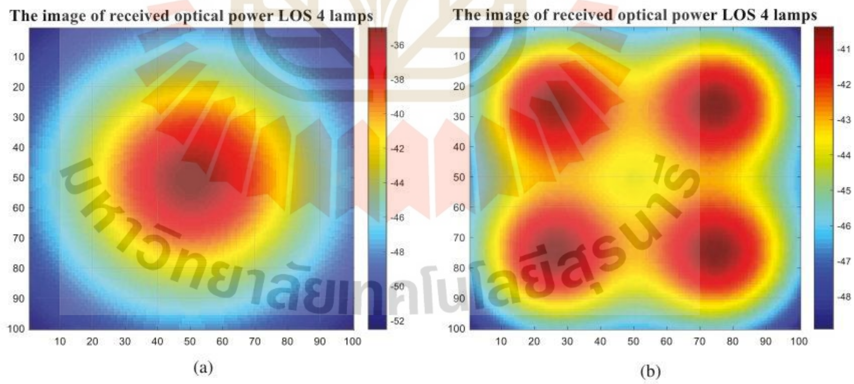

Figure 6: The image of received optical power LOS, (a) and (b) are transmitter at different places

2.3 Channel Modelling of the OWVLC-I2 V Using MIMO Technique

The distribution of the radiation intensity pattern is modeled using a generalized Lambertian radiant intensity as Eq. (1) [47,49]. The luminous intensity is used for expressing the brightness of an array LEDs. The transmitted optical power indicates the total energy radiated from an array LEDs. Luminous intensity is given in [26], that is the luminous flux per solid angle. From the topic (2.2), the transmitted power is $nLED \times nLED \times P_{LED}$, which is the power of the transmitted optical power that is given by

$$P_t = nLED \times nLED \times P_{LED} \tag{6}$$

Consider the channel DC gain on direct paths (LOS paths), which is given by

$$H_{LOS}(0) = \begin{cases} \dfrac{A_r(m+1)}{2\pi d^2}\cos^m(\phi)\,T_s(\psi)\,g(\psi)\cos(\psi), & 0 \le \psi \le \psi_c \\ 0, & eleswhere \end{cases} \tag{7}$$

where $T_s(\psi)$ is the optical filter transmission gain, $g(\psi)$ is the concentrator gain at the receiver, ψ_c is the field of view (FOV) of detector, A_r is the physical area of the photodetector, ϕ is the irradiance angle of the transmitter, ψ is the incidence angle at the receiver. The received optical power P_r expressed as the Eq. (4) or $P_r = P_t H_{los}(0)$. The propagation of light is based on the LOS link. We do not consider the channel DC gain on the reflection path. The channel response of light propagation from the transmitter to the receiver can be calculated as the Eq. (8) that is the impulse response of an LED array to the receiver.

$$h_{LOS}(t) = \frac{A_r(m+1)}{2\pi d^2}\cos^m(\phi)\,T_s(\psi)\,g(\psi)\cos(\psi)\,\delta\left(t - \frac{d}{c}\right) \tag{8}$$

where $h_{LOS}(t)$ is the impulse response of light propagation between the transmitter and the receiver, $\delta(.)$ is the Dirac function, and $\delta(t - d/c)$ represents the signal propagation delay. This function expression assumes that $\phi < 90°$, $\psi < FOV$ and $d >> \sqrt{A_r}$.

Many MIMO systems are employed with the VLC system [21]. The optical signal is arrived at the receiver from a multiple directions of LOS links. For MIMO optical wireless channel, the LOS impulse response $h_{ij}^{LOS}(t)$ from the $K - LED$ in the transmitter i^{th} to the receiver j^{th} is given as Eq. (9).

$$h_{ij}^{LOS}(t) = \begin{cases} \sum_{k=1}^{K}\dfrac{A_{rj}(m+1)}{2\pi d_{ijk}^2}\cos^m(\phi_{ijk})\,T_s(\psi_{ijk})\,g(\psi_{ijk})\cos(\psi_{ijk}), & 0 \le \psi_{ijk} \le \psi_c \\ 0, & elsewhere \end{cases} \tag{9}$$

where A_{rj} is the collection area of the j^{th} receiver, d_{ijk}^2 is the distance from the i^{th} transmitter to the j^{th} receiver, ϕ_{ijk} is the irradiance angle of transmitter, ψ_{ijk} is the angle of incidence on the receiver, ψ_c is the receiver field of view (FOV). m is the Lambertian number given as Eq. (2), g is the concentrator gain at the receiver and T_s is the filter transmission.

This section describes the channel model for the OWVLC-I2 V system using multiple input single output (MISO). This configuration is to study the channel impulse response when added more transmitters and placed the receiver at the edge of the communication area. We added the transmitters with 4 lamps. Transmitters are placed at Tx_1 (9.5, 9.5, 6), Tx_2 (10.5, 9.5, 6), Tx_3 (9.5, 10.5, 6), and Tx_4 (10.5, 10.5, 6) as shown in Fig. 3. The single receiver is placed on two positions that are Rx (19.95, 0.5, 1.10) and Rx (19.0, 5.0, 1.10). The receiver position is fixed to illustrate the channel impulse response of the OWVLC-I2 V system using MISO technique. Fig. 7 shows the channel impulse response of the where $NLOS$ is the number of LOS links position, R_x is the number of receivers, Therefore, the transmitter has more lamps and then the Eq. (10) can be modified to

$$h_{LOS}(t, R_x) = \sum_{nLOS=1}^{NLOS} \sum_{nLamp=1}^{NLamp} h_{nLOS,nLamp,ij}(t). \tag{11}$$

where $NLamp$ is the number of transmitter, $NLOS$ is the number of LOS links position and ij is the i^{th} transmitter to the j^{th} receiver. We designed to experiment with the channel impulse response of the OWVLC-I2 V system using MIMO technique. The experimental divided to LOS 3 links, LOS 5 links, and LOS 7 links along the way of the vehicle movement. All the parameters for the OWVLC-I2V system using the MIMO technique are shown in Tab. 2.

Table 2: The simulation parameters for the OWVLC-I2 V system using MIMO technique

Parameters	Values	Parameters	Values
Dimension road plane (x, y)	20 m × 20 m	Array LED (25 LEDs)	5 × 5
Height street lamp (z)	6 m	Detector physical area	1 cm^2
Receiver plane height	1.10 m	Photodiode responsibility (R_{PD})	0.55
LED power	1 W	Field of view (FOV)	120°
A street light (1 lamp)	25 LEDs	Refractive lens	1
Number of transmitters (Tx_1, Tx_2, Tx_3, and Tx_4)	4	Number of receivers (Rx_1, Rx_2, Rx_3, and Rx_4)	4

3.1 *LOS 3 Links*

Fig. 8 shows the configuration of the OWVLC-I2 V system using MIMO technique to study the characteristic of channel impulse response of the light propagation. The receiver position is defined as Tab. 3.

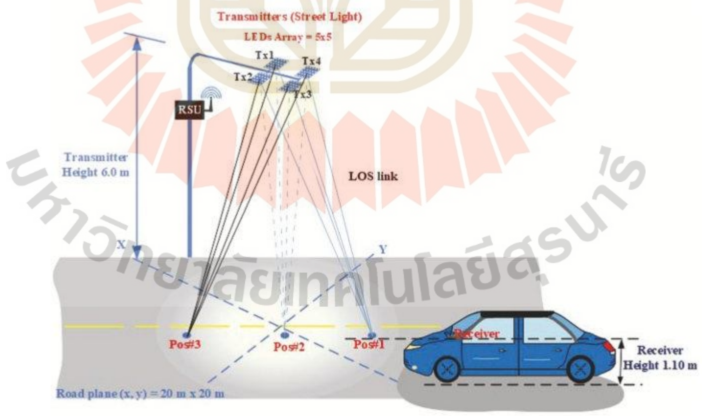

Figure 8: The light propagation of OWVLC-I2 V system using MIMO technique for LOS 3 links

Table 3: Receiver positions of each LOS 3 links

Position		LOS_1	LOS_2	LOS_3
Distance	x	10 m	10 m	10 m
	y	6.6 m	13.2 m	19.8 m

Fig. 9 shows the channel impulse response of the OWVLC-I2 V using MIMO technique which considers the number LOS of 3 positions while the receiver is on the move. The CIR signal is normalized to 1.

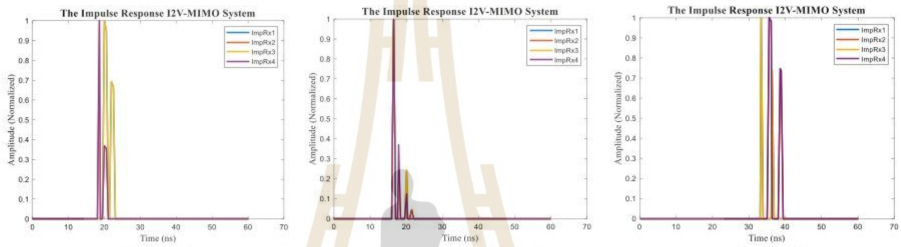

Position 1 Position 2 Position 3

Figure 9: The simulation result for CIR of the OWVLC-I2 V system using MIMO technique with LOS 3 links

3.2 LOS 5 Links

Fig. 10 illustrates the five LOS links for the OWVLC-I2 V system using MIMO technique. This is the modelling configuration to investigate the channel impulse response. The receiver position for five LOS links are shown in Tab. 4.

3.3 LOS 7 Links

Fig. 12 illustrates the seven line-of-sight links for the OWVLC-I2 V system using MIMO technique. This is the modelling configuration to investigate the channel impulse response. The receiver position for seven LOS links are shown in Tab. 5. For example, the LOS_1 receiver center position are placed as x = 10 m and y = 2.85 m. The receivers are 4 array photodetectors.

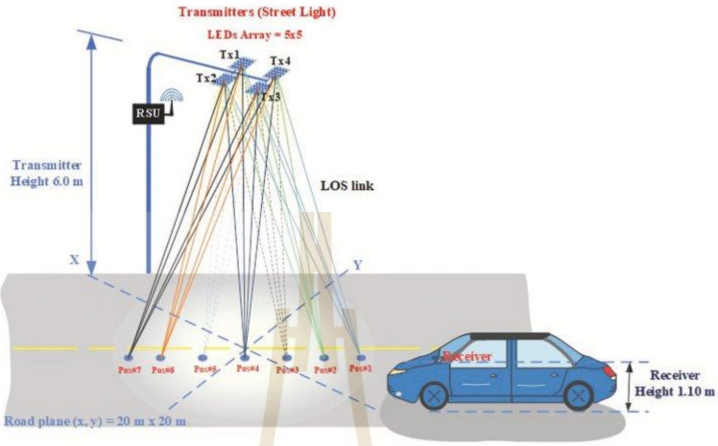

Figure 10: The light propagation of the OWVLC-I2 V system using MIMO technique for LOS 5 links

Table 4: Receiver positions of each LOS 5 links

Position		LOS_1	LOS_2	LOS_3	LOS_4	LOS_5
Distance	**x**	10 m	10 m	10 m	10 m	10 m
	y	4.0 m	8.0 m	12.0 m	16.0 m	20.0 m

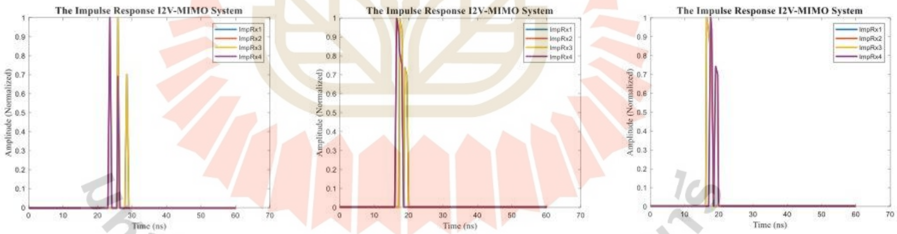

Position 1 Position 2 Position 3

Figure 11: (Continued)

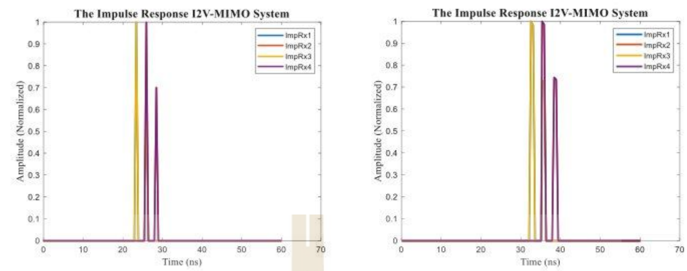

Position 4 Position 5

Figure 11: The simulation result for channel impulse response (CIR) of the OWVLC-I2 V using MIMO system LOS 5 links

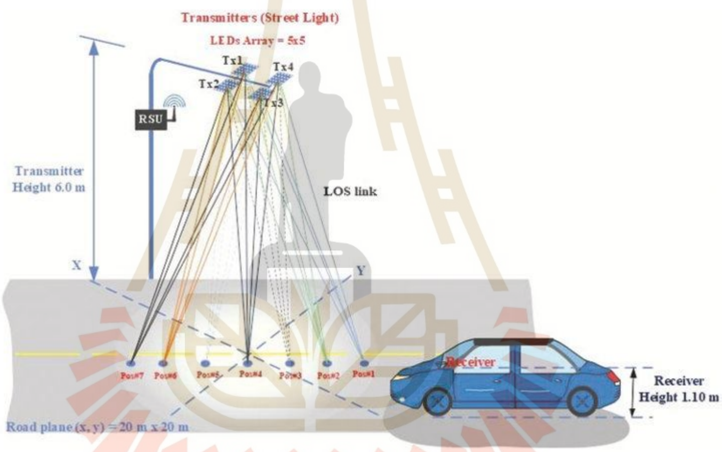

Figure 12: The light propagation of the OWVLC-I2 V system using MIMO technique for LOS 7 links

Table 5: Receiver positions of each LOS 7 links

Position		LOS_1	LOS_2	LOS_3	LOS_4	LOS_5	LOS_6	LOS_7
Distance	**x**	10 m	10 m	10 m	10 m	10 m	10 m	10 m
	y	2.85 m	5.7 m	8.55 m	11.4 m	14.25 m	17.1 m	19.95 m

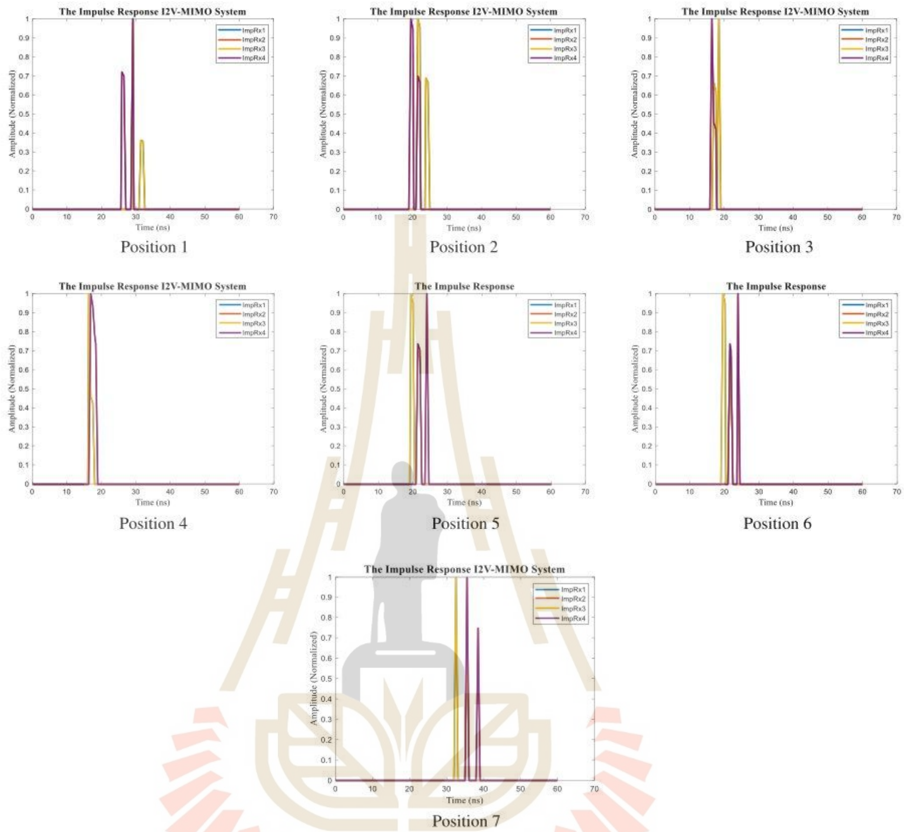

Figure 13: The simulation result for channel impulse response (CIR) of the OWVLC-I2 V using MIMO system LOS 7 links

3.4 Characteristic of Channel Impulse Response with the Different Data Rate

This section is the characteristic of channel impulse response of the OWVLC-I2 V system using MIMO technique by varying the data rate of 10 Mbps. The result shows the impulse response signal of light propagation from four transmitters to four receivers. As shown in Figs. 14a and 14c, the impulse response of along the cover communication area is overlapped by the light signal from Tx_1 with Tx_3 and Tx_2 with Tx_4, that is normalized signal. For the CIR of the OWVLC-I2 V MIMO system of LOS 3 links, data rate is 10 Mbps. We can compare with Fig. 9 that is the same as LOS 3 links. It can be seen that the data rate is related to the signal frequency of CIR. Figs. 14a and 14b show the light propagation time around of 20 ns and Fig. 14c move up near to 40 ns. We can compare Figs. 14 with 9 for different data rate.

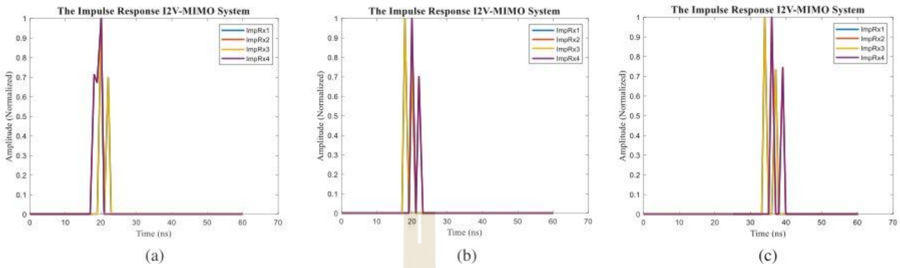

Figure 14: The simulation result for channel impulse response of the OWVLC-I2 V using MIMO system LOS 3 links

Figs. 14–16 show the CIR of the OWVLC-I2 V using MIMO technique as LOS 3, LOS 5 and LOS 7 links. We can compare with Figs. 9, 11, and Fig. 13 for each LOS 3, LOS 5 links and LOS 7 links positions respectively. The CIR with different data rate had important rise time and fall time for data rate of 10 Mbps and 20 Mbps.

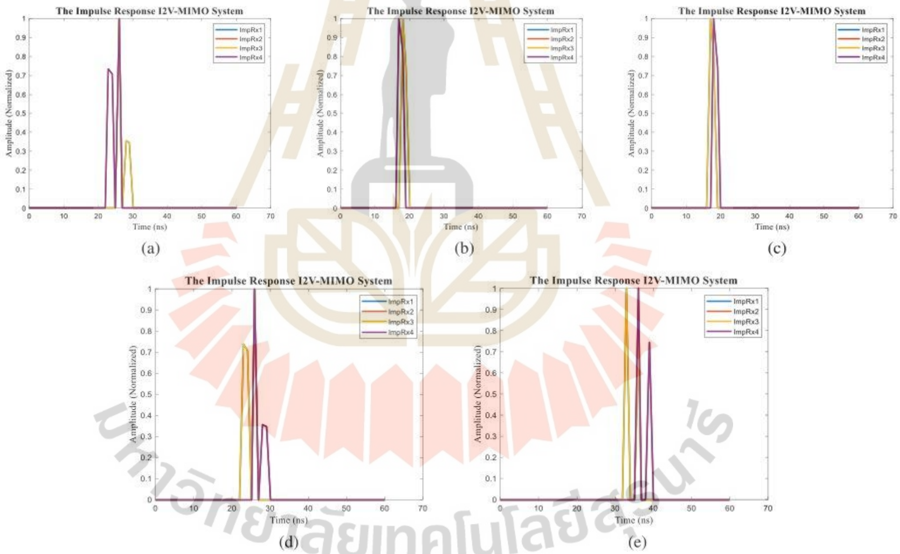

Figure 15: The simulation result for channel impulse response (CIR) of the OWVLC-I2 V using MIMO system LOS 5 links

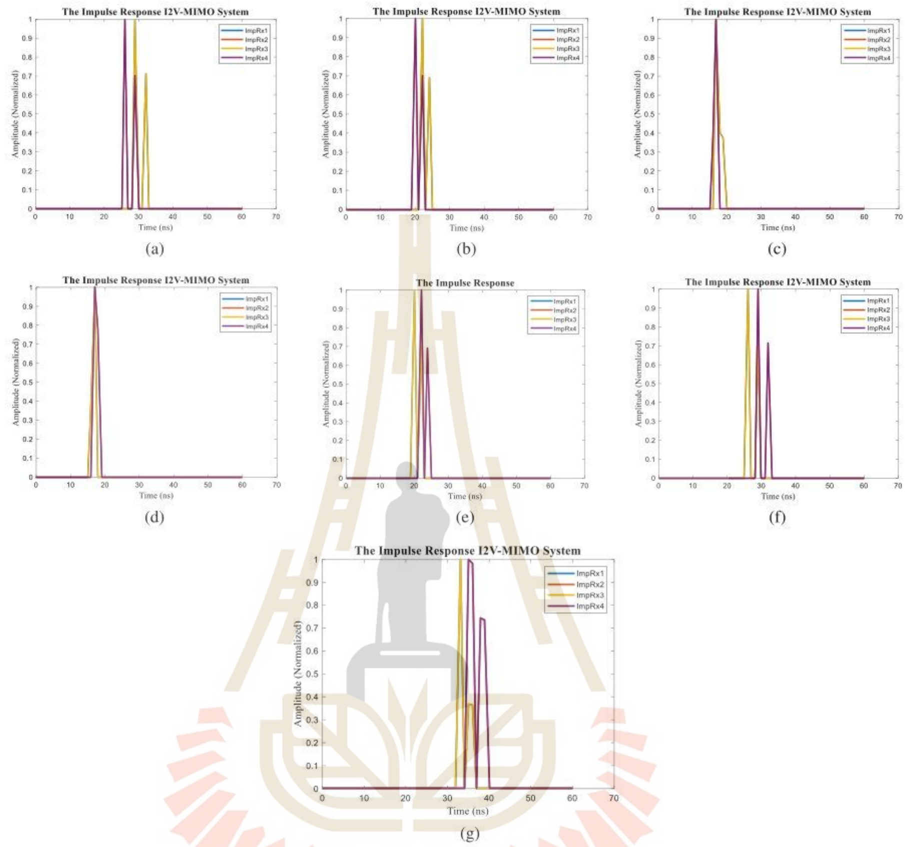

Figure 16: The simulation result for channel impulse response (CIR) of the OWVLC-I2 V MIMO system LOS 7 links

The light is converted to the electrical current as $i = (P_t)\, R_{PD}$. To study the signal to noise ratio (SNR) for the OWVLC-I2 V system, the SNR can be expressed in term of the received optical power (P_r), the photodetector responsibility (R_{PD}) (Ampere/Watt), and noise variance that is [49]

$$SNR = \frac{(R_{PD}P_r)^2}{\sigma_{shot}^2 + \sigma_{amp}^2} \tag{12}$$

where the shot noise and amplifier noise variances are given by [50]

$$\sigma_{shot}^2 = 2qB_n\,(R_{PD}P_r + P_n) \tag{13}$$

$$\sigma_{amp}^2 = i_{amplifier}^2 B_a \tag{14}$$

where B_n is noise bandwidth $B_n = I_2 R_b$, I_2 is the noise bandwidth factor, R_b is the data rate, q is the electron mass, P_n is the noise power of the ambient light, B_a is the amplifier bandwidth, and I^2_{amp} is the amplifier noise density. The total noise is given by

$$\sigma^2_{total} = 2qR_{PD}B_n(P_r + P_n) + i^2_{amp}B_a \tag{15}$$

The bit error rate can be calculated from the SNR as $BER = Q\sqrt{SNR}$, where $Q(x) = \frac{1}{2}\int_x^\infty e^{\frac{-y^2}{2}}dy$ [49].

4 The Performance of the OWVLC-I2 V System Using MIMO Technique

In this section, we perform the data transmission for the OWVLC-I2 V system using MIMO technique. The data input is a serial of [0, 1, 0, 1, . . .] stream, which is converted into a number of the transmitters. The data sequence is modulated by on-of-keying (OOK), which is the modulated signal to drive the street light. Then, data streams are convolved with the LED impulse response $h_{LED}(t)$ [49]. It is the street light luminance. We assumed that the array LEDs have the Lambertian radiant intensity as Eq. (3). The receiver consists of the concentrator lens for four photodetectors and a preamplifier. Then, the signal is low pass filtered and equalized if necessary. The data streams are concatenated to form a single received data stream compared to the input data stream to calculate the BER.

The measurement performance of the OWVLC-I2 V system is illustrated in the Bit Error Rate (BER). The BER performance at a data rate is 20 Mbps. Fig. 17 shows the BER of the OWVLC-I2 V system using the MIMO technique with LOS 3 links, which is related to the CIR of Fig. 9 that we have designed to investigate the CIR of the OWVLC-I2 V system when the vehicle moves through the communication area. We divided the communication links into 3, 5, and 7 links to study the performance of each link and which one is better for the I2 V system. It will represent the I2 V communication system during the vehicle movement through the street light.

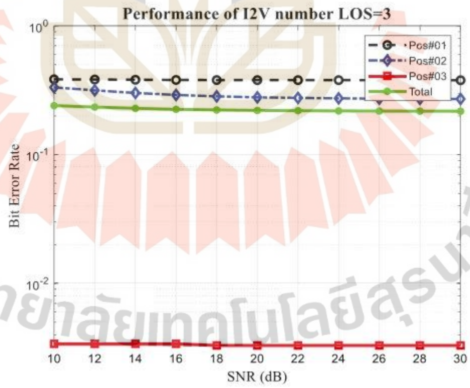

Figure 17: Bit error rate of the OWVLC-I2 V system using MIMO technique with LOS 3 links

Fig. 18 shows the BER performance of the OWVLC-I2 V system that used the characteristics of the LOS 5 and 7 links as Figs. 18a and 18b, respectively, at the data rate of 20 Mbps. It can be seen that the BER performance for all LOS links, the LOS 3 links looked better than the LOS 5 and 7 links.

Therefore, BER was too high from our study for all the LOS 3, 5, and 7 links in terms of Inter-Symbol Interference (ISI) of the received signal. One is the simple receiver design for signal processing. The satisfied LOS links to represent the OWVLC-I2 V system is LOS 3 links that we decided from the BER performance.

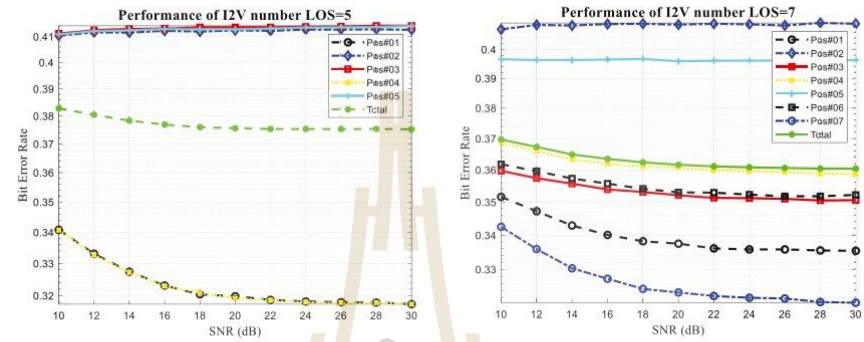

(a) (b)

Figure 18: Bit error rate of the OWVLC-I2 V system using MIMO technique (a) with LOS 5 links, and (b) with LOS 7 links

Fig. 19 shows the performance of the vehicle speed versus the data throughput of the OWVLC-I2 V system using the MIMO technique while the vehicle passes a street light. We compared two data rates, 10 Mbps and 20 Mbps, according to the characteristics of LOS links of both data rates. There is a significant difference in throughput at a low vehicle speed of 20 km/hr. Furthermore, there is a slight difference in high vehicle speed of 140 km/hr.

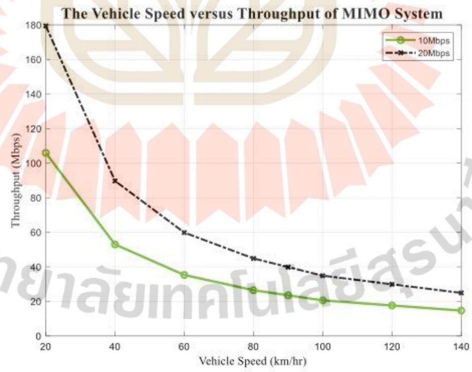

Figure 19: Data throughput of the OWVLC-I2 V system using MIMO technique

5 Conclusion

ITS is used by information and communication technologies for managing transportation and traffic to improve the efficiency of the road system, public transportation systems, and traffic safety to reduce accidents and congestion in the traffic. The advantages of ITS are that the warning signs appear before the drivers arrive at the accident point, allowing them to avoid the accident, and the limited speed signs, which can change the speeds before they arrive at regulated areas. Due to the presence of vehicle lights and the existing traffic light infrastructure, VLC could be used for vehicular communication. Outdoor wireless visible light communication is applied for infrastructure to vehicles in ITS. We investigated the channel impulse response of the MISO system for the I2 V communication system. The system analysis in this paper represents the channel impulse response of MISO and MIMO techniques while the receiver is on the move, and it may be that some perform the relation between vehicle speed and received data. It is worthy of further work to improve the data rate even more than our current configuration system. The BER performance of the OWVLC-I2 V system using the MIMO technique needs to be improved further in the following work. The performance BER of the OWVLC-I2 V system unachieved the BER of 10^{-4}. Therefore, there are many challenges to improve the OWVLC-I2 V system, such as robust noise effects, distance communication, coverage area, and daytime communication, which will be considered for study in the next future.

Acknowledgement: The authors would like to thank the Ministry of Higher Education, Science and Research Innovation of Thailand for supporting the scholarship to study Ph.D. and thanks the Nakhon Pathom Rajabhat University for supporting the full-time study.

Funding Statement: This work was supported in part by the Ministry of Higher Education, Science and Research Innovation of Thailand.

Conflicts of Interest: The authors declare that they have no conflicts of interest to report regarding the present study.

References

[1] World Health Organization (WHO) "Global status report on road safety 2018," [Online]. Available: https://www.who.int/violence_injury_prevention/road_safety_status/2018/en/.

[2] A. -M. Cailean, B. Cagneau, L. Chassagne, V. Popa and M. Dimian, "A survey on the usage of DSRC and VLC in communication-based vehicle safety applications," in *IEEE 21st Symp. on Communications and Vehicular Technology in the Benelux (SCVT)*, Delft, The Netherlands, pp. 69–74, Nov. 2014.

[3] O. K. Tonguz, N. Wisitpongphan, J. S. Parikh, F. Bai, P. Mudalige *et al.*, "On the broadcast storm problem in ad hoc wireless networks," in *3rd Int. Conf. on Broadband Communications, Networks and Systems*, San Jose, CA, USA, Oct. 2006, pp. 1–11, 2016.

[4] N. Wisitpongphan, O. K. Tonguz, J. S. Parikh, P. Mudalige, F. Bai *et al.*, "Broadcast storm mitigation techniques in vehicular ad hoc networks," *IEEE Wireless Communications*, vol. 14, no. 6, pp. 84–94, 2007.

[5] P. Papadimitratos, A. De La Fortelle, K. Evenssen, R. Brignolo and S. Cosenza, "Vehicular communication systems: Enabling technologies, applications, and future outlook on intelligent transportation," *IEEE Communications Magazine*, vol. 47, no. 11, pp. 84–95, 2009.

[6] I. Takai, S. Ito, K. Yasutomi, K. Kagawa, M. Andoh *et al.*, "LED and CMOS image sensor based optical wireless communication system for automotive applications," *IEEE Photonics Journal*, vol. 5, no. 5, Art. no. 6801418, 2013.

[7] I. Takai, T. Harada, M. Andoh, K. Yasutomi, K. Kagawa *et al.*, "Optical vehicle-to-vehicle communication system using LED transmitter and camera receiver," *IEEE Photonics Journal*, vol. 6, no. 5, Art. no. 7902513, 2014.

[8] T. Yamazato, I. Takai, H. Okada, T. Fujii, T. Yendo *et al.,* "Image-sensor-based visible light communication for automotive applications," *IEEE Communications Magazine*, vol. 52, no. 7, pp. 88–97, 2014.

[9] Y. Goto, I. Takai, T. Yamazato, H. Okada, T. Fujii *et al.,* "A new automotive VLC system using optical communication image sensor," *IEEE Photonics Journal*, vol. 8, no. 3, pp. 1–17, 2016.

[10] S. Okada, T. Yendo, T. Yamazato, T. Fujii, M. Tanimoto *et al.,* "On-vehicle receiver for distant visible light road-to vehicle communication," in *IEEE Intelligent Vehicles Symp. (IV)*, Xi'an, China, pp. 1033–1038, 14 July 2009.

[11] A. -M. Cailean, B. Cagneau, L. Chassagne, M. Dimian and V. Popa, "Novel receiver sensor for visible light communications in automotive applications," *IEEE Sensors Journal*, vol. 15, no. 8, pp. 4632–4639, 2015.

[12] N. Lourenço, D. Terra, N. Kumar, L. N. Alves and R. L. Aguiar, "Visible light communication system for outdoor applications," in *8th Int. Symp. on Communication Systems, Networks & Digital Signal Processing (CSNDSP)*, Poznañ, Poland, July 2012, pp. 1–6, 2012, July 2012.

[13] A. -M. C˘ailean and M. Dimian, "Current challenges for visible light communications usage in vehicle applications: A survey," in *IEEE Communication Surveys & Tutorials*, Fourth Quarter, vol. 19, no. 4, pp. 2681–2703, 2017.

[14] D. Gesbert, M. Shafi, D. -S. Shiu, P. J. Smith and A. Naguib, "From theory to practice: An overview of MIMO space-time coded wireless systems," *IEEE Journal Selected Areas in Communications*, vol. 21, pp. 281–302, 2003.

[15] S. G. Wilson, M. Brandt-Pearce, Q. Cao and J. Leveque, "Optical MIMO transmission using Q-ary PPM for atmospheric channels," *The Thirty-Seventh Asilomar Conference on Signals, Systems & Computers*, vol. 1, pp. 1090–1094, 2003.

[16] S. Jivkova, B. A. Hristov and M. Kavehrad, "Power-efficient multi-spot-diffuse multiple-input-multiple-output approach to broad-band optical wireless communications," *IEEE Transaction on Vehicular Technology*, vol. 53, no. 3, pp. 882–889, 2004.

[17] S. Hranilovic and F. R. Kschischang, "A pixelated MIMO wireless optical communication system," *IEEE Journal of Selected Topics in Quantum Electronics*, vol. 12, no. 4, pp. 859–874, 2006.

[18] M. Garfield, C. Liang, P. Kurzweg and K. R. Dandekar, "MIMO Space-time coding for diffuse optical communication," *Microwave and Optical Technology Letters*, vol. 48, pp. 1108–10, 2006.

[19] D. O'Brien, "Indoor optical wireless communications: Recent developments and future challenges," in *Proc. SPIE 7464 Free-Space Laser Communications IX*, San Diego, CA, USA, vol. 7464, pp. 74640B-12, 2009.

[20] A. G. Kirk, "Free-Space Optical Interconnects," in *Optical Interconnects: The Silicon Approach*, L. Pavesi and G. G. Guillot, Eds. Berlin: Springer, 2006.

[21] L. Zeng, D. O'Brien, H. L. Minh, G. E. Faulkner, K. Lee *et al.,* "High data rate multiple input multiple output (MIMO) optical wireless communications using white LED lighting," *IEEE Journal Selected Areas in Communications*, vol. 27, no. 9, pp. 1654–1662, 2009.

[22] M. Abualhoul, "Visible light and radio communication for cooperative autonomous driving: Applied to vehicle convoy," *Ph.D. Thesis*, MINES ParisTech, Paris, France, 2016.

[23] S. Arnon, "Optimised optical wireless car-to-traffic-light communication," *Transactions on Emerging Telecommunications Technologies*, vol. 25, pp. 660–665, 2014.

[24] X. Tang, H. Le-Minh, W. Viriyasitavat, Z. Ghassemlooy, H. M. Tsai *et al., Car-to-Car Visible Light Communications. in Visible Light Communications*, CRC Press: Boca Raton, FL, USA, pp. 275–304, 2017.

[25] S. Ucar, S. C. Ergen and O. Ozkasap, "IEEE 802.11 p and visible light hybrid communication based secure autonomous platoon," *IEEE Transactions on Vehicular Technology*, vol. 67, pp. 8667–8681, 2018.

[26] N. Kumar, N. Lourenço, D. Terra, L. N. Alves and R. L. Aguiar, "Visible light communications in intelligent transportation systems," in *2012 IEEE Intelligent Vehicles Symp.*, Madrid, Spain, pp. 748–753, June 2012.

[27] M. Uysal, Z. Ghassemlooy, A. Bekkali, A. Kadri and H. Menouar, "Visible light communication for vehicular networking: Performance study of a V2V system using a measured headlamp beam pattern model," *IEEE Vehicular Technology Magazine*, vol. 10, pp. 45–53, 2015.

[28] N. Wang, C. Liu, Y. Lu and J. Shen, "A visible light communication (VLC) based intelligent transportation system for lorry fleet," in *2017 16th Int. Conf. on Optical Communications and Networks (ICOCN)*, Wuzhen, China, 7–10 August, pp. 1–3, 2017.
[29] Q. -H. Dang and M. Yoo, "Handover procedure and algorithm in vehicle to infrastructure visible light communication," *IEEE Access*, vol. 5, pp. 26466–26475, 2017.
[30] L. Cheng, W. Viriyasitavat, M. Boban and H. M. Tsai, "Comparison of radio frequency and visible light propagation channels for vehicular communications," *IEEE Access*, vol. 6, pp. 2634–2644, 2017.
[31] W. Sun, G. C. Zhang, X. R. Zhang, X. Zhang and N. N. Ge, "Fine-grained vehicle type classification using lightweight convolutional neural network with feature optimization and joint learning strategy," *Multimedia Tools and Applications*, vol. 80, no. 20, pp. 30803–30816, 2021.
[32] W. Sun, X. Zhang, S. Peeta, X. He and Y. Li, "A Real-time fatigue driving recognition method incorporating contextual features and two fusion levels," *IEEE Transactions on Intelligent Transportation Systems*, vol. 18, no. 12, pp. 3408–3420, 2017.
[33] R. Raj, K. Jindal and A. Dixit, "Fairness enhancement of non-orthogonal multiple access in VLC-based IoT networks for intravehicular applications," *IEEE Transactions on Vehicular Technology*, (https://doi.org/10.1109/TVT.2022.3167091), 2022.
[34] X. Deng, W. Fan, T. B. Cunha, S. Ma, C. Chen *et al.,* "Two-dimensional power allocation for optical MIMO-OFDM systems over low-pass channels," *IEEE Transactions on Vehicular Technology*, (https://doi.org/10.1109/TVT.2022.3162621), 2022.
[35] H. B. Eldeeb, S. M. Saiit and M. Uysal, "Visible light communication for connected vehicles: How to achieve the omnidirectional coverage?," *IEEE Access*, vol. 9, pp. 103885–103905, 2021.
[36] N. Kumar, D. Terra, N. Lourenco, L. N. Alves and R. L. Aguiar, "Visible light communication for intelligent transportation in road safety applications," in *Proc. 7th Int. Wireless Communication Mobile Computer Conf.*, Istanbul, Turkey, Jul 2011, pp. 1513–1518, 2011.
[37] K. Cui, G. Chen, Z. Xu and R. D. Roberts, "Traffic light to vehicle visible light communication channel characterization," *Applied Optics*, vol. 51, no. 27, pp. 6594–6605, 2012.
[38] J. -H. Lee and S. -Y. Jung, "SNR analyses of the multi-spectral light channel for optical wireless LED communications in intelligent transportation system," in *Proc. IEEE 79th Vehicular Technology Conf. (VTC Spring)*, Seoul, Korea (South), pp. 1–5, May 2014.
[39] T. Nawaz, M. Seminara, S. Caputo, L. Mucchi, F. S. Cataliotti *et al.,* "IEEE 802.15. 7-compliant ultra-low latency relaying VLC system for safety-critical ITS," *IEEE Transaction on Vehicular Technology*, vol. 68, no. 12, pp. 12040–12051, 2019.
[40] M. Seminara, T. Nawaz, S. Caputo, L. Mucchi and J. Catani, "Characterization of field of view in visible light communication systems for intelligent transportation systems," *IEEE Photonics Journal*, vol. 12, no. 4, pp. 1–16, Aug. 2020.
[41] X. You, Y. Zhong, J. Chen and C. Yu, "Mobile channel estimation based on decision feedback in vehicle-to-infrastructure visible light communication systems," *Optics Communications*, vol. 462, Art. no. 125261, 2020.
[42] M. S. Demir, H. B. Eldeeb and M. Uysal, "CoMP-based dynamic handover for vehicular VLC networks," *IEEE Communications Letters*, vol. 24, no. 9, pp. 2024–2028, 2020.
[43] B. Turan, O. Narmanlioglu, O. N. Koc, E. Kar, S. Coleri *et al.,* "Measurement based non-line-of-sight vehicular visible light communication channel characterization," *Electrical Engineering and Systems Science in Signal Processing*, (arXiv:2111.11369[eess. SP]), 2021.
[44] P. Sharda, M. R. Bhatnagar and Z. Ghassemlooy, "Modeling of a vehicle-to-vehicle based visible light communication system under shadowing and investigation of the diversity-multiplexing tradeoff," *IEEE Transactions on Vehicular Technology*, (https://doi.org/10.1109/TVT.2022.3176907), 2022.
[45] G. Singh, A. Srivastava and V. A. Bohara, "Visible light and reconfigurable intelligent surfaces for beyond 5G V2X communication networks at road intersections," *IEEE Transactions on Vehicular Technology*, (https://doi.org/10.1109/TVT.2022.3174131), 2022.

[46] M. Fouda, S. Hashima, S. Sakib, Z. Fadlullah, K. Hatano *et al.,* "Optimal channel selection in hybrid RF/VLC networks: A multi-armed bandit approach," *IEEE Transactions on Vehicular Technology*, vol. 71, no. 6, pp. 6853–6858, 2022.
[47] T. Komine and M. Nakagawa, "Fundamental analysis for visible-light communication system using LED lights," *IEEE Transactions on Consumer Electronics*, vol. 50, pp. 100–107, 2004.
[48] J. M. Kahn and J. R. Barry, "Wireless infrared communications," *Proceedings of the IEEE*, vol. 85, no. 2, pp. 265–298, 1997.
[49] Z. Ghassemlooy, W. Popoola and S. Rajbhandari, "Optical wireless communications: System and channel modelling with matlab®," *CRC Press*, Chapter 3, pp. 77–159, 2019.
[50] L. Zeng, D. O'Brien, H. L. Minh, K. Lee, D. Jung *et al.,* "Improvement of date rate by using equalization in an indoor visible light communication system," in *2008 4th IEEE Int. Conf. on Circuits and Systems for Communications*, Shanghai, China, pp. 678–682, 2008.

จำลองระบบการสื่อสารด้วยแสงที่มองเห็นเพื่อประยุกต์ใช้งานระหว่างไฟส่องสว่างบนถนนกับยานยนต์

Modelling of Outdoor Wireless Visible Light Communication for Street Lamp to Vehicle Application

อดิศร แก้วภักดี[1] พีระพงษ์ อุฑารสกุล[1] และ เจษฎา สาททอง[2]

[1]สาขาวิชาวิศวกรรมโทรคมนาคมและคอมพิวเตอร์ สำนักวิชาวิศวกรรมศาสตร์ มหาวิทยาลัยเทคโนโลยีสุรนารี d6040512@g.sut.ac.th

[2]สาขาวิชาวิศวกรรมไฟฟ้า แขนงวิชาวิศวกรรมไฟฟ้าสื่อสาร คณะวิทยาศาสตร์และเทคโนโลยี มหาวิทยาลัยราชภัฏนครปฐม

PH-6

บทคัดย่อ

อุบัติเหตุทางจราจรและผู้ประสบภัยที่เกี่ยวข้องมีจำนวนเพิ่มขึ้นอย่างน่าสนใจ ด้วยเครือข่ายการสื่อสารข้อมูลเป็นสิ่งดีที่ช่วยเพิ่มความปลอดภัยบนท้องถนน บทความนี้นำเสนอแบบจำลองระบบการสื่อสารด้วยแสงที่มองเห็นเพื่อประยุกต์ใช้งานระหว่างไฟส่องสว่างบนถนนกับยานยนต์ เพื่อนำไปใช้งานกับระบบขนส่งอัจฉริยะ ที่ไฟส่องสว่างบนถนนทำงานในช่วงเวลากลางคืนและสามารถกระจายสัญญาณข้อมูลการจราจรจากสถานีกระจายสัญญาณข้างถนนของระบบขนส่งอัจฉริยะไปยังยานยนต์ที่กำลังเคลื่อนที่บนถนน จำลองไฟส่องสว่างเป็นหลอดแอลอีดีที่มีคุณสมบัติเฉพาะที่ให้แสงสว่างและแพร่กระจายข้อมูลได้ด้วย ตัวรับสัญญาณเป็นโฟโตไดโอดติดตั้งที่ยานยนต์รับสัญญาณแสงเปลี่ยนเป็นสัญญาณไฟฟ้าผ่านวงจรภาครับเพื่อถอดรหัสให้ได้ข้อมูลข่าวสารกลับคืน

คำสำคัญ: การสื่อสารไร้สายด้วยแสงที่มองเห็นภายนอกอาคาร ระบบขนส่งอัจฉริยะ โครงสร้างพื้นฐานกับยานยนต์

Abstract

Currently, traffic incidents and related victims have increased dramatically. With the data communication network is a great thing to improve transportation safety. Intelligent Transportation System (ITS) is promising to employ for distributing the traffic information to the vehicle on the road. This paper demonstrates a modelling of Outdoor Wireless Visible Light Communication (OWVLC) for Infrastructure to Vehicle (I2V) application. The transmitter is a Street Lamp (SL), Light Emitting Diode (LED) is widely used for illuminance on the road at nighttime. It not only for the luminance but also able to broadcast the traffic data. OWVLC can support an ITS by cooperating with the Road Side Unit (RSU) which is alternative communication for ITS. We show the model configuration of OWVLC-I2V system. The results illustrate that OWVLC-I2V system can communicate base on the simulation programming.

Keywords: Outdoor Wireless Visible Light Communication, Intelligent Transportation System, Infrastructure to Vehicle

1. บทนำ

องค์การอนามัยโลกรายงานการเสียชีวิตจากอุบัติเหตุบนท้องถนนมีจำนวน 1.35 ล้านคน ในปี ค.ศ. 2018 [1] เป็นอันดับที่ 8 ของการเสียชีวิต นักวิจัยพยายามนำเทคโนโลยีมาใช้งานกับการจราจร เพื่อช่วยลดจำนวนอุบัติเหตุและผู้เสียชีวิต ช่วยอำนวยความสะดวกด้านการจราจร ลดปัญหารถติด ลดการใช้พลังงาน ลดการปล่อยก๊าซคาร์บอนไดออกไซด์ซึ่งเป็นปัญหาหลักของสภาวะโลกร้อน เทคโนโลยีระบบขนส่งอัจฉริยะ (Intelligent Transportation System: ITS) นำเครือข่ายการสื่อสารยานยนต์เฉพาะกิจ (Vehicular Ad-hoc Networks: VANETs) ซึ่งมีหลายรูปแบบด้วยกัน อาทิเช่น การสื่อสารระยะสั้น (Dedicated Short-Range Communication: DSRC) การสื่อสารไร้สายแบบแอดฮอกสำหรับยานยนต์ (Wireless Ad-hoc Vehicular Environment: WAVE) และการสื่อสารด้วยโครงข่ายเซลลูล่าสำหรับยานยนต์กับทุกสรรพสิ่ง (Cellular-Vehicles to Everything: C-V2x) ในปัจจุบัน DSRC และ C-V2x ได้ทดลองใช้งานจริงโดยบริษัท Qualcomm Technologies, Inc. [2] เป็นการสร้างระบบ C-V2x เพื่อใช้งานด้านความปลอดภัยต่อเนื่องไปยังการใช้งานใน 5G NR C-V2x สำหรับยานยนต์ขับเคลื่อนอัตโนมัติในอนาคต คาดว่านำมาใช้งานร่วมกับระบบ DSRC ที่ใช้มาตรฐาน IEEE 802.11p ซึ่งพัฒนามาจาก IEEE 802.11a

การสื่อสารด้วยคลื่นความถี่วิทยุ (Radio Frequency: RF) มีย่านความถี่ที่ใช้งานจำกัด และมีต้นทุนที่สูง จึงได้พยายามนำเทคโนโลยีการสื่อสารด้วยแสงที่มองเห็น (Visible Light Communication : VLC) ประยุกต์ใช้งานกับ ITS เพื่อเป็นทางเลือก หรือใช้งานร่วมกับระบบ RF ด้วยเทคโนโลยีหลอดแอลอีดี (Light Emitting Diode: LED) [3-4] ที่ให้แสงสว่างที่มากพอและใช้ส่งข้อมูลข่าวสารได้ คาดว่าหลอดแอลอีดีจะถูกนำมาแทนหลอดไฟแบบเดิม [3] ซึ่งงานวิจัยด้าน VLC ในระบบการสื่อสารไร้สายด้วยแสงที่มองเห็นภายในอาคาร (Indoor Wireless Visible Light Communication: IWVLC) [5] ถูกพัฒนาให้การสื่อสารไร้สายภายในอาคารสามารถส่งข้อมูลระดับกิกะบิตต่อวินาที (Gb/s) [6]

พัฒนาไปสู่การสื่อสารไร้สายด้วยแสงที่มองเห็นภายนอกอาคาร (Outdoor Wireless Visible Light Communication: OWVLC) [7] งานวิจัยที่เกี่ยวข้องกับการสื่อสารไร้สายด้วยแสงที่มองเห็นเพื่อยานยนต์นั้นถือว่ามีความท้าทาย จาก [8] ได้จำลองสถานการณ์ระบบ VLC เป็นการใช้งานบนทางหลวง เป็นการสื่อสารแบบ V2V ยานยนต์ที่ได้รับข้อมูลการจราจรด้วยตัวตรวจจับแสงและส่งข้อมูลที่ได้รับไปยังยานยนต์ที่อยู่บริเวณใกล้เคียงกันด้วยไฟหน้าและไฟท้าย และมีงานวิจัยที่แสดงให้เห็นว่าระบบ VLC สามารถตอบสนองความต้องการต่อข้อกำหนดในเครือข่ายการสื่อสารของยานยนต์ในสภาพการใช้งานจริง [9] และ [10] ถูกค้นพบว่าเป็นระบบที่ทำงานร่วมกันได้กับการสื่อสารระหว่างยานยนต์จาก [11] ส่วนงานวิจัยใน

เชิงปฏิบัติเป็นการสื่อสารระหว่างไฟจราจรกับยานยนต์ [12] และการสื่อสารแบบ VLC-I2V สามารถทำงานร่วมกันได้กับไฟส่องสว่างบนถนนกับยานยนต์ [13] และ [14] ซึ่งแสดงเป็นระยะทางสั้นแบบคงที่ระหว่างไฟส่องสว่างบนถนนกับยานยนต์ที่ใช้กำลังงานที่สูงทำให้ช่วยเพิ่มอัตรการส่งข้อมูลได้ ทำให้มีเสถียรภาพการสื่อสารที่เพิ่มขึ้น ทำให้ VLC-I2V มีศักยภาพที่สูงในการพัฒนาต่อในอนาคต

งานวิจัยฉบับนี้นำเสนอแบบจำลองการสื่อสารไร้สายด้วยแสงที่มองเห็นภายนอกอาคารเพื่อประยุกต์ใช้งานระหว่างไฟส่องสว่างบนถนนกันยานยนต์ (OWVLC-I2V) จำลองตัวส่งเป็นไฟส่องสว่างบนถนน (Street Light) เป็นหลอดแอลอีดีแบบอาเรย์ (Array LED) ทำการส่งสัญญาณข้อมูลการจราจรผ่านช่องสัญญาณทางแสง เพื่อศึกษาการแพร่กระจายแสงของความสว่าง และการแพร่กระจายกำลังงานแสงที่ได้ของระนาบตัวรับสัญญาณแสง กำหนดให้ภาครับเป็นโฟโตดีเทคเตอร์ (Photodetector) ทำหน้าที่เปลี่ยนสัญญาณแสงเป็นสัญญาณไฟฟ้า ส่งไปยังภาคถอดรหัสให้ได้สัญญาณข้อมูลข่าวสารกลับคืน

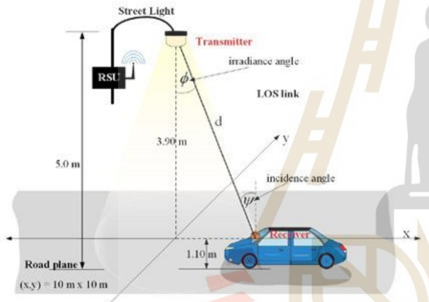

รูปที่ 1 จำลองระบบการสื่อสาร OWVLC-I2V

งานวิจัยประกอบด้วย อธิบายแบบจำลองระบบการสื่อสารไร้สายด้วยแสงที่มองเห็นภายนอกอาคารเพื่อประยุกต์ใช้งานระหว่างไฟส่องสว่างบนถนนกับยานยนต์ ช่องสัญญาณการสื่อสารของระบบรวมถึงสัญญาณผลตอบสนองของช่องสัญญาณการสื่อสาร สัญญาณรบกวนของระบบ การทำงานของภาครับ ในหัวข้อที่สอง หัวข้อที่สามอภิปรายผลการทดลองเชิงตัวเลข และหัวข้อที่สี่สรุปผลการทดลอง

2. แบบจำลองระบบการสื่อสารไร้สายด้วยแสงที่มองเห็นเพื่อประยุกต์ใช้งานระหว่างไฟส่องสว่างบนถนนกับยานยนต์

นักวิจัยได้ทำการออกแบบจำลองระบบการสื่อสารไร้สายด้วยแสงที่มองเห็นภายนอกอาคารเพื่อประยุกต์ใช้งานระหว่างไฟส่องสว่างบนถนนกับยานยนต์ (A modelling of OWVLC-I2V system) แสดงดังรูปที่ 1 ให้ตัวส่งสัญญาณเป็นไฟส่องสว่างบนถนน (Street Light) คือหลอดแอลอีดีอาเรย์ (Array LED) ขนาด 5 x 5 กำหนดแต่ละหลอดมีกำลัง 1 วัตต์ ตัวสถานีกระจายสัญญาณข้างถนน (RSU) ที่รับสัญญาณการจราจรจากศูนย์กลางการควบคุมจราจร (Traffic Control Center) เชื่อมต่อกับตัวส่งเพื่อให้ไฟส่องสว่างทำหน้าที่กระจายข้อมูลข่าวสารไปยังยานยนต์ที่กำลังเคลื่อนที่อยู่บนถนน ดังตารางที่ 1 แสดงค่าตัวแปรของระบบ OWVLC-I2V ที่ได้ทำการออกแบบซึ่งประยุกต์จากระบบ IWVLC [5] และ [15] ที่มีการพัฒนาใช้งานภายในอาคาร รูปที่ 2 เป็นตำแหน่งและขนาดของพื้นที่สำหรับวิเคราะห์แบบจำลอง

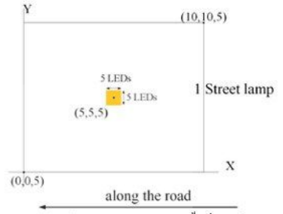

รูปที่ 2 ตำแหน่งตัวส่งและแสดงขนาดของพื้นที่ถนนในระนาบ (x,y)

ตารางที่ 1 พารามิเตอร์สำหรับจำลองระบบ OWVLC-I2V

พารามิเตอร์ (Parameter)	ขนาด (Value)
หลอดแอลอีดีอาเรย์	5 x 5 หลอด
กำลังงานหลอดแอลอีดี 1 หลอด	1 วัตต์
ความสว่างศูนย์กลาง (center luminous)	2500 ลูเมน
มุมการกระจายแสงของหลอดแอลอีดี	70 องศา
ขนาดพื้นที่ถนน (กว้าง x ยาว)	10 x 10 เมตร
ความสูงของตัวส่งจากพื้นถนน	5 เมตร
ความสูงของตัวรับจากพื้นถนน	1.10 เมตร
มุม Field of View (FOV) ของตัวรับ	120 องศา
สัมประสิทธิ์การสะท้อนของเลนน์ตัวรับ	1.0
ระยะทางจากตัวส่งไปยังตัวรับ (แนวตั้ง)	3.9 เมตร

2.1 การกระจายความแสงสว่างและกำลังงานแสงของไฟส่องสว่างบนถนน

ในอุตสาหกรรมไฟส่องสว่างบนถนน (Street Light) พบว่าได้นำหลอดแอลอีดีมาใช้งานแทนหลอดไฟแบบเดิมอย่างเห็นได้ชัด โดยเฉพาะอย่างยิ่งหลอดแอลอีดีแสงสีขาว (White LED) จากแบบจำลองระบบ OWVLC-I2V กำหนดให้ตำแหน่งไฟส่องสว่างบนถนนได้จัดวางไว้จุดศูนย์กลางของถนนขนาด 10 x 10 x 5 เมตร คือที่ตำแหน่ง (x,y,z) = (5,5,5) สมมติให้แอลอีดีอาเรย์เป็นหลอดไฟส่องสว่างบนถนนหนึ่งดวง ที่มีลักษณะการแพร่กระความเข้มแสงในแนวนอนแบบแลมเบอร์เซียน (Lambertian radiation) [15] แสดงดังสมการที่ (1)

$$E_{hor}(x,y,z) = I(\phi)/d^2.\cos(\psi) \tag{1}$$

เมื่อ $I(\phi) = I(0)\cos^m(\phi)$ คือเป็นค่าความเข้มแสงจากหลอดแอลอีดีที่มุม ϕ คือมุมที่แสงแพร่ออกมาจากหลอดแอลอีดี เป็นฟังก์ชันโคไซน์ยกกำลังด้วยค่าคงที่ d คือระยะทางระหว่างตัวส่งกับตัวรับ $I(0)$ คือความเข้มแสงศูนย์กลางของหลอดไฟแอลอีดี m คือตัวเลขแลมเบอร์เซียนแสดงตามสมการที่ (2) [15]

$$m = -\ln(2)/\ln(\cos\phi_{1/2}) \tag{2}$$

PH-6

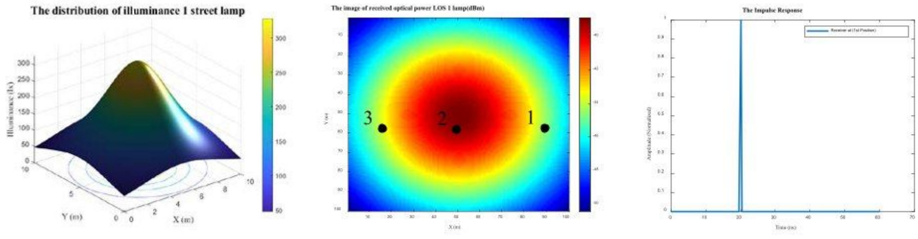

(ก) (ข) (ค)

รูปที่ 3 ผลการทดลองเชิงตัวเลขของระบบการสื่อสาร OWVLC-I2V (ก) การกระจายค่าความสว่างแสง (lux ลักซ์) (ข) การกระจายค่ากำลังงานแสง ของหลอดไฟส่องสว่างบนถนน (ค) สัญญาณผลตอบสนองช่องการสื่อสาร ณ ตำแหน่งที่ 1

โดย $\phi_{1/2}$ คือมุมครึ่งหนึ่งของมุมที่แสงแพร่จากตัวส่ง ψ คือมุมที่แสงตกกระทบที่ตัวรับซึ่งต้องมีค่าน้อยกว่ามุมมองของตัวรับ FOV จากการคำนวณทางตัวเลขสามารถแสดงการกระจายความเข้มแสงบริเวณพื้นที่ที่ได้กำหนดตามที่แสดงในรูปที่ 3 (ก) และค่าการกระจายกำลังงานแสงที่รับได้ในรูปที่ 3 (ข) จุดที่ 1 2 และ 3 เป็นตำแหน่งสำหรับหาสัญญาณผลตอบสนองของช่องสัญญาณในขณะที่ยานยนต์กำลังเคลื่อนที่ผ่าน ซึ่งคำนวณได้จากสมการที่ (3) และ (4) [14] [15]

$$P_r = P_t H_{LOS}(0) \tag{3}$$

เมื่อ P_t คือค่ากำลังงานแสงที่ตัวส่ง $H_{LOS}(0)$ คือค่าผลตอบสนองของช่องสัญญาณทางความถี่ฮาร์โมนิคที่ศูนย์ (Channel DC gain)

2.2 ช่องสัญญาณของระบบ OWVLC-I2V

โดยปกติรูปแบบการแพร่กระจายของแสงแบ่งเป็นสองรูปหลัก ๆ คือการแพร่แบบทางตรง (Line of Sight: LOS) และการแพร่แบบสะท้อน (Diffuse or Non-Line of Sight: NLOS) รายละเอียดสามารถศึกษาเพิ่มเติมจาก [5] สำหรับงานวิจัยนี้กำหนดให้การการแพร่ของแสงจากไฟถนน (ตัวส่ง) ไปยังยานยนต์ (ตัวรับ) มีรูปแบบการแพร่แบบ LOS แสดงได้ตามสมการที่ (4)

$$H_{LOS}(0) = \begin{cases} \dfrac{A_r(m+1)}{2\pi d^2}\cos^m(\phi)T_s(\psi)g(\psi)\cos(\psi), & 0 \le \psi \le \psi_c \\ 0, & eleswhere \end{cases} \tag{4}$$

เมื่อ A_r คือพื้นที่รับแสงของโฟโตไดโอด d คือระยะทางจากตัวส่งไปยังตัวรับ m คือเลขแลมเบอร์เชียน ϕ คือมุมการแผ่กระจายแสงจากหลอดแอลอีดี ψ คือมุมที่แสงตกกระทบที่พื้นที่ของตัวรับ $\cos(\phi)$ คือฟังก์ชันโคไซน์ของมุมการแผ่กระจายแสงของหลอดแอลอีดี $T_s(\psi)$ คือค่าสัมประสิทธิ์การสะท้อนของแสงที่มุมตกกระทบที่ตัวรับ $g(\psi)$ คือค่าสัมประสิทธิ์การทะลุผ่านของแสงที่มุมตกกระทบที่ตัวรับ $\cos(\psi)$ คือฟังก์ชันโคไซน์มุมของแสงตกกระทบที่ตัวรับ สัญญาณที่ได้รับสามารถแสดงด้วยสมการที่ (5)

$$y(t) = Rx(t) \otimes h(t) + n(t) \tag{5}$$

เมื่อ R คือผลตอบสนองของตัวรับสัญญาณ $x(t)$ คือสัญญาณทางไฟฟ้าที่ถูกส่งมาจากตัวส่ง หลอดแอลอีดีซึ่งสัญญาณผลตอบสนองของหลอดแอลอีดีเป็น $h_{LED}(t) = e^{-\omega_c t}$ [15] $h(t)$ คือผลตอบสนองของช่องสัญญาณการสื่อสารทางแสง และ $n(t)$ คือสัญญาณรบกวนในระบบการสื่อสารแสดงด้วยสมการที่ (6) [5] ซึ่งทำให้สามารถคำนวณหาบิตผิดพลาดที่เกิดขึ้น $BER = Q\left(\sqrt{SNR}\right)$

$$SNR = (RP_r)^2 / \sigma_{total}^2 \tag{6}$$

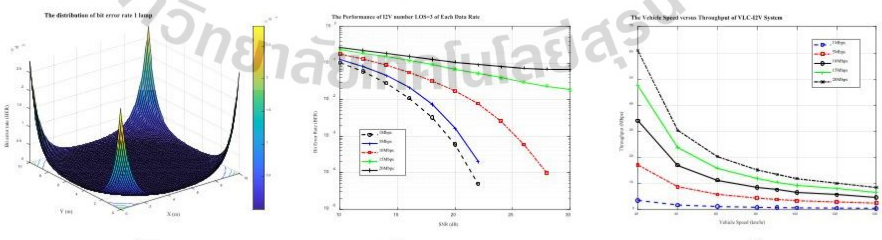

(ก) (ข) (ค)

รูปที่ 4 ผลการทดลองเชิงตัวเลขของระบบการสื่อสาร OWVLC-I2V (ก) การกระจายของบิตผิดพลาด (ข) บิตผิดพลาดของระบบในแต่ละอัตราการส่งข้อมูล (ค) ผลการส่งผ่านข้อมูลสำเร็จของระบบที่สัมพันธ์กับความเร็วของยานยนต์

2.3 การทดลองระบบ OWVLC-I2V

จากแบบจำลองระบบ OWVLC-I2V ที่ได้ออกแบบทดลองการสื่อสารระบบด้วยโปรแกรมการคำนวณเชิงตัวเลข (Matlab) ให้ตัวส่งทำการส่งสัญญาณดิจิทัลเบสแบนด์แบบ (On-Off Keying: OOK) ด้วยความถี่ 1 Mb/s 5 Mb/s 10 Mb/s 15 Mb/s และ 20 Mb/s ตัวรับที่ถูกติดตั้งบนยานยนต์เคลื่อนที่ด้วยความเร็ว 90 กม./ชม. กำหนดให้จำนวนช่องสัญญาณแบบ LOS เป็น 3 ตำแหน่งในบริเวณที่ยานยนต์เคลื่อนที่ผ่านพื้นที่การสื่อสาร เวลาที่ใช้รับ-ส่งข้อมูลภายในระยะทาง 10 เมตร เท่ากับ 0.4 วินาที

2.4 ผลการทดลอง

สมถรรนะของแบบจำลองการสื่อสาร OWVLC-I2V จากรูปที่ 4 (ก) เป็นการกระจายของบิตผิดพลาดที่เกิดขึ้นในพื้นที่ที่ทำการวิเคราะห์ 10 ตารางเมตร โดยสัมพันธ์กับการกระจายค่ากำลังงานแสงที่ได้รับของระบบตามสมการที่ (6) และในรูปที่ 4 (ข) หา *BER* ของระบบเมื่ออัตราการส่งข้อมูล จาก 1 Mb/s ถึง 20 Mb/s สุดท้ายผลการส่งผ่านข้อมูล (Throughput) ด้วยระบบ OWVLC-I2V มีความสัมพันธ์กับความเร็วของยานยนต์ที่เคลื่อนที่ผ่านพื้นที่ของการสื่อสาร ดังแสดงในรูปที่ 4 (ค) ดังนั้นความสัมพันธ์ระหว่างความเร็วของยานยนต์กับอัตราการส่งข้อมูลแสดงดังรูปที่ 4 (ค) พบว่าปริมาณข้อมูลที่ได้รับลดลงเมื่อยานยนต์มีความเร็วเพิ่มขึ้น

3. อภิปราย

ผลการทดลองแบบจำลองการสื่อสารไร้สายด้วยแสงที่มองเห็นเพื่อประยุกต์ใช้งานไฟส่องสว่างบนถนนกับยานยนต์ จากการจำลองระบบอย่างง่าย แสดงให้เห็นความสามารถประยุกต์ใช้ระบบ VLC กับการสื่อสารในระบบ ITS เพื่อเป็นแนวทางสำหรับการพัฒนาต่อเนื่องด้วยความต้องการข้อมูลการสื่อสารในยุค 5G และ 6G ที่ต้องการอัตราการส่งข้อมูลที่สูงขึ้นต่อเนื่องในระดับ Gb/s และ Tb/s ทำให้ระบบ VLC มีส่วนเข้ามารองรับการสื่อสารข้อมูลในระดับที่สูงด้วยความสามารถและข้อดีของระบบ VLC

4. สรุป

งานวิจัยฉบับนี้คือการนำเสนอแบบจำลองการสื่อสารไร้สายด้วยแสงที่มองเห็นเพื่อการประยุกต์ใช้งานระหว่างโครงสร้างพื้นฐานกับยานยนต์ (OWVLC-I2V) เป็นการประยุกต์ใช้งานระบบ VLC กับการสื่อสารข้อมูลในระบบขนส่งอัจฉริยะ (ITS) จำลองระบบการสื่อสารผ่านรูปแบบการทำงานด้วยโปรแกรมคอมพิวเตอร์ แสดงการแพร่กระจายความเข้มแสง แสดงผลตอบสนองช่องสัญญาณการสื่อสารด้วยแสงที่มองเห็น การส่งสัญญาณเบสแบนด์แบบ OOK และได้แสดงสมรรถนะของระบบด้วยอัตราบิตผิดพลาดข้อมูล (Bit Error Rate: BER) และสมรรถนะการส่งผ่านข้อมูลที่สัมพันธ์กับความเร็วยานยนต์

เอกสารอ้างอิง

[1] "Global status report on road safety 2018." [Online]. Available: https://www.who.int/violence_injury_prevention/road_safety_status/2018/en/.

[2] Qualcomm Technologies Inc., [Online]. Available https:// www.qualcomm.com/documents/nr-c-v2x-webinar-march-2020-presentation.

[3] T. Taguchi, "Technological innovation of high-brightness light emitting diodes (LEDs) and a view of white LED lighting system," OPTRONICS, vol. 19, no.228, pp.113-119, 2000.

[4] M. Ishida, "InGaN based LEDs and their application," OPTRONICS, vol.19, no.228, pp. 120-125, 2000.454446.

[5] T. Komine, "Visible Light Wireless Communications and Its Fundamental Study," in Thesis, 2005.

[6] L. Zeng, et al., "High Data Rate Multiple Input Multiple Output (MIMO) Optical Wireless Communications Using White LED Lighting," IEEE Journal on selected areas in communications , vol. 27, no. 9, December 2009, pp. 1654-1662.

[7] Kim, D. R., et al., (2012, August). Outdoor visible light communication for inter-vehicle communication using controller area network. In 2012 Fourth International Conference on Communications and Electronics (ICCE) (pp. 31-34). IEEE.

[8] A.-M. Cailean et al., "Novel receiver sensor for visible light communications in automotive applications," IEEE Sensors J., vol. 15, no. 8, pp. 4632–4639, Aug. 2015.

[9] C. Liu, B. Sadeghi, E.W. knightly, "Enabling vehicular visible light communication (V2LC) networks", Vanet'11, Las vegas, USA, 2011.

[10] M. Akanegawa, Y. Tanaka, M. Nakagawa, "Basic study on traffic information system using LED traffic lights," Intelligent Transportation Systems, IEEE Transactions on , vol.2, no.4, pp.197,203, Dec 2001.

[11] M.Y. Abualhoul, M. Marouf, O. Shagdar, F. Nashashibi, "Platooning control using visible light communications: A feasibility study," Intelligent Transportation Systems - (ITSC), 2013 16th International IEEE Conference on , vol., no., pp.1535,1540, 6-9 Oct. 2013.

[12] N. Kumar, N. Lourenço, D. Terra, L.N. Alves, R.L. Aguiar, Visible Light Communications in Intelligent Transportation Systems, IEEE Intelligent Vehicules Symposium 2012, 748-753.

[13] N. Kumar, "Smart and intelligent energy efficient public illumination system with ubiquitous communication for smart city," Smart Structures and Systems (ICSSS), 2013 IEEE International Conference on , vol., no., pp.152,157, 28-29 March 2013.

[14] S. Kitano, S. Haruyama, M Nakagawa, "LED road illumination communications system," Vehicular Technology Conference, 2003. VTC 2003-Fall. 2003 IEEE 58th , vol.5, no., pp.3346,3350 Vol.5, 6-9 Oct. 2003.

[15] Nguyen H. Q., et al., A Matlab-Based Simulation Program for Indoor Visible Light Communication System. CSNDSP2010 OWC-5. (2010); 537-541.

BIOGRAPHY

Adisorn Kaewpukdee, a male individual, was born on February 5, 1980, in the province of Sisaket, located in the country of Thailand. In the year 2000, he commenced his pursuit of a Bachelor's degree in Electronics Engineering at the Department of Electronics Engineering, located at King Mongkut's Institute of Technology Ladkrabang (KMITL), Chumporn Campus, situated in Chumporn Province, Thailand. After graduating, he secured employment at the MPT corporation in Ayutthaya Province, Thailand. In 2010, he pursued a Master's degree at the School of Data Storage Technology at King Mongkut's Institute of Technology Ladkrabang (KMITL) in Bangkok, Thailand. Subsequently, he held the position of lecturer and researcher at the Department of Electrical Engineering, Faculty of Science and Technology, Nakhon Pathom Rajabhat University (NPRU).